Toulouse, 11 June 2018

Dear Biogeosciences Editor

We have taken into account all the reviewer comments. Please find enclosed detailed answers to all reviewer comments and a revised version of the manuscript with highlighted changes with respect to the previous version. In addition, the main changes in the new version are indicated with boldface characters.

Yours sincerely,

Nemesio Rodriguez-Fernandez,

on behalf of all the authors

Referee # 1

The authors present an interesting work addressing the sensitivity of SMOS L-band vegetation optical depth (VOD) to biomass. The study is centered in the African continent and employs the three available data sets of SMOS VOD data currently available (L2,L3 and IC). As independent data sets, the authors chose four above-ground biomass sources (AGB), lidar-based tree height, MODIS vegetation indices and cumulated precipitation. The differences of the three SMOS products are clearly detailed and discussed. The analyses relating VOD to the independent data sets are performed in a scientifically sound manner. However, sometimes the pretensions of the authors with respect to the obtained results are too high, specially taking into account that they are only using one year of SMOS observations. Also, they report a higher sensitivity to AGB at L-band than at higher frequencies (K/X/C-bands), but they do not present a clear comparison of the different data sets. Therefore, I recommend this manuscript for publication after addressing the following issues:

We thank the referee for his/her constructive comments. We will add a discussion on how results would change if a different year is used for the study (see plots and table in the answer to comment 3). The results remain unchanged, but we agree with the referee, that the presentation and discussion would look more robust adding other years. With respect to VOD from higher frequencies, we develop below in comment 2.

In addition below, we give more details on these comments and we address all the other comments made by the referee.

1. The results should be re-organized in a more clear and structured way to facilitate readability and comprehension. There are many general references to relevant results in supplementary material that should directly point to a specific figure or table and be commented in the main text. Some choices made in the analysis and presentation of results are unclear (e.g. the stratification per land cover in two biomes should be further justified) and it is hard to follow the results presented in the main and the supp. material.

Taking into account the three reviewers comments (Referee #2 thinks that “too much importance is given to the inter-comparison of different VOD retrieval algorithms), we reckon that the best trade off is to leave in the supplement the results for SMOS L2 and L3 but to move to the main body of the analysis per biomes that was in the supplementary information (text and Fig. S6). The new Figures 6 and 7 show the results for all land cover classes and the discussion is done in the new Sect. 4.3, in the main body of the manuscript.

2. It is unclear how the authors obtain the results plotted in Fig. 4. It seems they do not use K/X/C-VOD data from year 2011 for a fair comparison to the presented results with L-band and NDVI. Instead, they show the results from Liu et al 2015, which are based on VOD time series from 1993 to 2012 and a significantly different approach. I believe the data is not directly comparable and the result presented in the figure is therefore misleading. I strongly suggest the authors to either a) include the K/X/C-VOD data from the same study period (yearly average) and detail in the methods or b) focus on the comparison of L-band VOD and NDVI and AGB. I would particularly encourage the latter. Also, the results on Fig 4 could be shown for the four different AGB data sets used in the study, for completeness.

This manuscript is devoted to SMOS L-Band VOD. That's the reason why we did not attempt to perform a complementary study with data from other radiometers at the present stage. However, we do think that it is interesting to discuss the new results by comparing to previous results reported in the literature for other frequency bands. Former Figure 4 (new Fig 8) does not contain any new result. It is a Figure for the discussion, where results presented earlier are compared to published results by Liu et al. 2015. However, we realized that the normalization used to plot L-VOD, K/X/C-VOD and NDVI in the same plot could be misleading. The normalization is not needed to compare with other VOD, only for NDVI. Therefore, new Fig, 8 presents the results in two panels. In the left panel L-VOD and NDVI were normalized to 1 using their maximum values. This is needed to plot the two quantities in the same figure. In the right panel, L-VOD and K/X/C-VOD relationship to Saatchi AGB are shown without using any normalization. The curves plotted here for the K/X/C-VOD are just those of Figure S4 from Liu et al. 2015, which were computed using Saatchi AGB and the same method that we used in the current study. Liu et al fitted their relationship using K/X/C-VOD data in the period 1998-2002 and Saatchi data acquired from 1995 to 2005 (page 6 of their supplementary information document). However, the non-linearity of the curve and the difference sensitivity to high AGB from different frequencies is driven by the high AGB values in the dense equatorial forest, which is not supposed to vary strongly in a few years time. These facts have been added to the new Sect 5.2.

The curves for the other AGB dataset with respect to L-VOD are already shown in Fig 5. They will not add much information to this discussion and we tried to show them in the figure below but it becomes unreadable.

3. The title is too ambitious and general. The focus is clearly on SMOS L-band VOD and biomass, but the results presented (using 1 year of observations over Africa) do not support the use of the words "high sensitivity". I would recommend the authors to provide a more specific title, more representative of its contents.

Taking into account comments from Referee #2 as well, we decided to change the title to:

An evaluation of SMOS L-band vegetation optical depth (L-VOD) data sets: a high sensitivity of L-VOD to above-ground biomass in Africa

Otherwise, by “high sensitivity” we meant that the AGB and L-VOD relationship is smooth and with a moderately low slope. This is not related to the number of years used for the study. However, as already mentioned, in the corrected version we using two years and both ascending and descending orbits and we show that it does not change the results. Figure 5 replaces the former Fig. S3. Both are almost indistinguishable, however Fig. 5 below has been computed using data from two years (2011 and 2012) and both ascending and descending orbits (taking into account the comment on the orbits below).

See also answer to comment 19 below.

4. Section 5 “Discussion” is too short. Results are already discussed in Section 4, and Section 5 adds a brief overview and a comparison to literature studies. I would recommend the authors to re-organize the manuscript and include the content of Section 5 either in the results or in the conclusions as “Discussion and Conclusion”.

The referee is right that there are a few comments on results from the literature already in Section 4 “Results”. They have been moved to section 5 “Discussion”. In addition section 4 was enlarged with the discussion of the results by biomes following the suggestions (here below) of the reviewer.

Here is a list of more specific comments and recommendations:

1. Abstract, last sentence. Consider changing “index” by “indicator”

We agree. This has been changed.

2. Page 2, lines 9-11. In presence of vegetation, part of the soil emission is absorbed and scattered. There are two microwave vegetation parameters that are used in the physical model to account for the effect of vegetation: the vegetation optical depth and the single effective scattering albedo. The authors should introduce here the albedo parameter, or at least mention it.

Thanks for pointing this out. We agree that the best is to introduce the tau-omega model already here, see Lines 12-13 of page 2.

3. Page 2, line 16. Specify how "thick" is the vegetation layer that microwaves penetrate, and introduce here a comparison between frequencies (this is later briefly discussed in line 30). Is the soil emission from tropical and boreal forests reaching the satellites operating at C/X/L bands? Add references and a brief discussion to support and clarify how the different frequencies are complementary.

"Thick" was removed (*VOD samples the vegetation including the woody vegetation under the green canopy*) as it is difficult to quantify it. We prefer to say that it is thicker than the layer sampled at higher frequencies as done in Line 34. Otherwise, the goal of this paragraph was to cite some examples of studies of the vegetation with VOD. The actual comparison of frequencies is done in the first paragraph of new page 3.

4. Page 3, first paragraph. Literature on SMAP L-band VOD is totally missing and should be added. For instance, a global comparison of SMAP VOD to lidar-based vegetation height is reported in Konings et al. 2017. A.G. Konings, M. Piles, N. Das, D.Entekhabi, L-Band Vegetation Optical Depth and Effective scattering Albedo Estimation from SMAP, Remote Sensing of the Environment, Vol. 198, pp 460-470, 2017.

This is a pertinent paper that has been added to the introduction, together with Konings, A. G.; Piles, M.; Rötzer, K.; McColl, K. A.; Chan, S. K. & Entekhabi, D. Vegetation optical depth and scattering albedo retrieval using time series of dual-polarized L-band radiometer observations Remote Sensing of Environment, 2016, 172, 178-189

5. Page 3, line 17. It should be relevant to (at least) mention briefly the difference between active and passive microwave sensing of vegetation.

The sentence was continued as follows (lines 26-29 of page 3):

[…] observations. In contrast to passive measurements, for which the goal is study how the thermal emission arising from the Earth is affected by the vegetation layer, active measurements allow to study how the radiation emitted by a human-made radiation source is backscattered by the vegetation, which depend mainly in vegetation water content and the vegetation structure.

6. Page 3, line 25. Please, add a reference to support that the quality of the ascending data is better than the descending. I would "a priori" recommend to use both to increase coverage.

Ascending orbits data have been shown to give somewhat better results than descending orbits to retrieve soil moisture in Europe, North America and the Sahel (see Kerr et al. 2016, RSE, and references therein). The reason is that in some regions they can be less affected by radio frequency interference and that at 6 AM (ascending orbits) the soil and canopy are closer to thermal equilibrium and there are less problems of convective precipitations than for descending orbits (6 PM). However, for a sensitivity study of VOD to vegetation and in particular biomass this does not necessarily apply.

See also answer to general comment 3 above and comment 19 below. We show that the results obtained using descending orbits are same as those obtained using ascending orbits.

In the revised version of the manuscript we used two years of data (2011-2012 and both ascending and descending orbits) as mentioned in the answer to general comment 3.

7. Page 4, line 7. SMOS is first introduced as a full-polarization radiometer but here it is stated that only dual-polarization measurements are used in the retrievals. Why? Too much information to constrain retrievals? Consider including a reference here.

The parameters Stokes 3 and 4 are actually used for filtering the SMOS brightness temperatures, for instance to detect RFI (Kerr et al. 2012, TGRS). Line 6-7 of page 4.

8. Page 4, line 14. The authors mention that previous L-VOD retrievals are used to constrain new retrievals. How many closest retrievals? Please, be more specific.

Due to the specificities of the SMOS geometry of observation, the profiles of brightness temperatures observed at the middle part of the field of view (~600 km centered on the satellite sub-track) have larger ranges of incidence angle than the outer pat of the field of view. For such observations, the retrieval system has more information content to discriminate the vegetation emission from the ground emission leading to more accurate retrieved soil moisture and VOD. The retrieved VODs and associated uncertainties for such grid points are used as prior first guess and uncertainties for the VOD retrieval of the next overpass of these grid-points (3 days later max) that will be observed, this time, at the outer part of the field of view with reduced range of incidence angle instead of using auxiliary data LAI, LAImax as first-guess values and fixed large prior uncertainties (see Kerr et al 2012).

This information was added to Sect, 2.1.1

9. Table S1. It would be relevant to include how albedo and soil roughness are computed in the different products. Also, please detail previous retrievals. ISEA should be ISEA4h9.

A) **Albedo and roughness:**

For SMOS IC the roughness and single scattering parameters are assigned per IBGP classes, based on Parrens et al. (2017a, b), and are averaged per pixel according to the fraction of classes present in the pixel (Fernandez-Moran et al. 2017).

For SMOS L2 and L3 algorithms, single scattering albedo and roughness values depend on the surface type and are taken from literature and/or specific SMOS studies. For low vegetated area the single scattering albedo is set to 0 and roughness set to 0.1. For forested areas the single scattering albedo is set to 0.06 for tropical and subtropical forest and 0.08 for Boreal forest and roughness set to 0.3 (Rahmoune et al. 2013,2014, Al Bitar et al. 2017).

Marie Parrens, Jean-Pierre Wigneron, Philippe Richaume, Ahmad Al Bitar, Arnaud Mialon, Roberto Fernandez-Moran, Amen Al-Yaari, Peggy O'Neill, and Yann Kerr, 2017. Considering Combined or Separated Roughness and Vegetation Effects in Soil Moisture Retrievals, International Journal of Applied Earth Observation and Geoinformation 55, 73-86.

M. Parrens, A. Al Bitar, A. Mialon, R. Fernandez-Moran, J.-P. Wigneron, P. Ferrazzoli, and Y. Kerr, 2017. Estimation of the L-band Effective Scattering Albedo of Tropical Forests using SMOS observations, IEEE GRS Letters 2017, 14, 1223-1227

See new sections 2.1.1, 2.1.2, 2.1.3 and new Table S1

b) **Previous retrievals:** see answer to the next comment #10.

c) **Grid name:** The name of the grid will be corrected to reflect the exact name.

10. Page 5, line 6. Mention how SMOS-IC is initialized and refer to Table S1.

In a first run the minimization is initialized with SM 0.2 m3/m3 and L-VOD 0.5. This allowed to compute a mean L-VOD map per each grid point. In a second run SM was initialized at 0.2 m3/m3 while the mean L-VOD for each grid point was used to initialize the L-VOD. This information was added to Sect 2.1.3 referring the Table S1 where it was already given but with a typo as the value quoted for the initialization of VOD in the first run was 0.2 instead of 0.5.

11. Page 5, line17. A reference is needed for Worldclim data.

Absolutely, thanks for pointing this out. The reference is: Fick, S. E. & Hijmans, R. J. WorldClim 2: new 1-km spatial resolution climate surfaces for global land areas *International Journal of Climatology*, *Wiley Online Library*, 2017

12. Page 5, line 21. change “sential” by “essential” (?)

Thanks for the typo correction.

13. Page 5, line 24. Consider adding a refernce for EVI and its main differences to NDVI.

The EVI description was extended and more references are given in the new section 2.2.2.

4. Page 5, line 7. Words “In a second step” are used in lines 5 and 7.

We assume it is page 6. The second “in a second step” was be replaced by “In the third step” and “in the third step” (line 8) will be replaced by “Finally”.

15. Page7, lines 15-16. It seems here that the authors hypothesize the AGB data set derived from L-band SAR is probably the more appropriate and therefore they restrict the study to its coverage (i.e. Africa). However, best results are obtained with Saatchi. The authors should better elaborate on why it is important to use this data set and reformulate this sentence.

One cannot summarize the results of this study saying that the best agreement of L-VOD is found with respect to Saatchi AGB dataset. Please, see the answers to comments 26 and 29 here below. Regarding the sentence referred to here, it will be reformulated as : […] *because one of the reference data-set is available only in Africa, in addition this dataset is particularly interesting because it has been obtained using radar observations at a lower frequency than other datasets, namely, in L-band, which is also the frequency of SMOS. The African continent contains […]*

16. Page 7, line 24. Please, specify which parameter is used to select the lower values of the cost function (chi-square?)

Yes, Chi2.

17. Page 7, line 28. There are different criteria to filter out the quality of SMOS observations. As a common practice, the DQX parameter is used. However, the authors here propose to use the Chi2 parameter larger than 3. A reference should be added to support this criteria.

The DQX is actually a standard deviation which informs only about the uncertainty of the retrieved solution which is driven by the forward model sensitivity at the solution point. It is the retrieved parameter post uncertainty computed using the inverse linear tangent model (Jacobian) at the solution used to translate the observation uncertainty (radiometric accuracy) into the parameter space uncertainty. It does not inform by itself about the correctness of the solution with is based on a quality of a fit. In other words, we can have a very wrong modeling (bad fit) with a retrieved parameters solution where the forward model is very sensitive resulting to low DQX. Moreover, the DQX values are not homoscedastic as our forward models are much more sensitive for lower values of the (SM,VOD) parameter space (leading to low DQX) than for higher values (leading to high DQX).

By filtering the DQX too strictly there is a serious risk to bias statistics toward lower retrieved SM and VOD, which would bias our results for tropical forest where both SM and VOD are high.

The DQX should be used as a weight in the parameters use e.g. as it is done by assimilation system. See for instance: A. Tarantola; Inverse Problem Theory and Methods for Model Parameter Estimation, SIAM, 2005.

In contrast, the Chi2, or alternatively its probability, which is naturally used in the retrieval procedure is currently the preferred option to filter out the retrieved solution; it is the classical goodness-of-fit test. See for instance Román-Gascon et al 2017 (using Chi2 < 3.5) or Bircher et al. (2013), who used Chi2 probability.

Román-Cascón, Carlos, et al. "Correcting satellite-based precipitation products through SMOS soil moisture data assimilation in two land-surface models of different complexity: API and SURFEX." *Remote Sensing of Environment* 200 (2017): 295-310.

Validation of SMOS L1C and L2 Products and Important Parameters of the Retrieval Algorithm in the Skjern River Catchment, Western Denmark, IEEE Transactions on Geoscience and Remote Sensing, pp 2969 – 2985. S. Bircher, N. Skou, Y. H. Kerr, 2013, DOI - 10.1109/TGRS.2012.2215041, Vol 51, Issue 5, ssn 0196-2892

The manuscript text was modified as follows:

Several quality indicators are present in the SMOS products. The DQX parameter uses the inverse linear tangent model (Jacobian) to translate the observation uncertainty (radiometric accuracy) into the parameter space uncertainty. The forward models are much more sensitive for lower values of the (SM,VOD) parameter space (leading to low DQX) than for higher values (leading to high DQX). Therefore, filtering using DQX implies a risk to bias our results for tropical forest where both SM and VOD are high. In addition, the DQX parameter does not give information about the correctness of the solution, which is based on a quality of a fit. Therefore, the Chi2 parameter (goodness of the fit) was used to filter out the retrieved solutions. Several tests were done and a value of 3, corresponding approximately to the peak of the Chi2 probability distribution was found to be a good threshold. This is in agreement with the values used in other studies (see for instance, Roman-Cascon et al. 2017).

18. Page 7, line 30. It would be important to show a map with the final number of samples used per pixel, after the filtering criteria is applied. It would also be relevant to show a map of the standard deviation of the estimates (apart from the average on Fig. 1). This is critical, since the study is based on a final comparison of spatial maps.

In a corrected version of the manuscript Fig 1 was splitted in two different figures: one for maps that have been averaged on time and another one for AGB and cumulated precipitations datasets. The first one adds the STD and the number of points in the times series for each grid point.

19. Page 8, line 3. The authors average on a yearly basis since they chose only one year of observations. A seasonal study would be interesting, but of coarse more years would be needed. The choice of using only one year of SMOS observations should be further justified. Also, the impact of using one year in the results should be (at least) discussed later in the manuscript.

Actually, the shape of the scatter plots is very similar using data for other years. See for instance the next figure and compare to Fig S3.

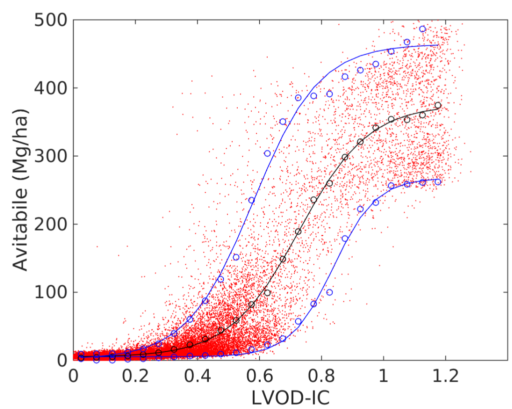

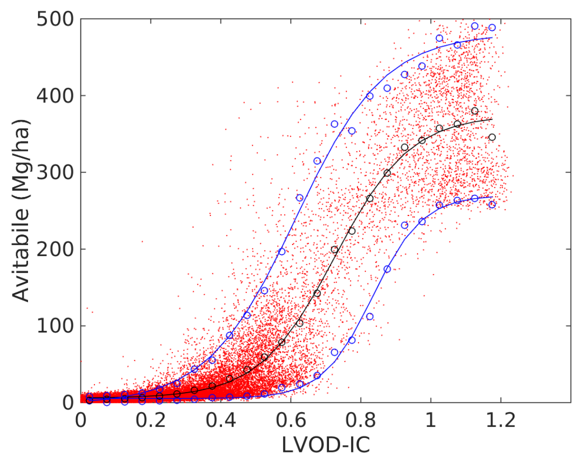

Fig. Left : 2012 Ascending orbits. Right: 2012 Descending orbits

The next table shows the parameters of the fits using ascending or descending orbits in 2012. The values can be compared to those of former Table S2. They have almost the same numeric values.

AGB	Year	Orbit	curve	a	b	c	d	R^2
Avitabile	2012	A	05th	262.697	14.406	0.838	5.347	0.99548
Avitabile	2012	A	Mean	370.615	8.920	0.727	4.915	0.99917
Avitabile	2012	A	95th	462.962	9.398	0.580	1.613	0.99243
Saatchi	2012	A	05th	333.496	4.642	0.906	-3.338	0.99080
Saatchi	2012	A	Mean	280.675	6.686	0.684	14.439	0.99334
Saatchi	2012	A	95th	291.444	9.661	0.545	32.436	0.99372
Baccini	2012	A	05th	497.748	2.673	1.024	-41.748	0.98810
Baccini	2012	A	Mean	414.033	3.503	0.717	-27.346	0.99882
Baccini	2012	A	95th	383.823	4.950	0.550	-1.911	0.99757
Bouvet-Mermoz	2012	A	05th	292.291	4.800	0.963	4.717	0.97445
Bouvet-Mermoz	2012	A	Mean	319.123	5.261	0.760	7.879	0.99616
Bouvet-Mermoz	2012	A	95th	358.172	7.290	0.581	17.621	0.99226
Avitabile	2012	D	05th	264.867	13.984	0.833	5.353	0.99548
Avitabile	2012	D	Mean	368.991	9.271	0.726	5.795	0.99765
Avitabile	2012	D	95th	483.476	7.893	0.614	-2.245	0.99585
Saatchi	2012	D	05th	332.540	4.976	0.890	-5.476	0.99111
Saatchi	2012	D	Mean	287.547	6.436	0.691	12.981	0.99499
Saatchi	2012	D	95th	291.493	8.979	0.543	30.449	0.99324
Baccini	2012	D	05th	606.345	2.250	1.168	-53.195	0.98742
Baccini	2012	D	Mean	398.354	3.688	0.706	-21.945	0.99806
Baccini	2012	D	95th	379.008	5.076	0.567	6.162	0.99538
Bouvet-Mermoz	2012	D	05th	308.430	4.441	0.965	0.250	0.98165
Bouvet-Mermoz	2012	D	Mean	317.532	5.425	0.764	10.022	0.99729
Bouvet-Mermoz	2012	D	95th	375.791	6.420	0.604	12.619	0.99451

Therefore, there is no real impact of using just one year. However, in a revised version of the manuscript we will use two years of data both for ascending and descending orbits. The results will not change but they would look more robust to the reader. This will be discussed in a revised version of the manuscript. See also answer to General Comment 3.

21. Page 4, line 15. It would be relevant to detail the function used for the fitting in the main manuscript.

We think that the reviewer meant “Page 8” and his/her comment refers to Liu et al. 2015 function.

$$AGB = a \times \frac{\arctan(b(\mathrm{VOD}-c)) - \arctan(-bc))}{(\arctan(\infty) - \arctan(-bc)} + d,$$

This equation and the logistic function are now shown in the Methods section.

22. Page 8, line 22. Please, detail “the remaining static data sets” and comment on Figure 1 (e.g. main visual differences between the VOD products and the AGB ones)

In the new version the text has been extended describing explicitly the new Fig2 1 and 2. See the first two paragraphs of Sect 4 in the revised version of the manuscript

23. Figure 1. The reference to Mermoz is missing.

Thanks, it was added to the corrected version.

24. Page 9, line 1. Comment on Spearman and Kendall results, which confirm the results obtained with Pearson.

The referee is right that the table contains all values while the text commented only on Pearson. As he/she says, the Spearman and Kendall results confirm the Pearson results, which also means that the lower values obtained for the L3 dataset are not due to a correlation that could be good but more non-linear than those of the IC and the L2 dataset. Thus, we fully agree that the results should be further commented. It has been done in the new Sect. 4.1.

25. Page 9, line 20. It is interesting that only with Saatchi and Baccini there is a single AGB peak corresponding to the higher VOD values. Why do the authors

believe this peak is not appearing as clearly with the other two data sets? Is it consistent that the peak is higher for Baccini than for Saatchi? The authors should elaborate on the results presented.

We have analyzed the high AGB blobs of the scatter plots as follows:

Avitabile blob 1: VOD > 1 ; 230 < AGB < 330

Avitabile blob 2: VOD > 1 ; AGB > 330

Bouvet-Mermoz blob 1: VOD > 1 ; 170 < AGB < 260

Bouvet-Mermoz blob 2: VOD > 1 ; AGB > 270

Saatchi : VOD > 1; AGB > 240;

Baccini: VOD > 1; AGB > 240;

The next figure shows the spatial distribution of those peaks:

In the two upper rows, one sees that consistently for Bouvet-Mermoz and Avitabile the first blob (slightly lower AGB) is in the center of the equatorial region around the Congo river basin while the spatial distribution for the highest AGB blob surrounds the first one. This bi-modal behavior is not seen for the high AGB values in the Saatchi and Baccini datasets, where the whole equatorial forest shows more homogeneous distribution with similar values in the two regions. Definitely, L-VOD seems to be in more agreement with the two latter datasets, unless the high AGB blobs in Bouvet-Mermoz and Avitabile are more realistic and in this case, L-VOD would show signs of saturation since, it remains basically constant. This is the same discussion already done when commenting the scatter plots. Thus, we reckon that it is not necessary to add anything to a revised version of the manuscript. In any case, to our knowledge, it is not easy to say which of the four AGB datasets is more realistic in the densest parts of the equatorial forest.

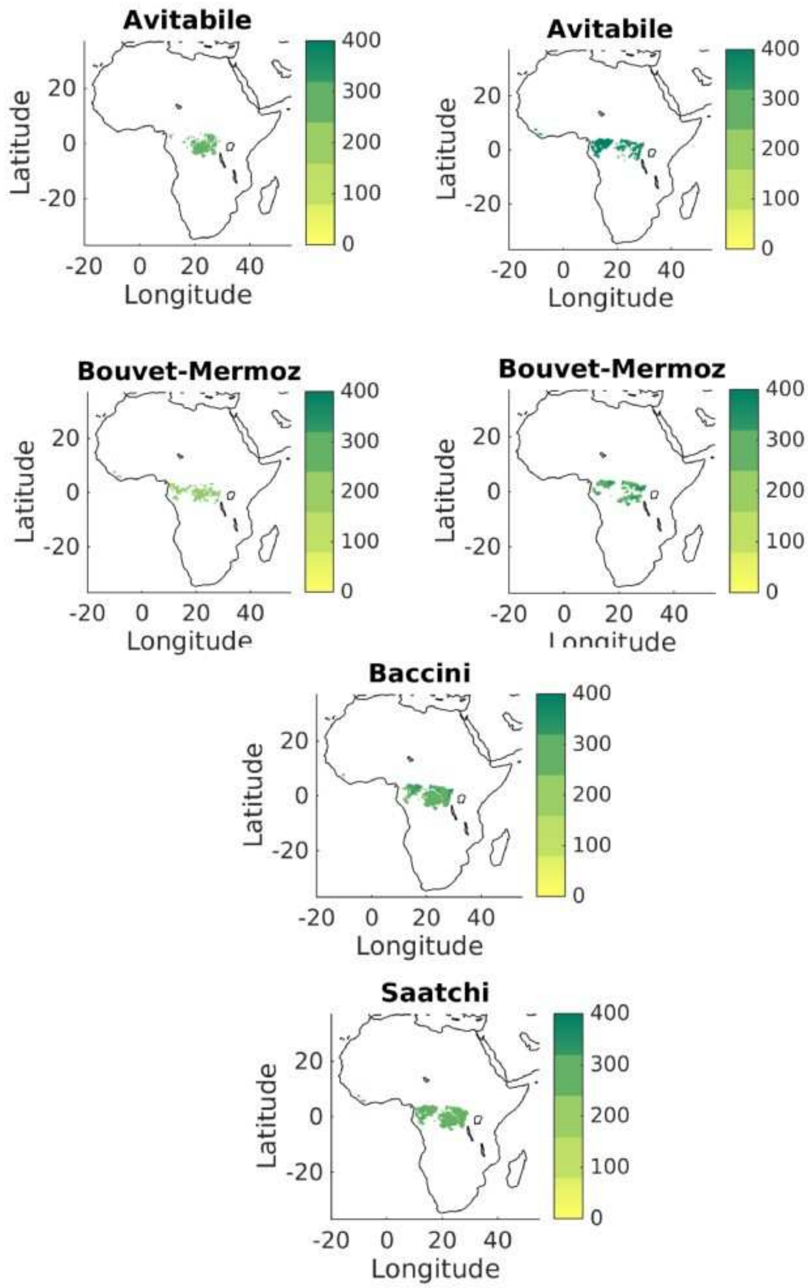

Note that the spatial distributions shown in the previous figures are not an artifact arising from the spatial averaging of the AGB to the SMOS resolution. If one plots the AGB data at the original resolution the differences are clear. See for instance in the next two figures that the Baccini original data (upper figure) is much more homogeneous than the Avitabile data (lower figure).

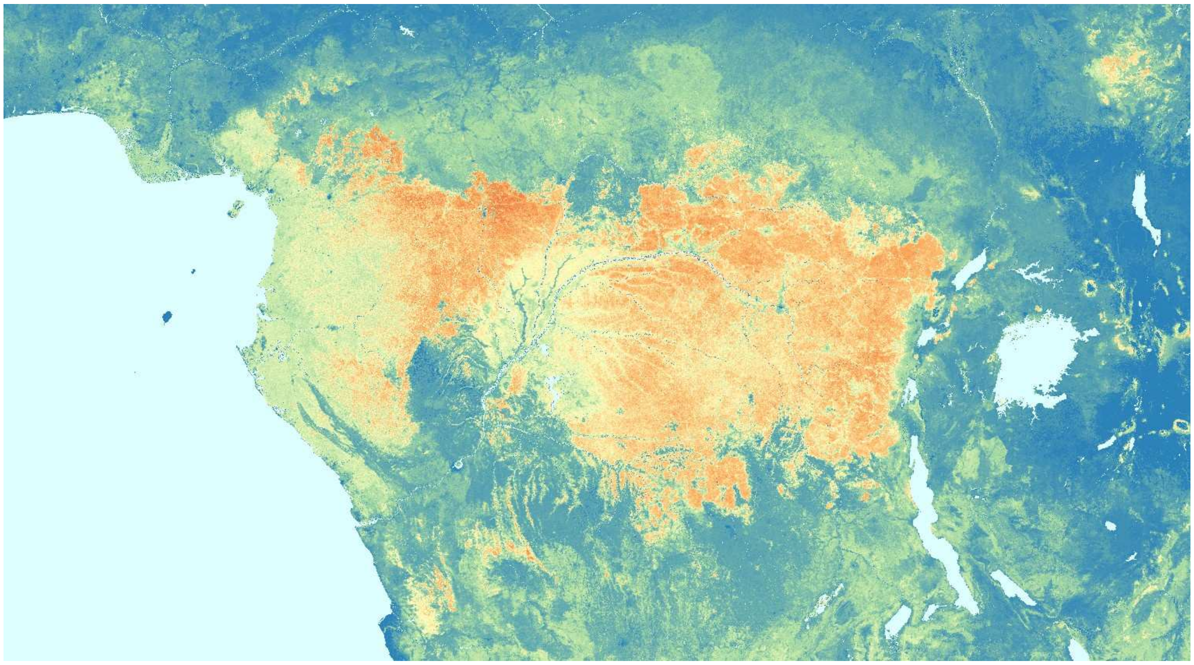

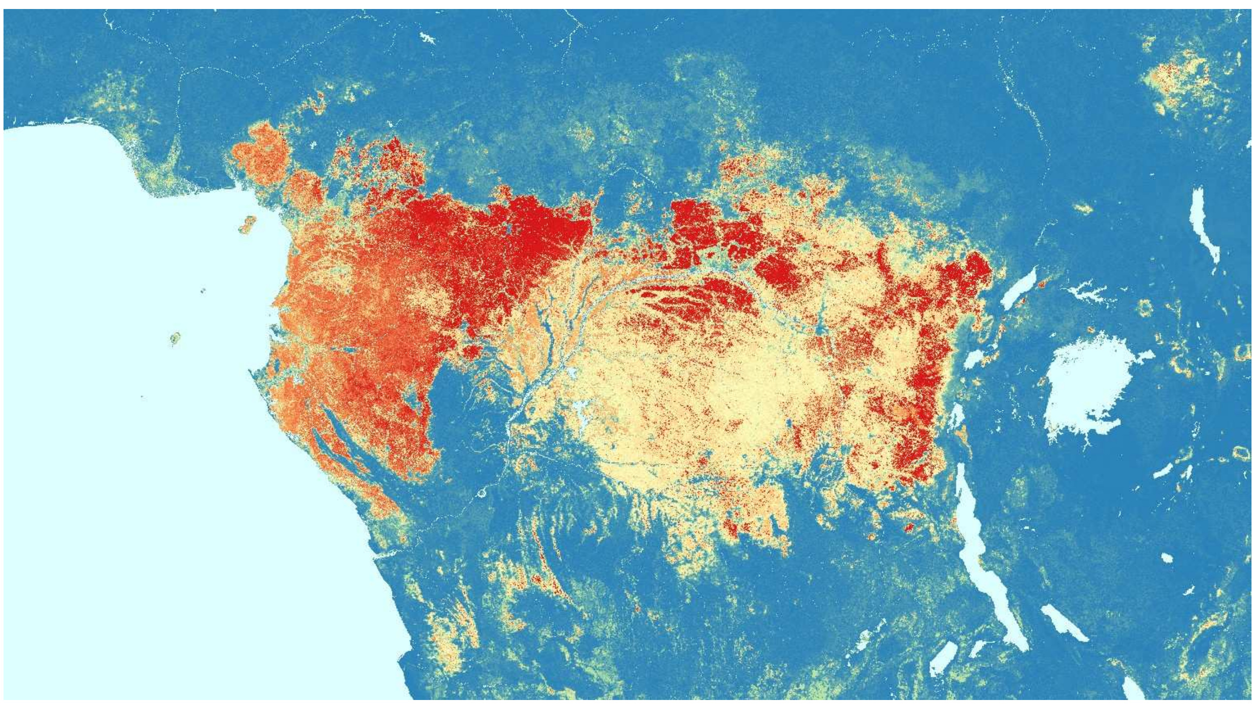

26. Page 9, line 22. It seems to me that also Saatchi shows a very low dispersion for low AGB values, but the plot is too small. Please, address.

That's true. Together with Bouvet-Mermoz, the Saatchi dataset show the highest correlation values with respect to SMOS L-VOD. In Fig. S6, one can see that correlation coefficients obtained with Saatchi's data are somewhat higher than those of Bouvet-Mermoz for low vegetation but lower for Savannahs. For woody savannah the situation is more complex for the mixed nature of this biome and because in the Bouvet-Mermoz datasets uses the Mermoz law for pixels classified as dense forest on the ESA CCI land cover dataset. Pixels classified as woody savannah using IGBP at the SMOS resolution can contain both woody savannnah and dense forest in the ESA CCI dataset. The scatterplot for woody savannah using the Bouvet-Mermoz dataset show these two populations for high L-VOD values, which decreases the Pearson correlation (which is lower than that obtained for Saatchi in woody Savannah) but still, Kendall and Spearman correlations are higher for the Bouvet-Mermoz dataset. A detailed discussion on the results for each AGB data set has been added to the new section 4.3.1

27. Page 9, line 29. The authors aggregate the data sets in two groups of biomes. This separation should be further justified. Also, there are many results shown in the supplementary material that are relevant and should at least be discussed in the text.

From this and comments from the other reviewers it is clear that the discussion in the main body on the manuscript with only two groups of biomes and more details in the supplementary information was misleading. Now the new Figures 6 and 7 show the results for all the biomes and they are is discussed in detail in the new sections 4.3.1 and 4.3.2.

28. Section 4.9. I would suggest the authors to include a box plot with the SMOS IC VOD results per land cover. It will give a general idea of the dispersion and the mean values of VOD per land cover. Perhaps it would also be good to show the box plots for the AGB data sets.

There is not section 4.9 and it is not fully clear to us what the reviewer is suggestion. Making box plots showing the distribution of LVOD for different land cover classes? We reckon that this will not add much information as the distribution can be seen also in the scatterplots per land cover class. Maybe he/she is proposing something else ?

29. Section 5. It would be nice to add a discussion on the consistency of the four AGB data sets and on why best correspondence is found between L-VOD and the approach of Saatchi (and not the one of L-band SAR).

We do not think that one can summarize the results of this study saying that the correspondence of L-VOD and AGB is better with Saatchi AGB. Figures 6 and 7 clearly shows this. All AGB datasets except that of Avitabile performs the best, comparing to L-VOD, for a few land cover classes. This is now discussed in detail in Sect. 4.3.1.

We thank the reviewer for the suggestion of developing this point in the discussion section. In the new version, it has been done in Sect 5.3

L-Band radar observations are thought to be very sensitive to biomass variations, in spite of a significant sensitivity to soil moisture as well. The high correlation with SMOS L-VOD, also at L-band, would confirm this fact. The strange behavior of Avitabile AGB probably comes from the fact that it is pure data driven method and that it is therefore very sensitive to the data used to train the method. In their training database, high AGB plots could be over-represented. Finally there are also some discussion on the peculiar Baccini AGB/LVOD relationship, which is the less non-linear one.

30. Figure 3. It would be interesting to know the number of pixels in the two groups of biomes, and whether they are balanced. Are all the correlation significant? To what level? This is important information that should be included either in the figure or the text.

The number of grid points in the two groups of biomes it is, of course, not the same. That is not the point here, the point is that groups from grassland, croplands, savannah and woody savannah show a similar slope, much lower than that of the equatorial forest therefore they were grouped in two groups because they show two "regimes" of the AGB vs L-VOD relationship. However, to avoid misunderstandings, the new Fig. 6 and 7 and Sect. 4.3.1 and 4.3.2 show/discuss all the biomes independently. All correlations are significant with very low P-values (<0.05).

31. Page 10, line 3. The authors should comment on the slope of NDVI per land cover and most relevant aspects shown in the supplementary information.

NDVI and EVI were added to the new Fig. 7. It is worth noting that, in contrast to AGB, the slope of the relationship decreases from low vegetation types to savannahs and dense forest as the optical/infrared indices saturates. It is noteworthy that no significant difference is seen on the behavior of EVI and NDVI for high L-VOD values. This is discussed in Sect. 4.3.2

32. Page 10, line 17. Please, specify which part of the supplemtary information is being referred to here.

The sentence was removed as the corresponding information was moved to the main document and discussed in detail there.

33. Figure 4. Legend reads "C/X VOD" but caption reads "K/X/C VOD". Please correct.

Thanks for pointing this out. The legend should actually show "K/X/C VOD". Corrected in new Fig. 8.

Referee # 2

The study is aimed to introduce the sensitivity of the vegetation optical depth (VOD) at L band to the biomass. Different SMOS datasets, produced by different algorithms, are compared to some above ground biomass (AGB) datasets over Africa. The analysis is carried out to show the higher correlation of the L band VOD with respect to higher frequencies VOD and optical vegetation indices. The paper also presents the correlation of the SMOS VOD with other parameters like tree height and cumulated precipitations.

We thank the reviewer for his/her constructive comments.

General comments:

The study's goal is well defined in the paper introduction where the authors claim that the retrieval of the VOD at L band can provide an important tool for the monitoring of the vegetation properties at large scales. In the first section of the manuscript is highlighted that, besides optical measurements, passive microwave observations acquired by the SMOS radiometer can provide an important complementary information to infer the state of vegetation. Here, several references are correctly reported to introduce the study and it is emphasized how the L band observations are less attenuated through the vegetation canopy. Therefore, L band VOD is expected to sample the vegetation layer up to higher biomass values compared to higher frequency observations. This aspect represents the key point of the manuscript and it is supported by the figure 4 of the results section. Anyway, just few comments are deserved to this point while a deeper explanation of the high sensitivity of the L band should be provided in the last section of the results.

First, following these comments and comments by reviewer #1, we have improved the presentation and the explanation of former Fig. 4, which became Fig. 8. Former Sect 4.4 was moved to the discussion (new Sect. 5.2) as the description of this figure, in particular using the curves of Fig S4 by Liu et al. 2015 is basically a discussion of new results on L-VOD/AGB with respect to published results by Liu et al. And we would like to avoid misunderstandings on this point. The new figure has two panels. In the left panel L-VOD and NDVI were normalized to 1 using their maximum values. This is needed to plot the two quantities in the same figure. In the right panel, L-VOD and K/X/C-VOD relationship to Saatchi AGB are shown without using any normalization, because they span basically the same range and following comment 2 by reviewer 1, we want to emphasize that the curves plotted here for the K/X/C-VOD are just those of Figure S4 from Liu et al., which were computed using Saatchi AGB and the same method that we used in the current study. Liu et al fitted their relationship using K/X/C-VOD data in the period 1998-2002 and Saatchi data acquired from 1995 to 2005 (page 6 of their supplementary information document). The fact that the dates of the different datasets vary is reminded explicitly in the text. We also remark that the non-linearity of the curve and the difference sensitivity to high AGB from different frequencies is driven by the high AGB values in the dense equatorial forest, which is not supposed to vary strongly in a few years time.

Finally, as suggested by reviewer #2, we remind that the different shapes of L-VOD vs AGB and K/X/C-VOD vs AGB curves in agreement with what it is expected from the radiation transfer theory (Wigneron et al. 1995, 2004, Ferrazzoli and Guerriero 1996) and previous results on L-VOD and X/C-VOD comparison by Grant et al. 2016 and Vittucci et al. 2015 (already cited in first paragraph of page 3). For instance, the right panel of the figure below clearly shows that for a given AGB, L-VOD is lower than VOD at higher frequencies, as expected. This facts were added explictly to the text discussing the new Figure in Sect. 5.2

Moreover, it seems that the presented research is a progress of a previous work in which some of the authors have already addressed the topic in 2016, including some results about the SMOS VOD sensitivity to tree height and AGB. I would suggest citing also this preliminary study in the introduction (doi 10.1109 / IGARSS.2016.7730383).

This research took, of course, as starting point a literature review and we tried to cite since the introduction all previous relevant studies. For instance, results about the SMOS VOD relationship to tree height were shown by Rahmoune et al. 2014 and Vittucci et al. 2016 (RSE 180). This last paper also included some results with respect to AGB. Both references are cited and commented in the manuscript. The conference contribution cited by the reviewer corresponds to the Vittucci et al. 2016 RSE paper. We reckon that there is not need to cite a conference paper with preliminary results when the full study has already been published in a peer-review journal.

Another general concern it is related to the use of three different VOD datasets derived from the SMOS data (L2, L3 and SMOS IC) that could confuse the reader.   In my opinion, this point of view is interesting but can defocus the attention from the study objective, that it is claimed in the manuscript title. In some parts of the article it seems that too much importance is given to the intercomparison of the different VOD retrieval algorithms, instead of supporting the relevance of the VOD at L band for AGB monitoring. Furthermore, a potential user of SMOS data, could ask himself what is the product to adopt between the L2, L3 and SMOS IC for vegetation monitoring, since the strengths and weaknesses of the different approaches can be highlighted more clearly. A suggestion to address this point could be to provide a general overview of the specific aims of the different products and maybe to update the title of the research to highlight that different L-band products are compared.

Title: referee #1 did also think that the title should be changed. Therefore, we decided to change the title to:

An evaluation of SMOS L-band vegetation optical depth (L-VOD) data sets: a high sensitivity of L-VOD to above-ground biomass in Africa

Comparison of SMOS L-VOD products: we agree completely with the reviewer, that is the reason we added most of the results on SMOS L2 and SMOS L3 as supplementary information. We will leave those Figures and the table summarizing the differences in the supplementary information. The Table has been improved with information on single scattering albedo and roughness parameters for the three approaches as recommended by reviewer #1 and by reviewer #2, here below.

In addition, lines 2-8 of page 4 were be moved before Sect. 2.1.1 to strength that those details are common to the three algorithm and so to focus Sects 2.1.1-2.1.3 on the differences.

Furthermore, the presentation of the results for different SMOS L-VOD data sets in Sect. 4.1 has been developed adding the discussion on Spearman and Kendall rank correlation values as follows:

The rank correlation values with respect to all the evaluation datasets are also higher for IC L-VOD (rho 0.78-0.91, tau 0.61-0.75), followed by L2 L-VOD (rho 0.67-0.83, tau 0.50-0.65) and L3 L-VOD (rho 0.66-0.80, tau 0.49-0.62). These results are in agreement with those obtained with the Pearson correlation and imply that the lower Pearson correlation values obtained for the L3 and L2 datasets are not due to a correlation that could be better but more non-linear than that of the IC dataset. Therefore, using eight vegetation-related evaluation data sets and three different metrics, the most consistent SMOS L-VOD data set is SMOS-IC. This result implies that, currently, the SMOS-IC dataset is the best SMOS L-VOD product to perform vegetation studies, and the rest of the current study will focus on SMOS-IC L-VOD.

We hope that a potentially interested reader asking himself what is the product to adopt between the L2, L3 and SMOS IC for vegetation monitoring would have a clearer statement to make a choice.

The relevance of L-VOD for AGB monitoring is addressed in the rest of Sect 4 and in the new Sect. 5.

Despite these general issues I believe that the topic is relevant, the results are obtained with a sounding scientific approach and the supporting figures and tables are clear. Therefore, I would recommend the paper for publication after a careful revision process.

We thank the reviewer for these encouraging comments.

Specific comments:

In the section 2, “Data”, is introduced the SMOS mission and the three different algorithms, considered to retrieve the L band VOD from the SMOS brightness temperature. At line 28 of page 2 is stated that only ascending orbits are considered in the study but the declaimed better overall quality of ascending pass acquisitions appears not justified. Therefore, the authors should provide a better explanation about this important constrain.

It is not really a constrain. The results do not depend significantly on the year or the type or orbits used as reference. The shape of the scatter plots is very similar using data for next years. See for instance the next figure and compare to Fig S3.

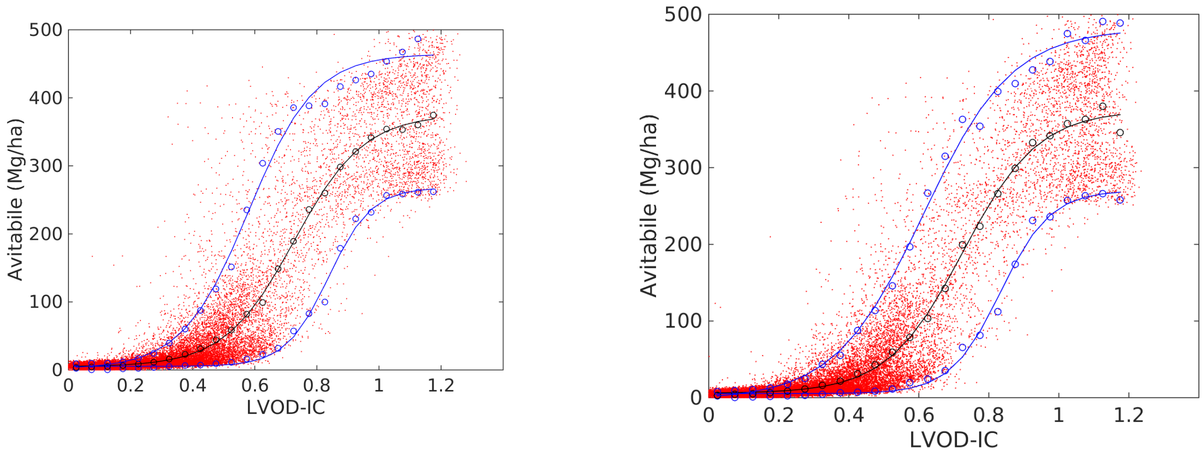

Fig. Left : 2012 Ascending orbits. Right: 2012 Descending orbits

The next table shows the parameters of the fits using ascending or descending orbits in 2012. The values can be compared to those of Table S2. They have almost the same numeric values.

AGB	Year	Orbit	curve	a	b	c	d	R^2
Avitabile	2012	A	05th	262.697	14.406	0.838	5.347	0.99548
Avitabile	2012	A	Mean	370.615	8.920	0.727	4.915	0.99917
Avitabile	2012	A	95th	462.962	9.398	0.580	1.613	0.99243
Saatchi	2012	A	05th	333.496	4.642	0.906	-3.338	0.99080
Saatchi	2012	A	Mean	280.675	6.686	0.684	14.439	0.99334
Saatchi	2012	A	95th	291.444	9.661	0.545	32.436	0.99372
Baccini	2012	A	05th	497.748	2.673	1.024	-41.748	0.98810
Baccini	2012	A	Mean	414.033	3.503	0.717	-27.346	0.99882
Baccini	2012	A	95th	383.823	4.950	0.550	-1.911	0.99757
Bouvet-Mermoz	2012	A	05th	292.291	4.800	0.963	4.717	0.97445
Bouvet-Mermoz	2012	A	Mean	319.123	5.261	0.760	7.879	0.99616
Bouvet-Mermoz	2012	A	95th	358.172	7.290	0.581	17.621	0.99226
Avitabile	2012	D	05th	264.867	13.984	0.833	5.353	0.99548
Avitabile	2012	D	Mean	368.991	9.271	0.726	5.795	0.99765
Avitabile	2012	D	95th	483.476	7.893	0.614	-2.245	0.99585
Saatchi	2012	D	05th	332.540	4.976	0.890	-5.476	0.99111
Saatchi	2012	D	Mean	287.547	6.436	0.691	12.981	0.99499
Saatchi	2012	D	95th	291.493	8.979	0.543	30.449	0.99324
Baccini	2012	D	05th	606.345	2.250	1.168	-53.195	0.98742
Baccini	2012	D	Mean	398.354	3.688	0.706	-21.945	0.99806
Baccini	2012	D	95th	379.008	5.076	0.567	6.162	0.99538
Bouvet-Mermoz	2012	D	05th	308.430	4.441	0.965	0.250	0.98165
Bouvet-Mermoz	2012	D	Mean	317.532	5.425	0.764	10.022	0.99729
Bouvet-Mermoz	2012	D	95th	375.791	6.420	0.604	12.619	0.99451

Therefore, there is no real impact of using just one year or using ascending or descending orbits. However, in a revised version of the manuscript we used two years of data both for ascending and descending orbits. The results will not change but they would look more robust to the reader. See also answer to General Comment 3.

In the following subsection are introduced the ESA L2 algorithm, the CATDS L3 algorithm and the INRA-CESBIO algorithm that were applied to obtain three different L band VOD data sets. If the Authors are inclined to stress the intercomparison between the outcomes of the different retrieval approach, a deeper discussion about the different algorithm could be effective to introduce the subsequent results, i.e. figure 1 and table 1. This choice, could be a good solution to solve some ambiguities between the study aim, as claimed on the paper title, and the interesting overview of the different algorithms performances. Anyway, a better explanation on the assumptions (i.e. soil roughness and albedo) under which the three different algorithms are based should be provided.

Thanks for pointing this out. This point has also been raised by referee #1.

In a revised version, first, the albedo will be cites earlier since the introduction citing presenting the tau-omega model. Therefore, the lines 10-14 of page 2 :

In the presence of vegetation, part of the soil emission is absorbed and scattered. This extinction effect is parameterized by the vegetation optical depth (VOD) that can be estimated using radiative transfer theory […] Wigneron et al. 2007).

were rephrased to:

In the presence of vegetation, part of the soil emission is absorbed and scattered. These effects can be parameterized using radiative transfer models such as the so-called tau-omega model (Refs), were tau is the optical depth and omega is the single scattering albedo. Tau was shown to be linked […] Wigneron et al. 2007). Therefore, tau is commonly known as Vegetation Optical Depth (VOD).

Regarding the actual values used for different SMOS product, the information was added more clearly in Sect. 2 and in Table S1. For SMOS IC the roughness and single scattering parameters are assigned per IBGP classes, based on Parrens et al. (2017a, b), and are averaged per pixel according to the fraction of classes present in the pixel (Fernandez-Moran et al. 2017).

For SMOS L2 and L3 algorithms, single scattering albedo and roughness values depend on the surface type and are taken from literature and/or specific SMOS studies. For low vegetated area the single scattering albedo is set to 0 and roughness set to 0.1. For forested areas the single scattering albedo is set to 0.06 for tropical and subtropical forest and 0.08 for Boreal forest and roughness set to 0.3 (Rahmoune et al. 2013,2014, Al Bitar et al. 2017).

Marie Parrens, Jean-Pierre Wigneron, Philippe Richaume, Ahmad Al Bitar, Arnaud Mialon, Roberto Fernandez-Moran, Amen Al-Yaari, Peggy O'Neill, and Yann Kerr, 2017. Considering Combined or Separated Roughness and Vegetation Effects in Soil Moisture Retrievals, International Journal of Applied Earth Observation and Geoinformation 55, 73-86.

M. Parrens, A. Al Bitar, A. Mialon, R. Fernandez-Moran, J.-P. Wigneron, P. Ferrazzoli, and Y. Kerr, 2017. Estimation of the L-band Effective Scattering Albedo of Tropical Forests using SMOS observations, IEEE GRS Letters 2017, 14, 1223-1227

After the introduction of the VOD datasets the different benchmark sets are presented. In the section 2.2.1 it is introduced the Worldclim data set, that is used to infer the relationship between the L band VOD and the mean annual precipitation. This analysis seems meaningless since, as it is reported at line 15 of page 5, the considered precipitation is extracted from a dataset ranging only between "1970-2000". This point should be clarified also considering that the relationship between the precipitation and the VOD are not well commented in the paper.

The new Fig. 7 shows the relationship of mean annual precipitations and L-VOD and the results are discussed in Sect 4.3.2. The regime of precipitations can be a driver of the vegetation growth. Thus, we show that there are basically two regimes. In the first one, as precipitation increases the amount of vegetation as traced by AGB maps, VOD or NDVI/EVI increases. In contrast, there is threshold of ~1500 mm/year over which AGB, VOD and NDVI are decoupled from the amount of the annual precipitations.

In the section 2.2.4 are presented the different AGB datasets considered as benchmarks. Here the sentence "This study used four static AGB benchmark maps (Baccini et al., 2012; Saatchi et al., 2011; Avitabile et al., 2016; Bouvet et al., 2018) each with specific strengths and limitations to assess L-VOD's ability to reflect aboveground biomass in different" is questionable and not well supported by the results. In particular, the Avitabile dataset is obtained by the fusion of the Baccini and Saatchi maps through a machine learning approach and it is proved to outperform the previous datasets in terms of retrieved AGB accuracy. The Authors should argue better the aspects related to the analysis carried out with these three different AGB data sets. On the contrary the consideration of the Bouvet dataset is very interesting and should be emphasized.

We are afraid we disagree. We do not see clear evidence that the Avitabile “outperforms” any other AGB dataset. We do think that AGB estimation from remote sensing measurements is complex and the errors of different retrieval methods are not easy to characterize. The fact that the Avitabile dataset is so different to both the Baccini and Saatchi maps used as input is actually puzzling, for instance the sharp decrease AGB from the Equatorial region with distance is not seen in any other AGB map. The Avitabile method can be biased to high AGB values because most of the plots used as reference are in dense forest. Furthermore, a totally independent observable such as L-VOD shows clear relationships for low AGB for all the datasets but Avitabile.

Otherwise, the analysis is performed in exactly the same way for all AGB datasets and in more detailed way in new Fig. 6 and Sect. 4.3.1 : The best correlations of AGB and L-VOD are found with (i) Bouvet-Mermoz for Shrublands and Savannahs (ii) Baccini for croplands and equatorial forest (iii) Saatchi for grasslands. Regarding natural vegetation and woody savannah the correlation values obtained with Saatchi and Baccini are very similar. One should note that correlation values obtained with Bouvet-Mermoz for woody savannah are degraded to the fact that for the highest values of AGB found in this class, at the SMOS resolution, the AGB estimation is a mix of Bouvet and Mermoz approaches. Therefore, all AGB datasets except that of Avitabile performs the best for a few land cover classes.

Interpreting where do this differences come from is not easy but an attempt is done in the discussion (Sect. 5.3). Radar observations in low vegetation regions such as shrublands and grasslands are thought to be very sensitive to biomass variations, in spite of a significant sensitivity to soil moisture. The high correlation of the two AGB maps mainly based of radar data (Saatchi and Bouvet-Mermoz) with SMOS L-VOD in grasslands would confirm this fact, as the high correlation in shrublands for Bouvet-Mermoz. The scatter plot found with Avitabile for woody-savannah shows a bimodal distribution that looks like an overlay of the scatter plot obtained with Baccini and the scatter plot obtained with Saatchi. The low AGB vs L-VOD slopes obtained for low vegetation classes, significantly lower than those found with the original Saatchi and Baccini datasets, are rather difficult to understand. The strange behavior of Avitabile AGB probably comes from the fact that it is pure data driven method and that it is therefore very sensitive to the data used to train the method. In their training database, high AGB plots could be over-represented. In addition as mentioned above, the distribution of Baccini AGB for woody savannah is significantly different to the other datasets, which much higher values.

In the Results section it should be provided a deeper explanation of the research outcomes, in particular the scatterplots reported in figure 2 need to be better commented.

We agree. We have realized from comments by Referees #1 and #2 that the explanation of the results should be improved. Therefore, as already mention in the answer to the previous comment, former Fig 2 and Fig. S6 were removed an replaced by Fig. 6 and 7 and discussed in detail in Sect. 4.3.1 and 4.3.2.

Anonymous Referee #3

The paper provides evidence that the vegetation optical depth VOD derived from passive microwave satellite data at L-band frequency has strong correlation with the above-ground biomass and can be used to monitor vegetation status. The paper is well-written and the methodology and results are sound and at the same intriguing, suggesting VOD as a potential satellite derived parameter to explore in future studies. I recommend the paper for publication but I have few suggestions and recommendations that may help improve the interpretation of the results before final publication of the paper.

We thank the reviewer for his/her encouraging comments

1. The paper does not provide a strong motivation of what VOD can be used for. Vegetation aboveground biomass is one of the most important global ecosystem variable for carbon cycle and climate mitigation. However, the strong correlation of VOD with biomass does not necessarily mean VOD from passive microwave at approximately 0.5-degree resolution is useful for biomass estimation or monitoring. VOD can be used to monitor vegetation water content at regional scales given its coarse resolution and frequent observation. I would like to suggest that although the authors correlate the result with biomass, they emphasize the use of VOD for monitoring vegetation water content. Biomass and water content are similar in magnitude with biomass being more static and water content more dynamic.

Examples of the use of VOD for vegetation, in general, and AGB monitoring, in particular, are given in the introduction. We do think that VOD, in particular L-VOD is useful to monitor the temporal evolution of AGB at a lower spatial resolution but with a higher temporal resolution than other types of observations at least until the launch of the ESA Biomass mission, whose goal is to produce a global biomass map twice per year. Liu et al. 2015 have provided a very good example on how L-VOD can be used to study the evolution of global carbon stocks. We do think that all this pieces of information are already in the manuscript since the abstract and the introduction. However, a very recent good example by Brandt et al. (2018) has been added to the introduction (line 16 page 2).

Regarding the use of VOD to monitor the VWC, the reviewer is right. Everything depends on the temporal scale of the study. The current manuscript being devoted mainly to AGB, long times periods were used. Studying the evolution of VWC requires to use much shorter time scales and it is an on-going work for a dedicated study. We agree that this was not fully explicit in the manuscript. In addition, a few important references were lacking:

Konings, A. G. & Gentine, P. Global variations in ecosystem-scale isohydricity Global change biology, Wiley Online Library, 2017, 23, 891-905

Li, Y.; Guan, K.; Gentine, P.; Konings, A. G.; Meinzer, F. C.; Kimball, J. S.; Xu, X.; Anderegg, W. R.; McDowell, N. G.; Martinez-Vilalta, J. & others Estimating Global Ecosystem Isohydry/Anisohydry Using

Active and Passive Microwave Satellite Data Journal of Geophysical Research: Biogeosciences, Wiley Online Library, 2017

Therefore, the new introduction adds the following information (*Lines 24-26, page 2*:

The VOD has also been used to study the VWC and variations in ecosystem-scale isohydricity (Konings and Gentine, 2017; Li et al., 2017).

and

Since this study is mainly devoted to AGB, long time averages (typically annual) will be used. Studying the evolution of VWC would require to use much shorter time scales. Lines 31-32, page 3

2. The method says: “The main evaluation strategy used in this study is to spatially compare L-VOD to the evaluation data set.” Although the pixel values are extracted from all the data sets to compare. However, this is not a spatial analysis because the spatial information almost disappears in the correlation studies. Unless a specific spatial correlation model was used to capture the pattern. Some of the vegetation classes are separated that can help with spatial variation of the data sets but again this is only a simple correlation study and does not include spatial analysis of data sets.

We agree. “Spatially” can be misleading. It was removed.

3. Figure 2. The density scatter plots with multiple parameters show that there is a strong relationship between VOD and all the parameters. Some of the most interesting ones are the optical data and precipitation showing a strong saturation with respect to VOD suggesting that VOD can be used as a complementary measurement to look at the vegetation. Wavelength is probably the most powerful aspect of the VOD measurements compared to optical data. If VOD correlated with EVI and NDVI over the entire range, then the interpretation of VOD could’ve been more difficult. I recommend the authors discuss this in the paper.

Following different reviewers comments, Fig. 2 and Fig. S6 were removed and replaced by Figs. 6 and 7, which are discussed in Sect. 4.3.1 and 4.3.2. Optical indices and precipitations are now discussed in Fig. 7 and Sect. 4.3.2.

The complementary of L-VOD with respect to NDVI and EVI is clear as both saturates strongly. In addition, it is interesting to remark that there are no significant differences in between NDVI and EVI, even if EVI is supposed to be more sensitive than NDVI to high AGB.

Regarding precipitations there are basically two regimes. In the first one, as precipitation increases the amount of vegetation as traced by AGB maps, VOD or NDVI/EVI increases. In contrast, there is threshold of ~1500 mm/year over which

AGB, VOD and NDVI are decoupled from the amount of the annual precipitations. This is discussed in the last paragraph of Sect. 4.3.2

4. The relationship between VOD and biomass from different products are interesting. The fact that L-band VOD does not show a clear saturation with biomass may be due to:

a. 1. At very coarse resolution (40-50 km), the variations of forest biomass on the landscape is dominated with the landscape heterogeneity. Larger heterogeneity (e.g. forest/non-forest mixture) will improve the relationship of VOD with biomass. This may mean that the VOD is also co-varying with the vegetation cover. In fact, the straighter relationship with Baccini data is the artifact of this effect. Baccini biomass is strongly correlated with MODIS VCF (vegetation continuous field) data and therefore causes a more linear relationship. Whereas other maps and including the vegetation height from Simard do not show this linear relationship. There is no reason for VOD and biomass to have a linear relationship. I recommend the authors discuss this point and may even include the MODIS VCF product as a layer similar to NDVI in the mix.

At *all* spatial resolutions the sensor output is a weighted average of the signal within the radiometer footprint or the CCD pixel and the instrument response. Since most of the time it is impossible to deconvolve the instrument response function and the function giving the 2D distribution of the signal, the physical parameters retrieved from the sensor output are “effective” values within that footprint or pixel. They are not independent of the 2D distribution. That said, we would like to remind that SMOS is sensitive to forest and non-forest biomass and that due to the long wavelength L-VOD samples “volume” biomass and not just the 2D distribution.

To get further insight into this questions, the reviewer suggestion of using MODIS VCF is a valuable one, and we will certainly process that data for subsequent studies. For the present study, for simplicity, we have preferred to compute the forest fraction from ECOCLIMAP because it is provided with some SMOS products such as the L2 and L3 datasets as the “FFO” parameter. FFO is the fraction of forest within the SMOS footprint computed from the 1 km ECOCLIMAP dataset. The following figure shows the SMOS IC L-VOD as a function of the fraction of forest cover from 60% to 100 %. The distribution shows two structures. In a first structure, the VOD varies from 0.2 to ~0.7 for those FFO values, showing a very small sensitivity to the exact value of the fraction of forest (small slope) because VOD does not only depend on the fraction of forest but also on the type and the properties of the vegetation within that fraction (and on the low vegetation present outside the forested cover fraction). For instance, it is possible to have almost 0.6 of L-VOD with FFO of 60 % and values as “low” as 0.4 for FFO of 100 %. The second structure also illustrates this effect, it is the high L-VOD (>1) peak for FFO 90%-100%. This is the same peak seen in the scatterplots with respect AGB and that corresponds to the equatorial forest, for which the L-VOD is higher than for other types of forest with the same cover fraction. This confirms, that even there is a relationship of the 2D forest fraction and L-VOD, forest fraction is not the main driver of L-VOD values.

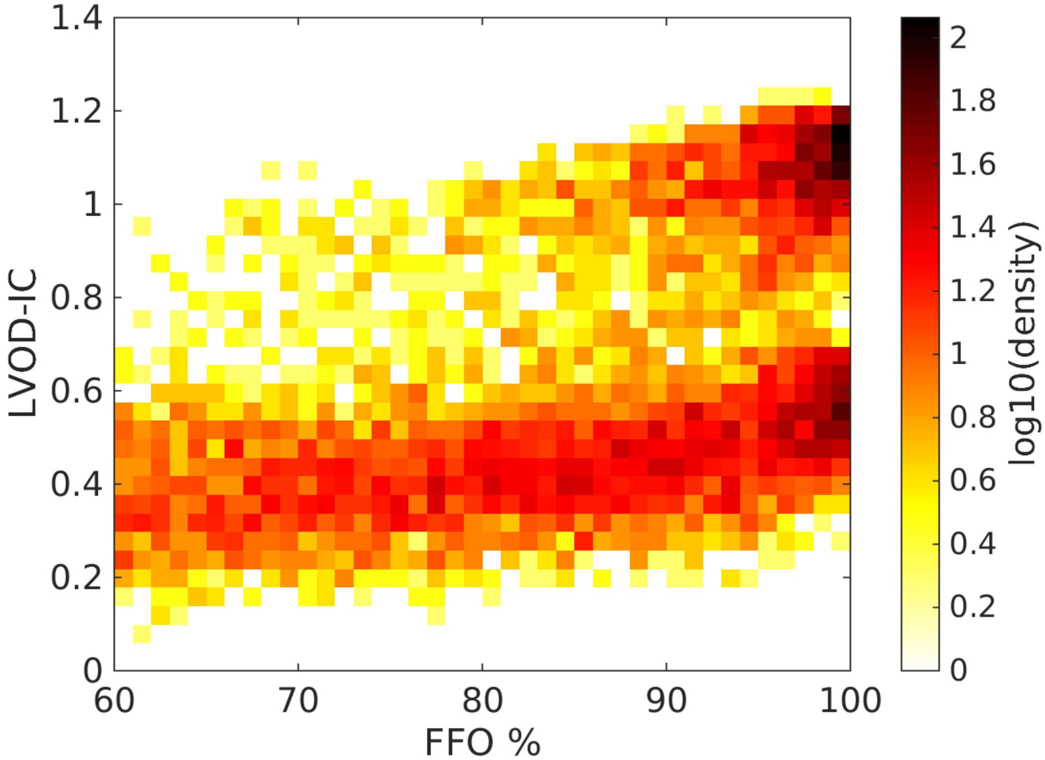

Coming back to Baccini AGB/L-VOD, even if variations of forest biomass on the landscape partly depend on the fraction of forest within the footprint but this cannot explain a close to linear relationship to Baccini AGB because the analysis was done consistently for all AGB datasets and the LVOD/AGB relationship with other datasets is much more non-linear. Therefore, the explanation should come from the Baccini dataset.

First, we would like to point out that analyzing the VOD-Baccini AGB per land cover class, the slopes change significantly. The reason that the global relationship looks close to linear is the high slope of the VOD-Baccini AGB relationship in woody Savannahs, which is close to that in evergreen broadleaf forest. With respect to the other three AGB datasets, the Baccini AGB dataset seems to overestimate AGB in woody savannahs with values of ~ 50 Mg/h for LVOD 0.2 to ~130 Mg/h for LVOD 0.6, while the regression lines for the other datasets show values lower than 100 Mg/h. However, unfortunately, the origin of this possible overestimation is not clear but it could be related to the processing done by Baccini to estimate AGB in this mixed land cover class (30%-60 % of forest). Which, as the reviewer says, uses only MODIS and cloud estimate an unrealistic (larger) forest covert fraction. The fact that Bacinni AGB shows a linear relationship with tree height is puzzling and not present in other datasets (Fig. S4) not expected from allometric relationships. This is commented in the new discussion section 5.3.

b. At coarse resolution, the global biomass values are much smaller on the average. Biomass at 1-ha can reach a very large number at some ecosystems. However, at 40 km as it is mixed with the heterogeneity the average is almost smaller. This is one more reason for better sensitivity to biomass. However, it would be interesting to focus on different range of biomass with VOD.

We refer to the answer to comment 4.a.1 regarding the sensitivity to biomass and heterogeneity.

Regarding the analysis for different ranges of biomass and VOD, we refer to the answer to comment 3 and to the discussion of the new figures 6 and 7. As now all biomes are treated independently, all different ranges of biomass and VOD are discussed independently.

c. Over Africa, all dense tropical forests are clustered around 300 Mg/ha of biomass on the graphs in figure 2. If the goal of the paper is sensitivity to biomass, it may not be a bad idea to separate areas of up to 150 Mg/ha that includes the first cluster from the second cluster and study it separately. The binary feature of biomass in Africa, from woodlands to dense humid tropical forests in area may introduce a false strong correlation with biomass that need to be discovered further. Figure 3 is supposed to show this effect. However, the authors mix this up with precipitation and NDVI and only show the result from Bouvet. It would be good to show this for all biomass maps so the variations of the relationships are discussed.

The referee is fully right, Figure 3 and Figure S6 were supposed to show that effect. Taking into account some comments from several reviewers, and as stated in the answers to comments 3 and 4.b, the former Figs. 3 andS6 were removed and the two new figures 6 and 7 are discussed in the main document showing all AGB datasets and not only Bouvet-Mermoz. The results are commented in Sect 4.3.1 and 4.3.2 and discussed in Sect 5.

We are confident that the new version with these figures is clearer and it address the concern raised here by the referee. In the new figures, it is possible to see that L-VOD and AGB correlation exist within each land cover class and not only when all classes are shown together.

d. Although the paper is written for the biogeoscience community, it would be important for the authors to provide some explanation of why L-band data from passive measurements may have better relations with biomass compared to active measurements at the same frequency.

Currently we do not have any clear evidence showing that passive L-band data may have better relations with biomass than active L-band data. We do not think we suggest this in the manuscript. The main reason is that all AGB maps used come from active observations. Fully independent AGB estimations as for instance from in situ estimations of AGB would be needed to address that question by comparing to both active and passive L-band observations. But due to the very different spatial resolution of active and passive instruments this will be very challenging.

e. How different are the relationships between VOD and different biomass maps and how can the difference be interpreted?

The best correlations of AGB and L-VOD are found with (i) Bouvet-Mermoz for Shrublands and Savannahs (ii) Baccini for croplands and equatorial forest (iii) Saatchi for grasslands. Regarding natural vegetation and woody savannah the correlation values obtained with Saatchi and Baccini are very similar. One should note that correlation values obtained with Bouvet-Mermoz for woody savannah are degraded to the fact that for the highest values of AGB found in this class, at the SMOS resolution, the AGB estimation is a mix of Bouvet and Mermoz approaches. Therefore, all AGB datasets except that of Avitabile performs the best for a few land cover classes.

Interpreting where do this differences come from is not easy. Radar observations in low vegetation regions such as shrublands and grasslands are thought to be very sensitive to biomass variations, in spite of a significant sensitivity to soil moisture. The high correlation of the two AGB maps mainly based of radar data (Saatchi and Bouvet-Mermoz) with SMOS L-VOD in grasslands would confirm this fact, as the high correlation in shrublands for Bouvet-Mermoz.

The scatter plot found with Avitabile for woody-savannah resembles an overlay of the scatterplot obtained with Baccini and the scatter plot obtained with Saatchi. The low AGB vs L-VOD slopes obtained for low vegetation classes, significantly lower than those found with the original Saatchi and Baccini datasets, are rather difficult to understand. The strange behavior of Avitabile AGB probably comes from the fact that it is pure data driven method and that it is therefore very sensitive to the data used to train the method. In their training database, high AGB plots could be over-represented.

In addition as mentioned above, the distribution of Baccini AGB for woody savannah is significanly different to the other datasets, which much higher values.

These elements were added to the new Sect 5.3.

f. In table 1, there are three metrics to show the relations between VOD and biomass and other parameters. However, only Baccini result is highlighted in the abstract. Why? The table does not necessarily support this. Furthermore, there is not physical reason that the scattering or emissivity has to be linearly related to biomass.

We understand the point by the reviewer that only Baccini is cited explicitly in the abstract and this could look strange. First, it a good style practice not to make citations in the abstract. In addition, the statement saying that the relationship of Baccini and L-VOD is linear was not correct. It as been removed from the abstract.

[…] four AGB data sets. The relationships between L-VOD and the AGB data sets were linear per land cover class, but with a changing slope depending on the class type, which makes a global non-linear relationship. In contrast, the relationship linking L-VOD to tree height ($R = 0.87$) was ***close*** *to linear. For low vegetation classes […]*

Actually, saying that the relationship with respect to Baccini is linear was motivated by the fact that it is closer to linear than those obtained with the other datasets. The degree of non-linearity of the L-VOD/AGB relationship clearly increases from Baccini to Saatchi and Bouvet-Mermoz (which are similar) and to Avitabile, which is strongly non-linear. Finally, we do not reckon that it is needed to give those details in the abstract and that it is better to say that the global relationship is non-linear in all the cases but basically linear per land cover class. The new Figs 6 and 7 showing all the land cover classes shows clearly that the relationship of L-VOD and Baccini is not linear with slopes going from only 2.16-43 Mg/h for shrublands and grasslands to 100-170 for croplands and savannahs and to 220-260 for woody savannah and evergreen broadleaf forest.

Thanks for pointing this out. We agree that there is not physical reason that the scattering or emissivity has to be linearly related to biomass. And furthermore, emissivity is not linearly related to L-VOD either.

5. Figure 4 is a bit difficult to understand. The colors and what the legend provide cannot be easily deciphered. It seems one should the see the saturation of NDVI and a much linear relationship with VOD but I am not sure the figure explicitly shows this. I recommend either making the figure a bit simple or provide more information in the caption and change colors so the points are clear.

We have completely re-thought the best way to present this figure, which basically does not contain any new result and the goal is to illustrate the discussion by comparing L-VOD to results presented earlier and published results by Liu et al. 2015. Therefore, following reviewers comments, and to avoid misunderstandings the text on Sect. 4.4 discussing this figure were moved to Sect. 5 “Discussion”. In addition, the new text will add more explanations on how the figure was done.

To make a clearer figure we decided to make a new one with two panels (see below).

In the right panel of the new figure 8, the L-VOD and K/X/C-VOD relationships to Saatchi AGB are shown without using any normalization as we realized that the normalization used to plot L-VOD, K/X/C-VOD and NDVI in the same plot could be misleading. The normalization is not needed to compare with other VOD, only for NDVI because their dynamic ranges are very different. The curves plotted here for the K/X/C-VOD are just those of Figure S4 from Liu et al. 2015, which were computed using Saatchi AGB and the same method that we used in the current study. Liu et al fitted their relationship using K/X/C-VOD data in the period 1998-2002 and Saatchi data acquired from 1995 to 2005 (page 6 of their supplementary information document). This will be reminded explicitly in the discussion section of a revised version of the manuscript. However, the non-linearity of the curve and the difference sensitivity to high AGB from different frequencies is driven by the high AGB values in the dense equatorial forest, which is not supposed to vary strongly in a few years time.

In the left panel of Fig 8 L-VOD and NDVI relationships with respect to Saatchi AGB. In this case L-VOD and NDVI were normalized to 1 using their maximum values (1.24 and 0.83, respectively) to have both quantities with the same dynamic range in the same figure. We hope the figure is clearer now. The text in Sect. 5.2 updated accordingly

The curves for the other AGB datasets with respect to L-VOD are already shown in Fig 5. They will not add much information to this discussion and we tried to show them in the figure below but it becomes unreadable and even more difficult to understand.

~~The high sensitivity~~ An evaluation of SMOS L-Band vegetation optical depth (L-VOD) data sets: a high sensitivity of L-VOD to above-ground biomass in Africa

Nemesio J. Rodríguez-Fernández[1], Arnaud Mialon[1], Stephane Mermoz[1], Alexandre Bouvet[1], Philippe Richaume[1], Ahmad Al Bitar[1], Amen Al-Yaari[2], Martin Brandt[3], Thomas Kaminski[4], Thuy Le Toan[1], Yann H. Kerr[1], and Jean-Pierre Wigneron[2]

[1]Centre d'Etudes Spatiales de la Biosphère (CESBIO), Université de Toulouse, Centre National d'Etudes Spatiales (CNES), Centre National de la Recherche Scientifique (CNRS), Institut de Recherche pour le Dévelopement (IRD), Université Paul Sabatier, 18 av. Edouard Belin, bpi 2801, 31401 Toulouse, France
[2]Interactions Sol Plante Atmosphére (ISPA), Unité Mixte de Recherche 1391, Institut National de la Recherche Agronomique (INRA), CS 20032, 33882 Villenave d'Ornon cedex, France
[3]Department of Geosciences and Natural Resources Management, University of Copenhagen, 1350 Copenhagen, Denmark
[4]The inversion Lab, Hamburg, Germany

Correspondence to: N.J. Rodríguez-Fernández (nemesio.rodriguez@cesbio.cnes.fr)

Abstract. The vegetation optical depth (VOD) measured at microwave frequencies is related to the vegetation water content and provides information complementary to visible/infra-red vegetation indices. This study is devoted to the characterisation of a new VOD data set obtained from SMOS (Soil Moisture and Ocean Salinity) satellite observations at L-band (1.4 GHz). Three different SMOS L-band VOD (L-VOD) data sets (SMOS Level 2, Level 3 and SMOS-IC) were compared with data sets on tree height, visible/infra-red indexes (NDVI, EVI), ~~cumulated~~ mean annual precipitation, and above ground biomass (AGB) for the African continent. For all relationships, SMOS-IC showed the lowest dispersion and highest correlation. Overall, we found a strong ($R > 0.85$) correlation with no clear sign of saturation between L-VOD and four AGB data sets. ~~The relationship linking L-VOD to tree height ($R = 0.87$) and Baccini's AGB ($R = 0.94$) was strong and linear. The relationships between L-VOD and three other AGB data sets were linear per land cover class, but with a changing slope depending on the land cover type. For low vegetation classes,~~ **The relationships between L-VOD and the AGB data sets were linear per land cover class, but with a changing slope depending on the class type, which makes a global non-linear relationship. In contrast, the relationship linking L-VOD to tree height ($R = 0.87$) was close to linear. For vegetation classes other than evergreen broadleaf forest,** the annual mean of L-VOD spans a range from 0 to 0.7 and it is linearly correlated with the amount of the average annual precipitations. SMOS L-VOD showed a higher sensitivity to AGB as compared to NDVI and K/X/C-VOD (VOD measured, respectively, at 19, 10.7, and 6.9 GHz). The results showed that although the spatial resolution of L-VOD is coarse (~ 40 km), the high temporal frequency and sensitivity to AGB makes SMOS L-VOD a very promising ~~index~~ **indicator** for large scale monitoring of the vegetation status, in particular biomass.

1 Introduction

Large scale monitoring of vegetation properties is crucial to understand water, carbon and energy cycles. The Normalized Difference Vegetation Index (NDVI, Tucker, 1979) computed from space-borne observations at visible and infra-red wavelengths has been widely used since the 1980s to study vegetation changes and its implications on animal ecology (Pettorelli et al., 2005, 2011), global fire emissions (Van der Werf et al., 2010), deforestation and urban development (Esau et al., 2016), global patterns of land-atmosphere carbon fluxes (Jung et al., 2011) and the vegetation response to climate (Herrmann et al., 2005) and extreme events such as droughts (Vicente-Serrano et al., 2013). NDVI is sensitive to the abundance of chlorophyll and therefore to the photosynthetically active biomass (which includes herbaceous vegetation and the leaves of trees), but insensitive to wood mass. NDVI is thus not considered as an accurate proxy of total above ground biomass (AGB), except in areas of low vegetation density (Todd et al., 1998). Contrastingly, being sensitive to both green and non-green vegetation components, passive microwave observations can provide important complementary information on the state and time changes of the vegetation features, in particular regarding the AGB dynamics (Liu et al., 2015).

The thermal emission arising from the Earth surface at microwave frequencies depends on the soil characteristics such as soil temperature, soil roughness and soil moisture content, which controls the soil emissivity (Ulaby, 1976). In the presence of vegetation, part of the soil emission is absorbed and scattered. ~~This extinction effect is parameterized by the vegetation optical depth (VOD) that can be estimated using radiative transfer theory (Mo et al., 1982; Ulaby and Wilson, 1985; Ferrazzoli and Guerriero, 1996; Wig~~ ~~VOD~~ **These effects can be parameterized using radiative transfer models such as the so-called $\tau-\omega$ model (Mo et al., 1982; Ulaby a** **where τ is the optical depth and ω is the single scattering albedo. τ** was shown to be linked to the vegetation water content (VWC, kg/m^2) (Kirdiashev et al., 1979; Mo et al., 1982; Jackson and Schmugge, 1991) and to other vegetation properties such as the Leaf Area Index (Jackson and Schmugge, 1991; Van de Griend and Wigneron, 2004; Wigneron et al., 2007). **Therefore, τ is commonly known as Vegetation Optical Depth (VOD).** VOD is also a function of the vegetation structure which determines its dependence on the incidence angle and on the polarization of the radiation (Ulaby and Wilson, 1985; Wigneron et al., 1995, 2004; Hornbuckle et al., 2003; Schwank et al., 2005).

Passive microwave radiometry is therefore a promising tool to monitor the vegetation at global scale. VOD samples ~~a thick layer of~~ the vegetation canopy including woody vegetation, which uses root zone soil moisture (Andela et al., 2013). VOD was used to study deforestation in South America (Van Marle et al., 2016) and Africa (Brandt et al., 2017). Using VOD, it has been possible to reveal teleconnexions linking the state of the vegetation in Australia and El Niño Southern Oscillation (Liu et al., 2007). In addition, Liu et al. (2015) showed the high potential of microwave VOD to monitor the AGB dynamics at large scale. Using both VOD and NDVI contributes to provide a more robust assessment of the vegetation characteristics (Liu et al., 2011). **The VOD has also been used to study the VWC and variations in ecosystem-scale isohydricity (Konings and Gentine, 2017; Li et al., 2017) .**

The above mentioned studies used VOD derived from different radiometers operating at different frequencies (Liu et al., 2011): SSM/I at 19 GHz (K-band), TRMM-TMI at 10.7 GHz (X-band), and the Advanced Microwave Scanning Radiometer - Earth Observing System (AMSR-E) at 10.7 GHz and 6.9 GHz (C-band). It is worth noting that VOD is intrinsically dependent on the frequency of the electromagnetic radiation and VODs retrieved at different frequencies provide complementary information. Therefore, in the following, a specific VOD data set will be noted as B-VOD, where B stands for the microwave band (X-VOD, C-VOD,...). The lower the frequency, the lower the VOD for a given level of VWC (Wigneron et al., 1995, 2004; Ferrazzoli and Guerriero, 1996). Consequently, L-band (1.4 GHz, 21 cm) observations, which are less attenuated through the vegetation canopy, are capable of sampling the vegetation layer up to higher biomass values compared to higher frequency observations.

Currently, two missions are performing systematic L-band passive microwave observations: The Soil Moisture and Ocean Salinity (SMOS) satellite (Kerr et al., 2010), launched by ESA in November 2009, and the Soil Moisture Active Passive (SMAP) satellite (Entekhabi et al., 2010), launched by NASA in January 2015. **SMAP measures the brightness temperature for a single incidence angle in two polarizations. A single-angle dual polarization retrieval algorithm decreases the quality of the soil moisture retrievals (Konings et al., 2016) but using a multi-orbit approach assuming that the L-VOD does not vary significantly in a few days window, it is possible to estimate soil moisture and L-VOD (Konings et al., 2017) .** The full-polarization and multi-angular capabilities of SMOS allow to retrieve simultaneously the soil moisture content and L-VOD. Lawrence et al. (2014) and Grant et al. (2016) compared SMOS L-VOD to X-VOD and C-VOD measured by AMSR-E and to visible/infra-red vegetation indices. In crop zones, as the MODIS vegetation indices, L-VOD increases during the growing season and decreases during senescence (Lawrence et al., 2014). At global scale, L-VOD is less correlated to optical/visible vegetation indices than X/C-VOD, suggesting that L-VOD can add more complementary information with respect to optical/infrared indices than X/C-VOD (Grant et al., 2016). For instance, Rahmoune et al. (2014) found a significant correlation between L-VOD and tree height estimates. Vittucci et al. (2016) also discussed this relationship and compared it to the one estimated with X/C-VOD, which shows higher values for low tree-height than SMOS L-VOD, as expected. Vittucci et al. (2016) also showed a close to linear relationship between L-VOD and AGB at 20 selected points over Peru, Columbia, and Panama. **L-VOD has been recently used to study the evolution of carbon stocks in African drylands by Brandt et al. (2018) .**

In summary, L-VOD derived from the new SMOS L-Band observations is a promising tool for monitoring global vegetation characteristics. There is, however, a lack of in-depth studies on how L-VOD relates to established vegetation characteristics. The goal of the current study is to get further insight into the sensitivity of L-VOD to vegetation properties **(such as tree height and AGB)** and precipitations, which can drive the vegetation dynamics for some biomes. Taking into account the novelty of these observations, three distinct SMOS L-VOD data sets were evaluated against several data sets independent of L-VOD: (*i*) optical/infra-red indices (representing the greenness of vegetation, also often used as proxy for primary productivity), (*ii*) AGB benchmark maps, (*iii*) LIDAR derived tree height and (*iv*) precipitation data set. The area selected for this study is Africa, as it is a continent with several climate regions and biomes and with a large variability in the vegetation biomass from sparse shrubs to savannah and very dense rainforests. In addition, Bouvet et al. (2018) have recently discussed the first biomass map of African savannahs computed from L-band active microwave (synthetic aperture radar) observations. **In contrast to passive measurements, for which the goal is to study how the thermal emission arising from the Earth is affected by the vegetation layer, active measurements allow to study how the radiation emitted by a human-made radiation source is backscattered by the vegetation, which depends mainly of the vegetation water content and the vegetation structure.**

Since this study is mainly devoted to AGB, long time averages (typically annual) will be used. Studying the evolution of VWC would require using much shorter time scales. The document is organized as follows. Section 2 presents the different SMOS L-VOD data sets as well as the data sets used for the evaluation (tree height, cumulated precipitations, NDVI, EVI and four AGB data sets). Section 3 deals with the evaluation methods. Section 4 presents the results, which are discussed in Section 5, in particular the potential of L-VOD to estimate AGB at large scale. Finally, Section 6 summarizes the results and presents the conclusions of this study.

2 Data

2.1 SMOS data

The SMOS (Kerr et al., 2001, 2010) mission is an ESA-led mission with contributions from CNES (Centre National d'Etudes Spatiales, France) and CDTI (Centro Para el Desarrollo Tecnológico Industrial, Spain). The SMOS radiometer measures the thermal emission from the Earth in the protected frequency range around 1.4 GHz in full-polarization and for incidence angles from $0°$ to $\sim 60°$. **Stokes 3 and 4 parameters are used to filter the data, to detect radio frequency interference sources, for instance.** The footprint (full width at half maximum of the synthesized beam) is ~ 43 km on average (Kerr et al., 2010). The equator overpass time is 6:00 AM/PM for ascending/descending orbits. ~~Only ascending orbits are used in this study as the overall quality of the data is higher than the descending data.~~ **Ascending and descending orbits data from 2011 and 2012 are used in this study.** Taking into account the novelty of L-VOD estimates, three different L-VOD data sets were evaluated in this study: the ESA Level 2 (L2) product, the CATDS multi-orbit Level 3 (L3) product and the new INRA-CESBIO (IC) data set ~~.~~ ~~The differences between these data sets are discussed in the following~~ (Table S1 gives a summary of the main characteristics of those three products).

2.1.1 ~~SMOS Level 2 soil moisture and L-VOD~~

~~The~~

The three SMOS soil moisture and L-VOD L2 retrieval ~~algorithm was described by Kerr et al. (2012) . The algorithm uses~~ algorithms discussed below use the L-MEB (L-band Microwave Emission of the Biosphere) radiative transfer model (Wigneron et al., 2007), which is based on the $\tau-\omega$ ~~(optical depth - single scattering albedo) parameterization~~ parametrization to take into account the effect of vegetation. The soil temperature profile is estimated from European Centre for Medium Range Weather Forecasts (ECMWF) Integrated Forecast System (IFS) data. The difference between forward model estimates of the brightness temperatures at antenna reference frame and actual satellite measurements is minimized by varying the values of the soil moisture (SM) content and the L-VOD. The contributions from the soil and vegetation layers can be distinguished thanks to the multi-angular and dual-polarization measurements. ~~The soil temperature profile is estimated from European Centre for Medium Range Weather Forecasts (ECMWF) Integrated Forecast System (IFS) data~~

The differences between the three SMOS data sets are discussed in the following.

2.1.1 SMOS Level 2 soil moisture and L-VOD

The SMOS soil moisture and L-VOD L2 retrieval algorithm was described by Kerr et al. (2012) . The forward model contributions are computed at ~ 4 km resolution pixels and aggregated to the sensor resolution using the mean synthetic antenna pattern. For footprints with mixed land cover, the L2 algorithm distinguishes the minor and the major land cover (low vegetation or forest). The SMOS retrieval is performed only over the dominant land cover class within the footprint while the emission of the minor land cover is estimated from ECMWF SM and MODIS Leaf Area Index (LAI) data (Kerr et al., 2012). The version of the data used in the current study is 620. This data version uses auxiliary files including information on L-VOD computed from previous retrievals, surface roughness and Radio Frequency Interference (RFI) that are used to constrain the new retrievals. **Due to the specificities of the SMOS geometry of observation, the profiles of brightness temperatures observed at the middle part of the field of view (~600 km centered on the satellite sub-track) have larger ranges of incidence angles than the outer part of the field of view. For such observations, the retrieval system has more information content to discriminate the vegetation emission from the ground emission leading to more accurate retrieved soil moisture and VOD. The retrieved VODs and associated uncertainties for such grid points are used as prior first guess and uncertainties for the L-VOD retrieval of the next overpass of these grid-points (3 days later maximum) that will be observed, this time, at the outer part of the field of view with a reduced range of incidence angle. This avoids to use auxiliary LAI data to compute a first-guess L-VOD value (Kerr et al., 2012) .**

The SMOS L2 data are provided by ESA in an Icosahedral Equal Area (ISEA) 4H9 grid (Sahr et al., 2003) in swath mode with a sampling resolution of 15 km. **The single scattering albedo and roughness values depend on the surface type and are taken from literature and/or specific SMOS studies. For low vegetation areas, the single scattering albedo is set to 0 and roughness set to 0.1. For forested areas the single scattering albedo is set to 0.06 for tropical and subtropical forest and 0.08 for Boreal forest and roughness set to 0.3 (Rahmoune et al., 2013, 2014) .**

2.1.2 SMOS Level 3 soil moisture and L-VOD

The SMOS L3 soil moisture and L-VOD data set is provided by the CATDS (Centre Aval de Traitement de Données SMOS) from CNES (Centre National D'Etudes Spatiales) and IFREMER (Institut Français de Recherche pour l'Exploitation de la Mer) in an Equal-Area Scalable Earth (EASE) grid version 2 (Brodzik et al., 2012.) with a sampling resolution of 25 km. The data version used in this study is Version 300. The data set and the retrieval algorithm are described in Al Bitar et al. (2017). The L3 algorithm is based on the same physics and modelling as the ESA L2 single-orbit algorithm (Section 2.1.1). ~~Instead~~ However, instead of using information on prior retrievals to constrain the SM and L-VOD inversion, the Level 3 algorithm uses a multi-orbit approach with data from three different revisits over a seven day window. In contrast to soil moisture, L-VOD is not expected to change strongly over a short period of time. Therefore a Gaussian correlation function is used during the retrieval to penalize large L-VOD variations in the cost function. The standard deviation of the Gaussian correlation function is 21 days for forests and 7 days for low vegetation~~(Al Bitar et al., 2017) .~~. **The single scattering albedo and roughness parametrizations use the same approach and values of the L2 algorithm.**

2.1.3 SMOS INRA-CESBIO (IC) soil moisture and L-VOD

The SMOS INRA-CESBIO (SMOS-IC) algorithm was designed by INRA (Institut National de la Recherche Agronomique) and is produced by CESBIO (Centre d'Etudes Spatiales de la BIOsphère). A detailed description is given in Fernandez-Moran et al. (2017). One of the main goals of the SMOS-IC product is to be as independent as possible from auxiliary data, which are often also used for evaluation. ~~SMOS-IC is based on the same L-MEB (Wigneron et al., 2007) model used by the ESA L2 algorithm (Section 2.1.1) to perform global retrievals of SM and L-VOD but it uses some simplifications.~~ In contrast to the L2 and L3 algorithms, the IC algorithm considers the footprints to be homogeneous to avoid uncertainties and errors linked to possible inconsistencies in the auxiliary data sets which are used to characterize the footprint heterogeneity. ~~As for the L2 and L3 algorithms, the soil temperature profile is estimated from ECMWF Integrated Forecast System (IFS) data. However~~In addition, SMOS-IC differs from the SMOS L2 and L3 products in the initialization of the cost function minimization and in the modelling of heterogeneous pixels: no LAI nor ECMWF SM data are used. ~~Finally, the effective vegetation scattering albedo and soil roughness parameters were optimized as discussed by Fernandez-Moran et al. (2017) and are different to those used by the Level 2 and Level 3 algorithms.~~ **A first run was done with SM 0.2 m^3/m^3 and L-VOD 0.5 as initial guess for the minimization. This allowed to compute a mean L-VOD map per each grid point. The final inversion was done using this mean L-VOD map as first guess for L-VOD and a value of 0.2 m^3/m^3 as first guess for SM. The roughness and single scattering parameters are assigned per International Geosphere-Biosphere Program (IGBP, Loveland et al., 2000) land cover classes, based on Parrens et al. (2017b, a) , and are averaged within a footprint according to the fraction of classes present in the footprint.** The data used in this study is version 103 and it is provided in the 25 km EASEv2 grid.

2.2 Evaluation data sets

This study performs an evaluation of the SMOS L-VOD data sets by a comparison with other vegetation-related evaluation data sets which are described in the following.

2.2.1 Precipitations

The Worldclim data set (Fick and Hijmans, 2017) provides spatially interpolated monthly climate data for global land areas at a very high spatial resolution (approximately 1 km). It includes monthly temperature (minimum, maximum and average), precipitation, solar radiation, vapour pressure and wind speed, aggregated across a target temporal range of 1970-2000, using data from between 9000 and 60 000 weather stations. As precipitations drive the vegetation dynamics for some biomes, mean annual precipitation were used to evaluate the relationship with L-VOD.

2.2.2 MODIS vegetation indices

MODIS NDVI and Enhanced Vegetation Index (EVI) from the product MYD13C1 ~~(Huete et al., 2002)~~ (Tucker, 1979; Huete et al., 2002) c 6 were compared to the SMOS L-VOD data sets to test L-VOD's performance against green photosynthetically active vegetation. Both NDVI and EVI are directly linked to the ~~sential~~ essential climate variables FAPAR and LAI and they are widely used as proxy for green vegetation cover. The NDVI product contains atmospherically corrected bi-directional surface reflectances masked for water, clouds, and cloud shadows. ~~The~~

EVI uses the blue band to remove residual atmospheric contaminations caused by smoke and sub-pixel thin cirrus clouds, which also introduces uncertainties over tropical areas. ~~The EVI also uses feedback adjustment to minimize canopy background variations and to enhance its sensitivity from sparse to dense vegetation conditions.~~ EVI was designed to have a higher sensitivity in high biomass regions than NDVI by allowing to distinguish the vegetation and the atmosphere contributions to the signal (Huete et al., 2002) . Whereas the NDVI is chlorophyll sensitive, the EVI is more responsive to the canopy type and structure (including LAI) and, for example, it has allowed to study the Amazon green-up season (where other vegetation indexes such as NDVI do not show any particular pattern, Huete et al. (2006)).

Global MYD13C1 data are cloud-free spatial composites of the gridded 16-day 1 km MYD13A2, and are provided as a Level 3 product projected on a 0.05° geographic Climate Modeling Grid (CMG). Cloud-free global coverage is achieved by replacing clouds with the historical MODIS time series climatology record.

2.2.3 Lidar tree height

This study used global tree height data from Simard et al. (2011). This data set was produced using 2005 data from the Geoscience Laser Altimeter System (GLAS) aboard ICESat (Ice, Cloud, and land Elevation Satellite). The processing follows three steps. First, Simard et al. (2011) developed a procedure to select waveforms and correct slope-induced distortions and to calibrate canopy height estimates using field measurements. In a second step, GLAS canopy height estimations were found to be correlated to other ancillary data such as annual mean precipitation, precipitation seasonality, annual mean temperature, temperature seasonality, elevation, tree cover and classes of protection status. In a ~~second~~ third step, a machine learning approach (random forest) was trained using the ancillary variables as input and GLAS tree height as reference data. ~~In the third step~~Finally, the random forest algorithm was applied to the ancillary data to produce a forest canopy height map at 1 km resolution for areas not covered by GLAS waveforms.

2.2.4 Above ground biomass

This study used four static AGB benchmark maps (Baccini et al., 2012; Saatchi et al., 2011; Avitabile et al., 2016; Bouvet et al., 2018) each with specific strengths and limitations to assess L-VOD's ability to reflect aboveground biomass in different biomes: Whereas the maps produced by Saatchi, Baccini and Avitabile aim at covering all pan-tropical region, with focus on dense forests, the Bouvet's map focuses on African ~~savannas~~ savannahs with lower biomass values. To take advantage of ALOS/PALSAR L-band observations, in the current study the Bouvet data set has also been extended to rainforest (see below).

The first AGB map over Africa was extracted from the 1 km resolution pan-tropical AGB data set produced by Saatchi et al. (2011). The methodology to produce this data set involves roughly two steps:

(i) in situ inventory plots are used to derive AGB estimates from the Lorey's height (the basal area weighted height of all trees with a diameter of more than 10 cm) calculated from the ICESat GLAS measurements,

(ii) these punctual measurements are spatially extrapolated using MODIS and Quick Scatterometer (QuikSCAT) data through Maximum Entropy (MaxEnt) modeling. All in situ AGB measurements were made from year 1995 to year 2005, and the MODIS and QuikSCAT data used for spatial extrapolation were acquired in 2000-2001, so that the resulting biomass map is representative of AGB circa the year 2000.

This study also used data over Africa extracted from the pan-tropical AGB data set produced by Baccini et al. (2012). The methodology used to produce this data set is very similar to that of Saatchi et al. (2011), except that *(i)* only MODIS data are used for the spatial extrapolation, *(ii)* Random Forest is used instead of MaxEnt, *(iii)* the data set is representative of circa 2007-2008, and *(iv)* the AGB map is produced at a resolution of 500 m.

The Avitabile et al. (2016) was also used in this study. This forest biomass data set was obtained by merging the data sets by Saatchi et al. (2011) and Baccini et al. (2012) with machine learning techniques to compute a pan-tropical AGB map at 1-km spatial resolution. The merging method was trained using an independent reference data set with field observations and locally calibrated high-resolution biomass maps, harmonized and up-scaled to be representative of 1 km^2. They used a total of 14477 AGB samples in Australia, Southern Asia, Africa, South America and Central America, spanning AGB values from 0 to ~ 500 Mg/h and covering different biomes such as grasslands, shrublands, savannahs and ~~rainforest~~rainforests.

The fourth biomass map used in this study is based on Bouvet et al. (2018) map over ~~savannas~~ savannahs and from Mermoz et al. (2015) over dense forests. The map from Bouvet et al. (2018) at 25 meter resolution is the first biomass map for Africa with focus on ~~savannas~~ savannahs and was built from a L-band ALOS PALSAR mosaic produced with observations made in year 2010 (when SMOS was already in operation). A direct model was developed to relate the PALSAR backscatter to AGB with the help of in situ and ancillary data. In a subsequent step, a Bayesian inversion of the direct model was performed. Seasonal effects were taken into account by stratification into wet/dry season areas. In Bouvet et al. (2018), the method was originally applied to savannah and woodlands with typical AGB values of less than 85 Mg/h. In the current study, the Bouvet et al. data set was extended to regions with AGB values larger than 85 Mg/h using the methodology presented by Mermoz et al. (2014): the ESA CCI (Climate Change Initiative) land cover map was used to separate dense forest areas, over which AGB was estimated at 500 meter resolution using the results by Mermoz et al. (2015). The resulting data set will be referred to as the Bouvet-Mermoz data set in the following.

3 Methods

The region selected for this study was the African continent because the Bouvet-Mermoz data set, which is the only one that has been produced using SAR observations made in the same frequency band (L-band) as SMOS, is limited to Africa. The African continent contains arid, equatorial and temperate regions (Kottek et al., 2006) with deserts, shrublands, mediterranean woodlands, grasslands, savannah and rainforests (Olson et al., 2001). Therefore, this study covers a wide range of climate regions and biomes and allows to extend the analysis of L-VOD data to monitor vegetation properties, in particular biomass, at larger scales than previous studies (Grant et al., 2016; Lawrence et al., 2014; Vittucci et al., 2016).

Unlike SMOS-IC and SMOS L3 products, which are produced natively on the 25 km EASEv2 grid, the SMOS L2 L-VOD products are provided on the ISEA4H9 grid. A spatial interpolation was required to align the SMOS L2 L-VOD to the EASE 25 grid. In order to maintain as much as possible the meaning of the opacity e.g. close to the coastline or transitions between the two grid systems, this interpolated Level 2 (hereafter iL2) L-VOD is obtained using: *(i)* whenever possible a DeLaunay triangulation linear interpolation (three valid L2 L-VOD), *(ii)* or a linear interpolation (only two valid L2 L-VOD), *(iii)* or the nearest L2 L-VOD (only one valid L2 L-VOD) to EASE25 grid point within a neighbour defined by the 25km EASE square cell.

AGB, precipitation, tree height ~~,~~ and MODIS NDVI/EVI ~~and SMOS L2~~ data were aggregated and re-sampled to the EASEv2 grid common to the SMOS L3 and IC data sets using the Geospatial Data Abstraction Library (GDAL) routine `gdalwarp` in average mode. Regarding, the SMOS Level 2 data, several SMOS Level 2 retrievals are available for a given day for high northern and southern latitudes. At these latitudes, the best retrievals (corresponding to lower values of the cost function `Chi2`) were selected.

In spite of observing in a protected band dedicated to research observations, some radio frequency interferences (RFI) from human-built equipment affect the quality of the SMOS observations. ~~SMOS L2 and L3 data with low quality (goodness of the fit to the observed brightness temperatures as given by the `Chi2` parameter larger than 3) were filtered out.~~ **Several quality indicators are present in the SMOS L2 and L3 products. The `DQX` parameter uses the inverse linear tangent model (Jacobian) to translate the observation uncertainty (radiometric accuracy) into the parameter space uncertainty. The forward models are much more sensitive for lower values of the (SM, L-VOD) parameter space (leading to low `DQX`) than for higher values (leading to high `DQX`). Therefore, filtering to keep the lowest `DQX` implies a risk to bias our results toward lowest retrieved values, particularly for tropical forest where both SM and L-VOD are high. In addition, the `DQX` parameter does not give information about the correctness of the solution, which is based on a quality of a fit. Therefore, the `Chi2` (goodness of the fit) was used to filter out the retrieved solutions. Several tests were done and a value of 3, corresponding approximately to the peak of the `Chi2` probability distribution was found to be a good threshold. This is in agreement with the values used in other studies (see for instance, Román-Cascón et al., 2017) .**

In the case of SMOS-IC, data with a root mean squared difference between modelled and observed brightness temperatures larger than 10 K were filtered out. In addition, the L-VOD time series of the three products were analysed grid point-to-grid point, and values with a deviation (in absolute value) larger than 2.5 with respect to the grid point average σ (were σ is the standard deviation) were considered as outliers and also filtered out.

The main evaluation strategy used in this study is to ~~spatially~~ compare L-VOD data to the evaluation data sets presented in Sect. 2. These variables such as above ground biomass, tree height, or long-term averages of ~~yearly rainfall~~ mean annual precipitations are not expected to change quickly over time. ~~Therefore, the L-VOD data were averaged on a yearly basis to avoid short-term variations due to changes in the vegetation water content over short time periods.~~ The biomass data sets discussed in Sect. 2 were produced with observations done from years 1995 to 2010. The comparison of L-VOD with the other data sets was done using L-VOD ~~data computed in 2011, as 2011 is the first complete year after the SMOS commissioning phase, which ended in June 2010.~~ **data from 2011 and 2012, as 2011 is the first complete year after the SMOS commissioning**

phase, which ended in June 2010. The L-VOD data for 2011 and 2012 were averaged to avoid short-term variations due to changes in the vegetation water content over short time periods.

To get a quantitative assessment of the correlation and the dispersion of L-VOD versus the evaluation data sets, three correlation coefficients were computed. The Pearson correlation coefficient R is a measure of the linear correlation between two variables. If the relationship linking these variables is linear with no dispersion, R equals 1 (both variables increase together) or -1 (one variable increases when the other decreases). However, the relationships between L-VOD and the evaluation data are not expected to be linear in most of the cases. Therefore, the Spearman and Kendall rank correlations (which can range from -1 to 1) were also computed to quantify monotonic relationships whether linear or not (~~more details are provided in the Supp.~~ the exact definition of the Spearman and Kendall rank correlations is given in the Supplementary Information).

~~The relationships linking~~ **The AGB and L-VOD** ~~**to the evaluation data**~~ **relationship was studied for different biomes** ~~**were fitted using linear fits. In addition, fits to**~~ **using the IGBP land cover classes (Loveland et al., 2000) . Table S2 summarizes the IGBP classes and Figure S1 shows their spatial distribution using the Bouvet-Mermoz AGB map. For a single biome, a linear function gives a good fit to the AGB and L-VOD relationships (see Sect. 4.3). In contrast, the global relationships linking** ~~**AGB**~~ **the AGB datasets and L-VOD are significantly non-linear, therefore fits were computed following the approach used by Liu et al. (2015). The L-VOD data** ~~**was**~~ **were binned in 0.05-width bins. For each L-VOD bin, the 5th and 95th percentiles and the mean of the AGB distribution were computed, providing three AGB curves as a function of L-VOD. The three curves were fitted with** ~~**Liu et al. (2015) function ,**~~ **the function used by Liu et al. (2015) ,**

$$AGB = a \times \frac{\arctan(b\,(vod - c)) - \arctan(-b\,c))}{(\arctan(\infty) - \arctan(-b\,c)} + d, \tag{1}$$

and with a logistic function~~**or with a generalized logistic function, obtaining results of the same quality (more details are provided in the Supp. Information).**~~ **,**

$$AGB = \frac{a}{1 + e^{-b\,(VOD - c)}} + d. \tag{2}$$

In Eqs. 1 and 2, the parameters a, b, c and d are varied to get the best fit to the curves. The fitted curves give AGB in Mg/h units as a function of L-VOD, which is a dimensionless quantity. Therefore the units of a and d are Mg/h and b and c are dimensionless quantities.

4 Results

~~Figure 2 shows the annual mean for 2011 of the three SMOS L-VOD products and of the MODIS NDVI and EVI indices. It also shows the remaining static data sets after resampling to a 25 km EASEv2 grid, when needed.~~

Figure 1 shows the average L-VOD computed over 2011 and 2012 using both ascending and descending orbits for the three SMOS L-VOD products. In addition, it also shows the standard deviation (STD) and the number of points of the local time series after applying the filters discussed in Sect 3. The three SMOS L-VOD products show a similar spatial distribution but the SMOS-IC L-VOD shows a smoother spatial distribution than the iL2 and L3 datasets. The highest values are found in equatorial forest regions and L-VOD decreases monotonically with distance to the equatorial forest in the tropical area and beyond. The STD of the L-VOD time series also increases towards the equatorial forest, in particular for the iL2 and L3 datasets. The number of points in the time series is lower for the IC dataset due to the lower revisit frequency arising from the requirement of having brightness temperature measurements spanning an incidence angle range of at least 20° (Fernandez-Moran et al., 2017) .

Figure 2 shows the evaluation data after resampling to a 25 km EASEv2 grid: the 2011-2012 average of the MODIS NDVI and EVI indices, tree height, mean annual precipitations and AGB datasets. EVI and NDVI also decrease with increasing distance to the equator but more slowly than L-VOD. The tree height map shows two main populations: the equatorial forest, with heights larger than 20 meters, and the rest of the continent, where most of the vegetation is lower than ~ 5 meters. In contrast to the previous quantities, AGB can vary in two orders of magnitude, therefore AGB maps are shown in logarithmic units in Fig. 2. The Baccini, Saatchi and Bouvet-Mermoz maps show a similar AGB distribution. In contrast, the Avitabile map shows a much sharper decrease of AGB from the equatorial forest region to the rest of the continent.

4.1 Comparison of the three L-VOD data sets

Figure 3 ~~show~~ shows the scatter plots of SMOS IC L-VOD with respect to the evaluation data. The scatter plots obtained with the ~~L2~~ iL2 and L3 data sets are shown in Figs. S2 and S3, respectively. A visual inspection shows that the scatter plots obtained with IC L-VOD are significantly different than those of ~~L2~~ iL2 and L3 L-VOD, as they show smoother relationships with lower dispersion with respect to all the evaluation data sets than the equivalent plots for ~~L2~~ iL2 and L3 L-VOD.

A quantitative assessment of the correlation and the dispersion of the different scatter plots can be found in Table 1, where Pearson, Spearman and Kendall correlation coefficients are given for the three L-VOD data sets with respect to the evaluation data sets. The lowest Pearson correlation coefficient values were obtained for L3 L-VOD ($R = 0.65 - 0.87$). The Pearson correlation coefficients obtained for ~~L2~~ iL2 L-VOD are similar ($R = 0.67 - 0.87$) ~~than~~ to those obtained for L3 L-VOD but systematically higher by up to 4%~~. The~~ , while the values obtained for IC L-VOD are the highest ($R = 0.77 - 0.94$) with respect to all the evaluation data sets. The correlation ~~increases~~ increase is in the range of 5%-10% with respect to ~~L2~~ iL2 L-VOD and up to 15 % with respect to L3 L-VOD. ~~Therefore, using eight vegetation-related evaluation data sets, the most consistent SMOS L-VOD data set is SMOS-IC.~~ **The rank correlation values with respect to all the evaluation datasets are also higher for IC L-VOD ($\rho = 0.78 - 0.91$, $\tau = 0.61 - 0.75$), followed by iL2 L-VOD ($\rho = 0.67 - 0.83$, $\tau = 0.50 - 0.65$) and L3 L-VOD ($\rho = 0.66 - 0.80$, $\tau = 0.49 - 0.62$). These results are in agreement with those obtained with the Pearson correlation and imply that the lower Pearson correlation values obtained for the L3 and iL2 datasets are not due to a correlation that could be better but more non-linear than that of the IC dataset. Therefore, using eight vegetation-related evaluation**

data sets and three different metrics, the most consistent SMOS L-VOD data set is SMOS-IC. This result implies that, currently, the SMOS-IC dataset is the best SMOS L-VOD product to perform vegetation studies, and the rest of the current study will focus on SMOS-IC L-VOD.

4.2 Comparison of SMOS IC L-VOD to other data sets

~~Taking into account that the best results presented in Sect. 4.1 were obtained with SMOS-IC L-VOD, only the latter is considered in the following.~~

The relationship between tree height and IC L-VOD was found to be close to linear with a high Pearson correlation coefficient ($R = 0.87$, Table 1), in agreement with previous findings using SMOS L2 data ~~Rahmoune et al. (2013)~~ (Rahmoune et al., 2014) .

With respect to visible/infra-red indices such as EVI and NDVI, Figure 3 shows that both indices saturate even for moderate L-VOD values of ~ 0.5, in agreement with previous studies (Lawrence et al., 2014). The correlation coefficients are $R = 0.80-0.81$ and $\rho = 0.86-0.88$ for NDVI and EVI. Regarding precipitation, the scatter plots show more dispersion ($R = 0.77$, $\rho = 0.82$) than those obtained with NDVI and EVI but there is a saturation in the mean annual ~~cumulated~~ precipitation values for L-VOD values higher than $\sim 0.6-0.7$.

Regarding the different AGB data sets, most of the scatter plots show a clear non-linear relationship between L-VOD and AGB. ~~However, the~~ The relationship between Baccini et al. (2012) AGB versus IC L-VOD is ~~almost linear for the whole range of L-VOD and AGB values~~ the less non-linear one and the associated Pearson correlation ~~coefficients are~~ coefficient is the highest found ($R = 0.94$, $\rho = 0.90$). The relationship between Avitabile et al. (2016) AGB and L-VOD is the most non-linear one ($R = 0.85$, $\rho = 0.84$). It shows a low sensitivity to low L-VOD values and a large dispersion for high L-VOD values with AGB ranging from ~300 Mg/h to 500 Mg/h. The relationship between L-VOD and the Bouvet-Mermoz AGB data set ($R = 0.89$, $\rho = 0.91$) also shows a ~~large~~ significant dispersion for high L-VOD values with AGB spanning a range from 200 to 400 Mg/h. In contrast, the results obtained with the Saatchi et al. (2011) ($R = 0.92$, $\rho = 0.91$) and Baccini et al. (2012) data sets show a single AGB peak for the highest SMOS L-VOD values with values of ~ 280 Mg/h and ~ 320 Mg/h, respectively. ~~Interestingly, the Bouvet-Mermoz AGB data set, which has been obtained from L-band SAR data and is the only one developed with a particular focus on savannahs, shows a linear relationship between L-VOD and AGB with a very low dispersion for low L-VOD and AGB values.~~ In summary, IC L-VOD shows a high sensitivity to AGB, with smooth relationships without strong signs of saturation, in particular with respect to the AGB data sets from Saatchi et al. (2011), Baccini et al. (2012) and Bouvet-Mermoz.

To compare the relationship linking L-VOD and AGB to the relationship of other vegetation indices and AGB, scatter plots similar to those of Fig. 3 were computed using Saatchi's AGB with respect to MODIS NDVI and EVI (Fig. 4). There is a close-to-linear relationship for AGB lower than ~ 90 Mg/h and EVI or NDVI lower than 0.4 and 0.7, respectively. However, in contrast to L-VOD, the relationship saturates for EVI and NDVI higher than 0.5-0.6 and 0.7-0.8, respectively, for which AGB increases sharply from 90 to 300 Mg/h. This is expected as the visible/infra-red indices are sensible to the greenness of the canopy, which is not closely related to the total AGB in densely vegetated regions.

To get further insight into the global AGB versus L-VOD relationship, the fitting method described in Sect. 3 was used. Fits of the same quality were found using Liu's function (Eq. 1) and the logistic function (Eq. 2). Figure 5 shows the fits using a logistic function and Table S3 shows the best-fit parameters. Even if the overall form of the scatterplots of L-VOD and the four different AGB data sets are different, fits of the same quality were obtained for the four relationships. The Pearson correlation coefficients (R^2) of the fitted function with respect to the points to fit are in the range from 0.990 to 0.999 (Table S3). Eq. 2 with the best-fit coefficients of Table S3 for the "mean" curves can be used to transform SMOS IC L-VOD into AGB, while the 05th and 95th quantile best-fits can be used to provide an uncertainty interval.

4.3 Comparison of IC L-VOD to other data sets per land cover class

~~To get further insight into~~

4.3.1 AGB data sets

Figure 6 shows the relationship of ~~SMOS IC L-VOD and the evaluation data sets , an analysis per IGBP land cover class was performed. Figure ?? shows the relationships in between~~ L-VOD ~~and~~ versus the four AGB data sets (from left to right: Bouvet-Mermoz~~AGB, tree height, NDVI and precipitations for two groups of biomes using the~~, Saatchi, Baccini; Avitabile) for different IGBP land cover ~~classification: (*i*) evergreen broadleaf, and (*ii*) all other biomes (grasslands, croplands , shrublands, savannahs and woody savannahs). Figure S1 shows the spatial distribution of those two groups in the Bouvet-Mermoz map.~~ classes (from top to bottom: open shrublands; croplands; grasslands; croplands and natural vegetation mosaics; savannah; woody savannah; evergreen broadleaf). Each panel of Fig. ~~??~~ 6 shows the regression line ~~, and the~~ and the corresponding equation, as well as values of the Pearson R, Spearman ρ and Kendall τ coefficients. ~~Figure ?? shows scatter plots of SMOS-IC L-VOD with respect to the four AGB data sets and the tree height data computed for more specific land cover classes.~~

Maximum L-VOD values increase from grasslands, croplands~~and shrublands to savannahs~~, shrublands and savannahs, where L-VOD reaches a maximum value of ~ 0.4, to croplands and natural vegetation mosaics and woody savannahs, where L-VOD reaches a maximum value of ~~~ 0.7. The slope of the NDVI and~~ $\sim 0.6 - 0.7$. L-VOD ~~relationships for these biomes decreases smoothly and therefore the global relationship is non-linear. The slope is close to zero for evergreen broadleaf rainforest~~values higher than 0.7 were only found in the evergreen broadleaf equatorial forest, where the L-VOD range is $0.5 - 1.2$.

~~Although with a significant dispersion, the scatter plot of L-VOD and the cumulated precipitations outside the rainforest shows a close to linear relationship, with the cumulated precipitations increasing up to ~ 1700 mm for L-VOD ~ 0.7. As the relationship with NDVI, the~~ There are clear trends in the slope of the ~~precipitations and~~ regression lines. For Bouvet-Mermoz and Saatchi AGB data sets the trends are consistent. Slopes increase from 75-86 Mg/h from shrublands and croplands to 110-150 Mg/h for grasslands, croplands and natural vegetation mosaics, savannahs and woody savannahs. Finally the AGB versus L-VOD ~~relationship for~~ relationship slopes increase to 215-250 Mg/h for broadleaf evergreen forest. The general trends found with the ~~rainforest is low.~~

~~The scatter plot of tree height and L-VOD shows a similar slope out and within the rainforest, giving the global linear relationship showed in Fig. 3. Out of the rainforest, the maximum tree height value is ~ 20 m for L-VOD ~ 0.7.~~

~~The scatter plots showing the~~ Baccini AGB data set are in overall agreement with those of Bouvet-Mermoz and Saatchi but the slopes for shrublands and grasslands are significantly lower (2-44 Mg/h) while those for croplands and natural vegetation mosaics, savannahs and woody savannahs reach 160-210 Mg/h, which are values significantly higher than the ones obtained with Bouvet-Mermoz and Saatchi (122-156 Mg/h). The slope obtained for the evergreen broadleaf equatorial forest was in good agreement with the two other AGB datasets (265 Mg/h). On the other hand, the slopes of the Avitabile AGB and L-VOD ~~relationship shows a linear relationship out and within the rainforest. It is noteworthy that out of the rainforest, the relationship of L-VOD and AGB is the one showing the lowest dispersion ($\rho = 0.87$, $\tau = 0.68$) of all the evaluation~~ do not show the same trends of the other three AGB data sets. Slopes for shurblands, croplands, grasslands and savannahs are so low as 13-44 Mg/h. The slope increases for mosaics of croplands and natural vegetation up to 87 Mg/h, still significantly lower than the range of 132-174 Mg/h found with the other three AGB data sets. ~~Therefore, for African shrublands, grasslands, croplands and savannahs, the SMOS~~ The regression line for the scatter plot for Avitabile's woody savannah AGB increases up to 175 Mg/h, an intermediate value with respect to those found with Saatchi's (123 Mg/h) and Baccini's AGB (211 Mg/h), and actually the scatter plot shows signs of bimodality for L-VOD ~~data is in very good agreement with the independent AGB map obtained from L-band SAR observations by Bouvet et al. (2018) . The 0-85~~ values of 0.5-0.7. In contrast, the slope obtained for evergreen broadleaf forest using Avitabile's AGB is much higher (362 Mg/h) than those obtained with the other three AGB data sets (215-265 Mg/h~~range estimated by Bouvet et al. in these regions corresponds to the 0-0.7~~).

Many of the relationships are close to linear with Pearson coefficients R up to 0.70-0.87 and similar Spearman ρ values. SMOS L-VOD ~~range, where the vegetation characteristics seem to be closely related to the amount of annual precipitations. In contrast to tree height, the slope of the~~ is well-correlated to Bouvet-Mermoz and Saatchi's AGB for all IGBP classes with Pearson correlation coefficients R of $0.6-0.85$ (except with Saatchi AGB in shrublands, which is lower, $R = 0.49$). With respect to Baccini AGB, the Pearson correlation is high ($R = 0.7-0.87$) for all IGBP classes but for shrublands and grasslands, where it was found to be very low: $R = 0.03-0.39$. A similar behavior to that of Baccini AGB was found using Avitabile AGB, for which Pearson correlation values were also found to be low for shrublands and grasslands ($R = 0.31-0.44$), while they increase for savannahs and woody savannahs to $R = 0.51-0.56$ and to $R \sim 0.7$ for croplands, crops and natural vegetation mosaics, and evergreen broadleaf forest.

The best correlations of AGB and L-VOD ~~relationship increases by a factor of ~ 2 in~~ were found with: *(i)* Bouvet-Mermoz AGB for Shrublands ($R = 0.64$) and Savannahs ($R = 0.81$) *(ii)* Baccini AGB for croplands ($R = 0.76$) and evergreen broadleaf equatorial forest ($R = 0.78$) *(iii)* Saatchi AGB for grasslands ($R = 0.82$). Regarding croplands and natural vegetation mosaics, the highest correlation values were obtained with Saatchi and Baccini, which gave very similar results ($R = 0.85-0.87$) and somewhat higher than those obtained with Bouvet-Mermoz ($R = 0.81$). Finally, for woody savannah, the highest correlation values were also obtained with Saatchi and Baccini ($R = 0.67 - 0.70$, respectively) while with Bouvet-Mermoz ($R = 0.6$) and Avitabile ($R = 0.56$) the correlation was lower. One should note that Pearson correlation values obtained with Bouvet-Mermoz for woody savannah could be degraded by the fact that for the highest values of AGB found in this class at the SMOS resolution, the ~~rainforest, giving the global non-linear relationship shown in Fig. 3. The comparison of L-VOD to other AGB datasets for different biomes shows a behaviour consistent to that found~~ AGB estimation is a mix of Bouvet and Mermoz approaches. Actually, it is noteworthy that the highest rank correlations for woody savannahs and mosaics of croplands and natural vegetation were obtained with the Bouvet-Mermoz data set (~~Supp. Information).~~

4.4 ~~Sensitivity of L-VOD to AGB and comparison to other indices~~

~~To get further insight into the global AGB versus~~ $\rho = 0.77$ and $\rho = 0.91$, respectively). In summary, except for the Avitabile AGB dataset, all the other AGB datasets performs the best, as compared to L-VOD~~relationship, the fitting method described in Sect. 3 was used. Figure 5 shows the fits using a logistic function and Table S3 shows the best-fit parameters.~~ , for a few land cover classes.

~~Since Liu et al. (2015) discussed fits of Saatchi's AGB as a function K/X/C-VOD, in order to compare the performance of NDVI, K/X/C-VOD and~~

4.3.1 Other auxiliary data sets

Figure 7 is similar to Fig. 6 but it shows the relationship of L-VOD ~~to estimate AGB, the Saatchi data set was used. The scatter plot between Saatchi's AGB and NDVI was fitted using the method described in Sect. 3 and~~ versus other auxiliary data sets (from left to right: tree height, NDVI, EVI and mean annual precipitations) for different IGBP land cover classes.

Regarding tree height, the slope of the regression line is 17-27 m for all IGBP classes except for shrublands, where it is 12 m. The Pearson correlation is relatively low (~ 0.4) except for mosaics of croplands and natural vegetation and for evergreen broadleaf forest ($R = 0.61 - 0.73$).

Regarding the L-VOD and NDVI relationship in different biomes, the ~~fits to the 5th and 95th percentiles curves were plotted in Fig. 8. In addition, Fig. 8 shows the fits obtained by Liu et al. (2015) to the 5th and 95th percentiles curves of Saatchi's AGB versus K/X/C-VOD. Finally, Fig. 8 also shows the fits to Saatchi's AGB 5th and 95th percentiles curves as a function of SMOS-IC~~ slope of the regression line increases from 0.05 in shrublands to 0.57 in grasslands and 0.87 in mosaics of croplands and natural vegetation, before decreasing again to 0.6 in savannahs, 0.36 in woody savannahs and 0.11 in evergreen broadleaf forest as NDVI saturates. It is noteworthy that no significant difference is seen on the behavior of EVI and NDVI for high L-VOD ~~. For each data set, the area inside the 5th and 95th percentile fits was shaded. For ease of comparison, VOD and NDVI were normalized~~ values, in spite of the "enhanced" performance of EVI with respect to NDVI pointed out by some studies (Huete et al., 2006) .

Regarding the relationship of L-VOD and the average amount of annual precipitation, L-VOD increases from 0 ~~to 1 using their respective maximum values.~~

~~As expected, NDVI shows some sensitivity to AGB only for low AGB values (with a low slope) before showing a strong saturation for AGB values higher than ~ 70~~ up to ~ 0.7 for increasing precipitations up to ~ 1500 mm (values found for croplands and natural vegetation mosaics and woody savannah). In this range of L-VOD all other vegetation tracers increase as well. For instance, Bouvet-Mermoz and Saatchi's AGB increase up to 85 Mg/h ~~. The relationship between AGB and K/X/C-VOD shows a similar shape to that of AGB versus NDVI but it is slightly shifted to lower normalized VOD values. AGB increases from ~ 50 Mg/h to ~ 300~~ and ~ 100 Mg/~~h for K/X/C-VOD values higher than 70 % of their total value. In contrast, the relationship between AGB and L-VOD shows a more steady increase from low to high AGB and~~ h, respectively, and NDVI and EVI increase up to ~ 0.7 and ~ 0.45, respectively (Figs. 6 and 7). The Pearson correlation R and the slope of the regression line increase from 0.2-0.3 and 266-612 mm, respectively, for shrublands and grasslands to 0.4-0.65 and 1395-1914 mm for croplands, mosaics of croplands and natural vegetation and savannahs. The Pearson correlation coefficient R and the slope decrease to 0.25 and 741 mm, respectively, in woody savannahs. Finally, L-VOD values ~~. In particular, it does not show a threshold beyond which the relationship saturates and the slope increases significantly.~~ higher than 0.6-0.7, found only in evergreen broadleaf forest, are uncorrelated with the mean annual precipitation ($R = 0.04$ and slope of -64 mm). The mean annual precipitation could be one of the drivers of vegetation growth in drylands. In contrast, over that threshold of ~ 1500 mm of annual precipitations, which occur basically in the evergreen broadleaf forest, L-VOD and the other vegetation tracers are not coupled to the amount of precipitation.

5 Discussion

5.1 Sensitivity of L-VOD to AGB

As mentioned in Sect. 2, SMOS L2 and L3 products consider heterogeneous land covers inside the SMOS footprints, while SMOS-IC does not account for footprint heterogeneity. The better results obtained with the SMOS-IC data set suggests that the approach used to account for heterogeneous land covers introduce uncertainties in the Level 2 and 3 products. Nevertheless, independently of the choice of the SMOS L-VOD data set, the results showed a generally high sensitivity of L-VOD with respect to the vegetation-related variables/indices used for the evaluation, in particular with respect to AGB ($R = 0.78 - 0.94$).

The relationship between tree height and SMOS L-VOD was found to be close to linear, confirming previous findings by Rahmoune et al. (2014) using SMOS L2 L-VOD. Vittucci et al. (2016) estimated a correlation of L2 L-VOD and tree height of 0.81, which is in good agreement with the value reported here ($R = 0.79$, Table 1). However, for IC L-VOD the relationship ~~was found to be closer to a linear one, with~~ shows even less dispersion and a ~~significantly~~ higher correlation ($R = 0.87$).

The SMOS-IC L-VOD relationships with respect to NDVI and EVI were found in agreement with those discussed using SMOS L3 data by Grant et al. (2016) as there is a saturation in EVI and NDVI for high L-VOD values. In contrast, the relationships found in this study using SMOS-IC showed less dispersion than those found by Grant et al. (2016).

Regarding the comparison to AGB, Vittucci et al. (2016) discussed the relationship linking L2 L-VOD and biomass from the Carnegie Airborne Observatory (Asner et al., 2014) at 20 selected points over Peru, Columbia, and Panama spanning AGBs from ∼50 Mg/h to ∼280 Mg/h. The relationship was almost linear, in good agreement with the results discussed in Sect. 4 for SMOS IC L-VOD for evergreen broadleaf forest.

5.2 Comparison of L-band sensitivity to AGB to other frequencies

This study is devoted to L-VOD as estimated from SMOS observations but it is interesting to discuss the scatter plots presented in Sect. 4.2 in comparison those obtained for other frequencies. Figure 8a shows the fits to the 5th and 95th curves obtained analysing the Saatchi AGB and L-VOD distributions (Fig. 5c). The area in between both curves was shadowed in green color. In addition, the figure also shows the fits to the 5th and 95th curves obtained analysing the MODIS NDVI and L-VOD distributions (Fig. 4). The area in between both curves was shadowed in pink color. Since the dynamic range of L-VOD and NDVI are significantly different, both quantities were normalized from 0 to 1 dividing by their maximum values (1.24 and 0.83 for L-VOD and NDVI, respectively) in order to better show the sensitivity to AGB. As discussed in Sect. 4.2, NDVI shows some sensitivity to AGB only for low AGB values (with a low slope) before showing a strong saturation for AGB values higher than ∼ 70 Mg/h.

Regarding the VOD estimated with higher microwave frequencies, Liu et al. (2015) discussed fits of Saatchi's AGB as a function K/X/C-VOD. They used K/X/C-VOD data in the period 1998-2002 (as mentioned in Sect. 2, the data used to compute the Saatchi et al. (2011) maps were acquired from 1995 to 2005). Liu et al. (2015) computed the 5th and 95th quantiles of the AGB distribution in VOD bins obtaining two curves giving the "envelope" of the AGB versus and VOD distribution, which is the same method that was used in the current study (Sect. 3). Figure 8b shows the fits to the 5th and 95th curves shown in Fig. S4 of Liu et al. (2015) , which were reproduced using the function and the parameters given in their Eq. S2 and Table S1, respectively. The area in between both curves was shadowed in brown color. In addition, Figure 8b shows the fits to the 5th and 95th curves obtained analysing the Saatchi AGB and L-VOD distributions. The area in between both curves was shadowed in green color as in Fig. 8a. The relationship between AGB and K/X/C-VOD shows a similar shape to that of AGB versus L-VOD but it is somewhat shifted to higher VOD values. AGB increases from ∼ 50 Mg/h to ∼ 300 Mg/h for K/X/C-VOD values higher than ∼ 0.7. In contrast, the relationship between AGB and L-VOD shows a more steady increase from low to high AGB and L-VOD values. In particular, it does not show a threshold beyond which the relationship saturates and the slope increases significantly. **One must bear in mind that the time periods of the data used to compare with K/X/C-VOD are not the same, as the L-VOD period used in this study is 2011-2012 and that more detailed comparisons of the sensitivity to AGB of VOD at different frequencies would be interesting. However, the non-linearity of the curve and the difference sensitivity to high AGB from different frequencies is driven by the high AGB values in the dense equatorial forest, which is not supposed to vary strongly in a few years time at the SMOS spatial resolution. In addition, it is worth noting that the different shapes of the L-VOD and AGB relationships with respect to the K/X/C-VOD and AGB relationships are in agreement with what it is expected from the radiation transfer theory (Wigneron et al., 1995, 2004; Ferrazzoli and Guerriero, 1996) and previous results**

on L-VOD and X/C-VOD comparison by Grant et al. (2016) and Vittucci et al. (2016) as Fig. 8b shows that for a given AGB, L-VOD is lower than VOD at higher frequencies, as expected.

5.3 Comparison of the different AGB datasets

Estimating the AGB from remote sensing measurements is complex and the errors of different retrieval methods are not easy to characterize. Interpreting why L-VOD compares better to a given AGB data set for a given IGBP class (Sect. 4.3) is not easy.

The Avitabile AGB data set shows a sharp decrease from the Equatorial region with distance is not seen in any other AGB map nor in the L-VOD maps. Avitabile AGB and L-VOD scatter plots are also significantly different to those computed with the original Baccini and Saatchi maps. For instance, the low AGB versus L-VOD slopes obtained for low shrublands, grasslands and croplands are much lower than those found with the original Saatchi and Baccini datasets. The scatter plot found with Avitabile for woody-savannah resembles an overlay of the scatter plot obtained with Baccini and the scatter plot obtained with Saatchi. Finally, the slope of the AGB versus L-VOD in evergreen broadleaf forest is $\sim 30\%$ higher than those found with the other data sets. The singular behavior of Avitabile AGB could arise from the fact that it is a pure data driven method and that it is therefore very sensitive to the data used to train the method. In the Avitabile et al. (2016) training database, high AGB plots could be over-represented.

On the other hand, as mentioned in Sect. 4.3, the distribution of Baccini AGB for woody savannah is significantly different to the other datasets, which much higher values than those found for Bouvet-Mermoz and Saatchi AGB. Actually, with Baccini AGB, the value of the slope obtained for woody savannah is 80 % of that obtained for evergreen broadleaf forest, while this ratio is only 55% for Bouvet-Mermoz and Saatchi AGB. This high slope for woody savannah is responsible of the lower non-linearity of the global AGB and L-VOD relationship using the Baccini data set. Woody savannah in the IGBP classification is defined as herbaceous vegetation and a forest canopy cover between 30 % and 60 %. AGB could be overestimated in this heterogeneous land cover class in the Baccini dataset due to the fact that no microwave data but only MODIS is used for the spatial extrapolation (Sect. 2). Figure S4 shows scatter plots of the four AGB datasets as a function of the Simard et al. (2011) tree height estimation. The relationship is almost linear for Baccini et al. (2012) AGB, which is not the expected behavior from allometric relations (Chave et al., 2014) .

Radar observations in low vegetation regions such as shrublands and grasslands are thought to be very sensitive to biomass variations, in spite of a significant sensitivity to soil moisture. The high correlation of the two AGB maps involving radar data, either as the main source of information (Bouvet-Mermoz) or together with optical and elevation data (Saatchi), with SMOS L-VOD in grasslands would confirm this fact, as the high correlation in shrublands for Bouvet-Mermoz. The low slopes found for shrublands and grasslands when comparing to Baccini AGB also support this interpretation. Interestingly, the Bouvet-Mermoz AGB data set, which has been obtained from L-band SAR data and is the only one developed with a particular focus on savannahs, shows a linear relationship between L-VOD and AGB with a very low dispersion.

6 Conclusions

Three different SMOS-based L-VOD data sets were evaluated and compared to precipitation, tree height, NDVI, EVI and AGB data. Lower dispersion and smoother relationships were obtained by using SMOS-IC L-VOD, compared to the ~~L2~~ iL2 and L3 L-VOD data sets. Consistently, the rank correlation values obtained with SMOS-IC were significantly higher by 5-15 % than those obtained with Level 2 and Level 3 L-VOD data sets.

The relationships between AGB estimates and L-VOD were strong ($R = 0.85 - 0.94$) but differed among the products. For low vegetation classes (grasslands to woody savannah), the best performance was achieved with the ~~Bouvet's savannah biomass data set. The biomass data produced by Baccini and Saatchi performed well for all vegetation classes and show the best agreement with L-VOD for dense forest ($R = 0.70 - 0.79$). Avitabile's AGB data showed low correlation values with L-VOD for low vegetation classes and a similar performance to~~ Bouvet-Mermoz~~for dense forest ($R = 0.64 - 0.67$). Furthermore, we found a linear relationship for the Baccini data which was not the case for the remaining data. The AGB and L-VOD relationships can be fitted over the entire range of both variables with a single law using a sigmoid logistic function. However, an analysis per land cover class showed that within the same class, the L-VOD and AGB relationship is linear also for the Saatchi et al. (2011); Avitabile et al. (2016) and Bouvet-Mermoz data sets.~~ **, Baccini and Saatchi biomass data sets. The biomass data by Baccini and Saatchi showed the best agreement with L-VOD for dense forest ($R = 0.70 - 0.79$). Avitabile's AGB data showed low correlation values with L-VOD for low vegetation classes and a similar performance to Bouvet-Mermoz for dense forest ($R = 0.64 - 0.67$). The AGB and L-VOD relationships can be fitted over the entire range of both variables with a single law using a sigmoid logistic function. However, an analysis per land cover class showed that within the same land cover class, the L-VOD and AGB relationship is close to linear.** Therefore, the global non-linear relationship, found when all the different land cover are considered together, arises from different slopes in the L-VOD/AGB relationship obtained for different land cover classes considered separately. For low vegetation classes, the annual mean of L-VOD spans a range from 0 to 0.7 and ~~it shows a linear relationship with the amount of the average~~ could be related to the mean annual precipitations.

The relationship between AGB versus L-VOD was compared to the ones between AGB versus NDVI and AGB versus K/X/C-VOD from Liu et al. (2015). As expected, NDVI saturates strongly and it becomes weakly sensitive to AGB changes from ~ 70 to ~ 300 Mg/h. With respect to K/X/C-VOD, the AGB also increases slowly as VOD increases for most (~ 70 %) of the K/X/C-VOD dynamic range but ~~it saturates more gradually than for NDVI~~**it saturates for VOD > 0.8**. In contrast, AGB values show a steady increment as L-VOD increases over the whole L-VOD dynamic range.

The equations computed in this study can be used to estimate AGB from SMOS-IC L-VOD. Of course, these equations depend on the data set used as reference to fit the AGB and L-VOD relationship. Three of them (those determined with Baccini et al. (2012), Saatchi et al. (2011) and Bouvet-Mermoz) gave very similar values when the 5th and 95th percentiles of the distributions were taken into account.

The results obtained in this study showed that the L-VOD parameter estimated from the SMOS passive microwave observations is an interesting index to monitor AGB at coarse resolution (~ 40 km). ~~The advantage of this technique is that it~~

~~allows to add a temporal dimension to the static AGB maps estimated from other remote sensing observations with high spatial resolution. Despite its coarse spatial resolution, the high temporal resolution of the new SMOS L-VOD data will be useful to perform temporal estimations of the changes in the global carbon stocks at large scales.~~ **Despite its coarse spatial resolution, the advantage of using SMOS L-VOD is that it is possible to compute one AGB map per year, for instance, which allows to perform temporal estimations of the changes in the global carbon stocks at large scales (Brandt et al., 2018) .**

Author contributions. NJRF, AM, YK and JPW planned the research discussed in this manuscript and NJRF and AM performed most the computations. SM, AB and TLT provided the AGB data sets and expertise on AGB estimations. AM, JPW and AAY provided the SMOS-IC data. PR preprocessed the SMOS Level 2 data. TK, AAB and MB reviewed the system design and the results, in particular regarding the analysis per land cover classes. All authors participated in the writing and provided comments and suggestions.

Competing interests. The authors declare that they have no conflict of interest.

Acknowledgements. N.J.R.-F, J.-P.W, T.K., A.M. and Y.H.K. acknowledge partial support by the ESA contract No. 4000117645/16/NL/SW Support To Science Element SMOS+Vegetation and by CNES (Centre National d'Etudes Spatiales) TOSCA program. They also acknowledge and interesting discussions with other colleagues involved in the SMOS+Vegetation project (Marko Scholze, Matthias Drusch, Michael Vossbeck, Wolfgang Knorr, Cristina ~~Vitucci~~ Vittucci and Paolo Ferrazzoli). SMOS Level 3 data were obtained from the "Centre Aval de Traitement des Données SMOS" (CATDS), operated for the CNES (France) by IFREMER (Brest, France).

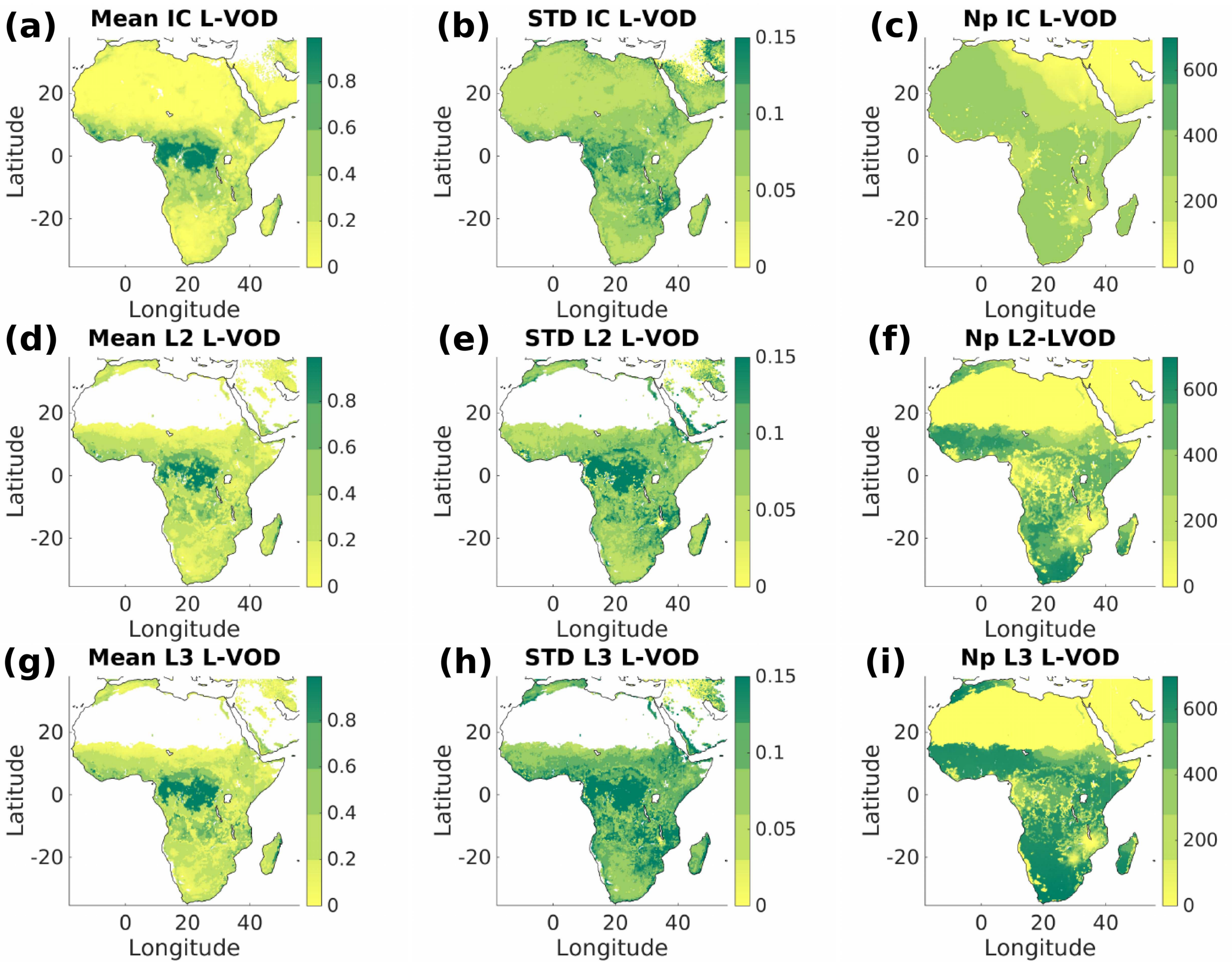

Figure 1. Years 2011-2012 average of L-VOD for the SMOS-IC, SMOS iL2 and SMOS L3 data sets (panels **a**, **d** and **g**, respectively), corresponding standard deviation (STD, panels **b**, **e** and **h**) and number of points (N_p, panels **c**, **f** and **i**) after filtering (Sect. 3) of the local L-VOD time series for the three products.

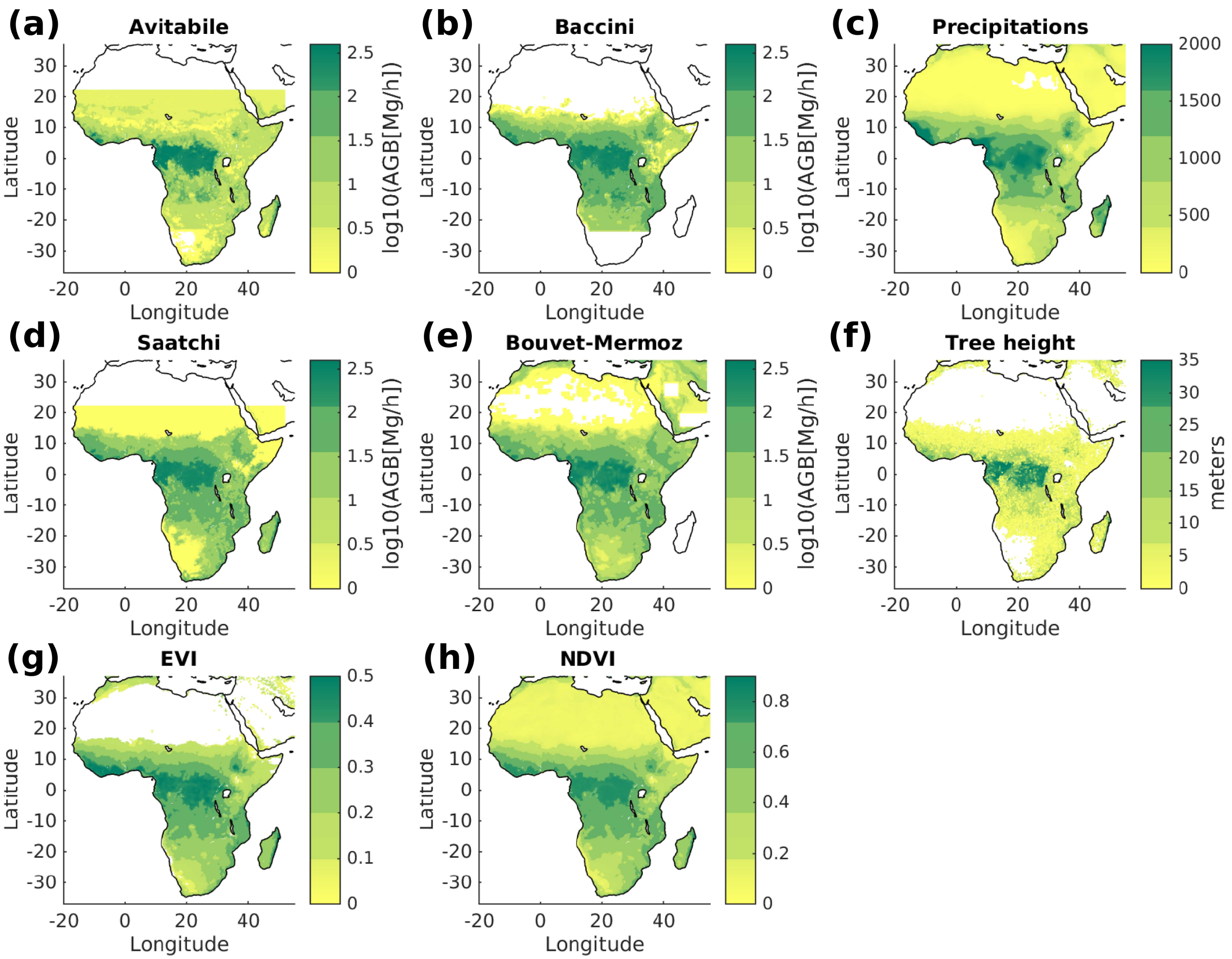

Figure 2. ~~Year 2011 annual mean of L-VOD for the SMOS-IC~~AGB maps from Avitabile et al. (2016) , ~~SMOS-L2~~ Baccini et al. (2012) , Saatchi et al. (2011) and ~~SMOS-L3~~ Bouvet et al. (2018) (panels ~~**a, d** and **g**~~**a, b, d, e**, respectively). ~~Data used to evaluate the SMOS L-VOD datasets (middle~~ Mean annual precipitations and ~~right~~ tree height (panels **c, f**, respectively). Year ~~(2011)~~ 2011-2012 average of MODIS EVI (~~**b**~~**g**) and NDVI (~~**e**). Simard et al. (2011) tree heigh (h). Worldclim average anual precipitations (j~~**h**).~~AGB maps from Avitabile et al. (2016) , Baccini et al. (2012) , Saatchi et al. (2011) and Bouvet et al. (2018) (panels **c, f, i, k**, respectively)~~

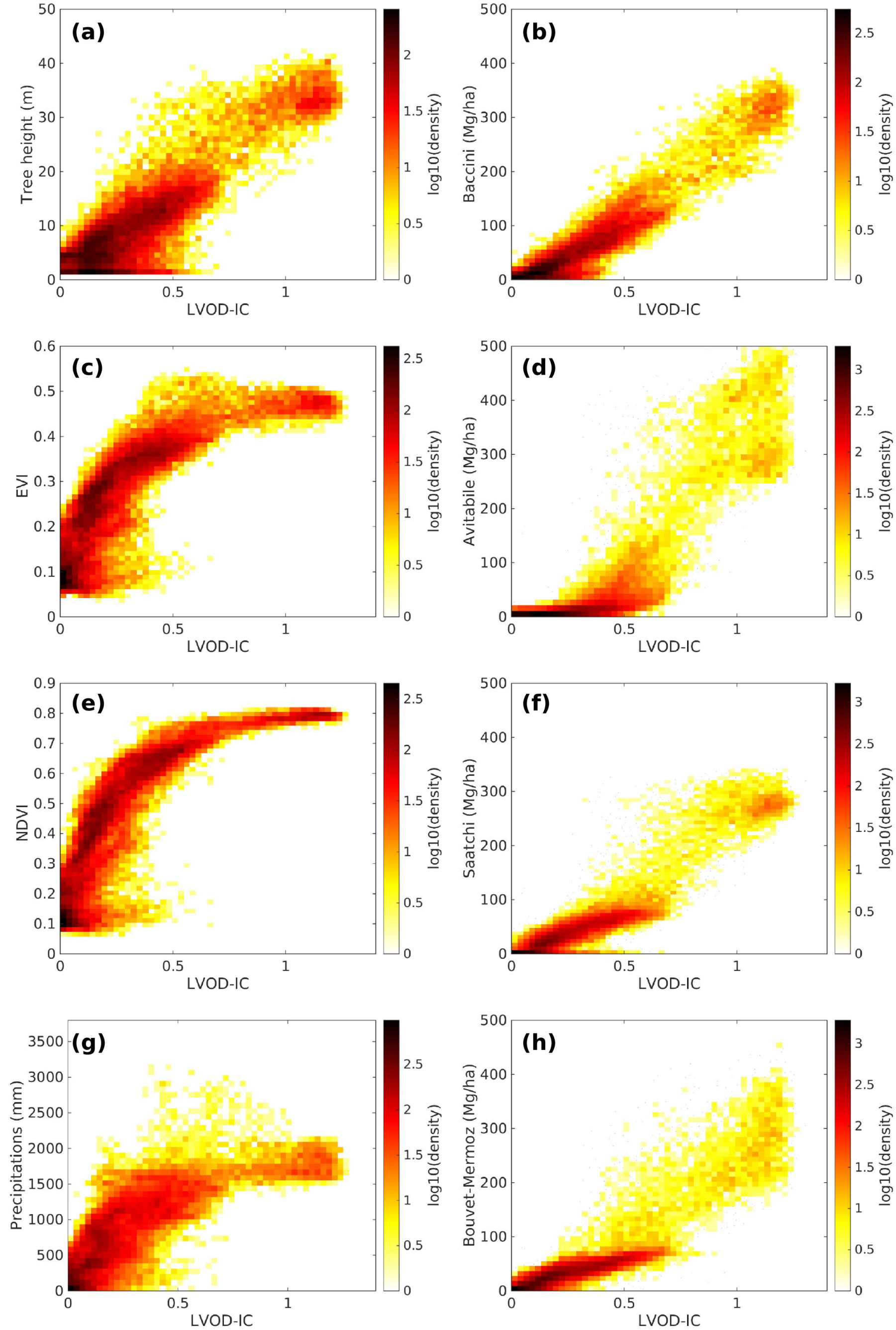

Figure 3. Density scatter plots of SMOS-IC L-VOD respect to: tree height (**a**), EVI (**c**), NDVI (**e**), cumulated precipitation (**g**), Baccini et al. (2012) AGB (**b**), Avitabile et al. (2016) AGB (**d**), Saatchi et al. (2011) AGB (**f**) and Bouvet-Mermoz AGB datasets (**h**).

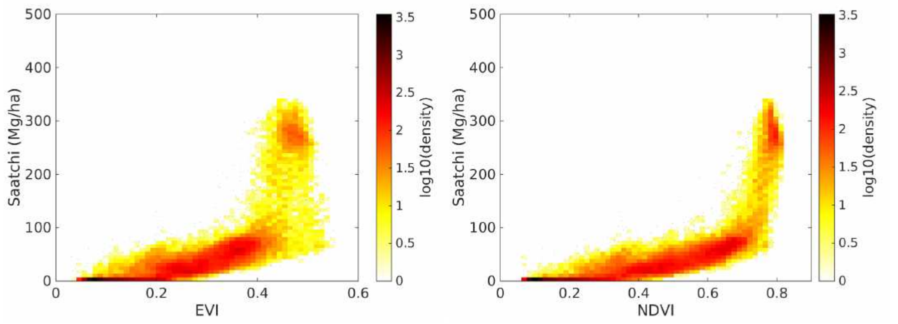

Figure 4. Scatter plots of MODIS NDVI and EVI with respect to Saatchi et al. (2011) AGB.

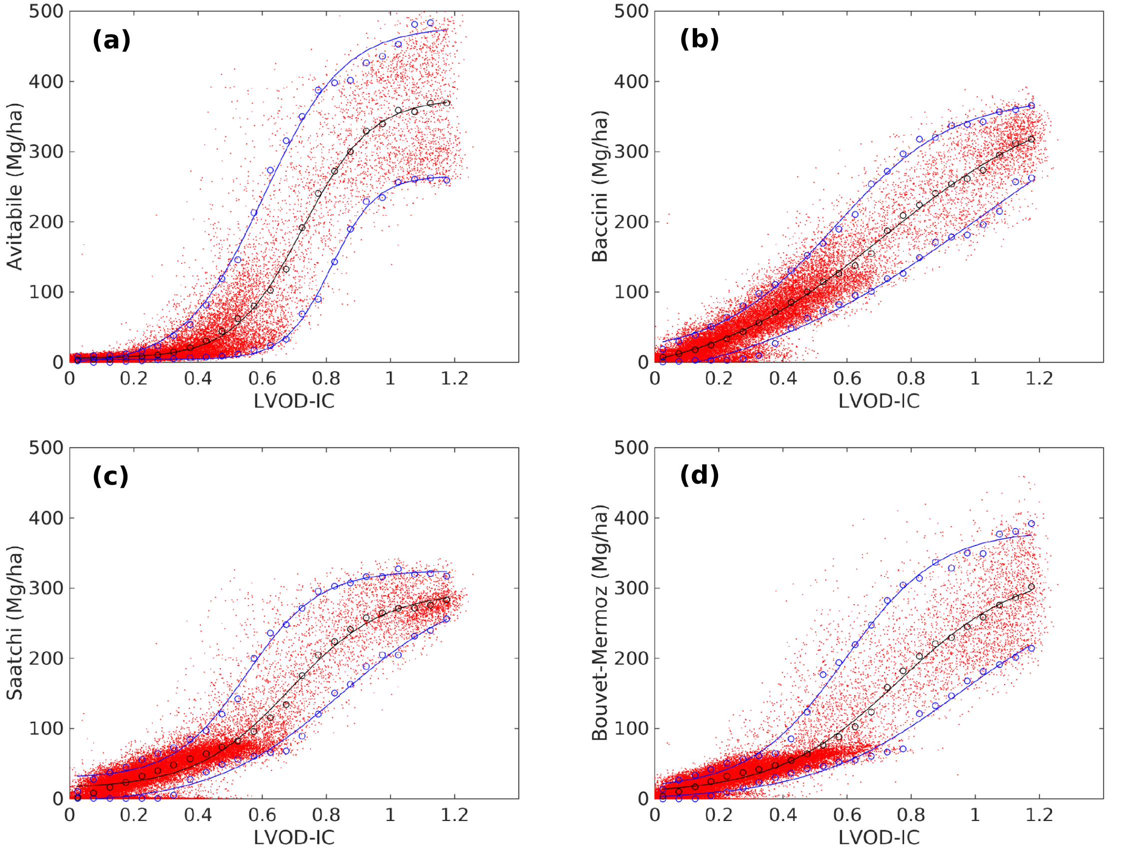

Figure 5. AGB versus L-VOD scatter plots of Fig. 3 but plotted as point scatter plots. In addition, on the right-hand panels, the 5th and 95th percentiles of the AGB distribution in bins of L-VOD are displayed as blue circles while the mean is displayed as black circles. Solid blue and black lines are the fits obtained using a logistic function (Eq. 2) with the parameters given in Table S3 for the 5th and 95th percentiles and the mean curves.

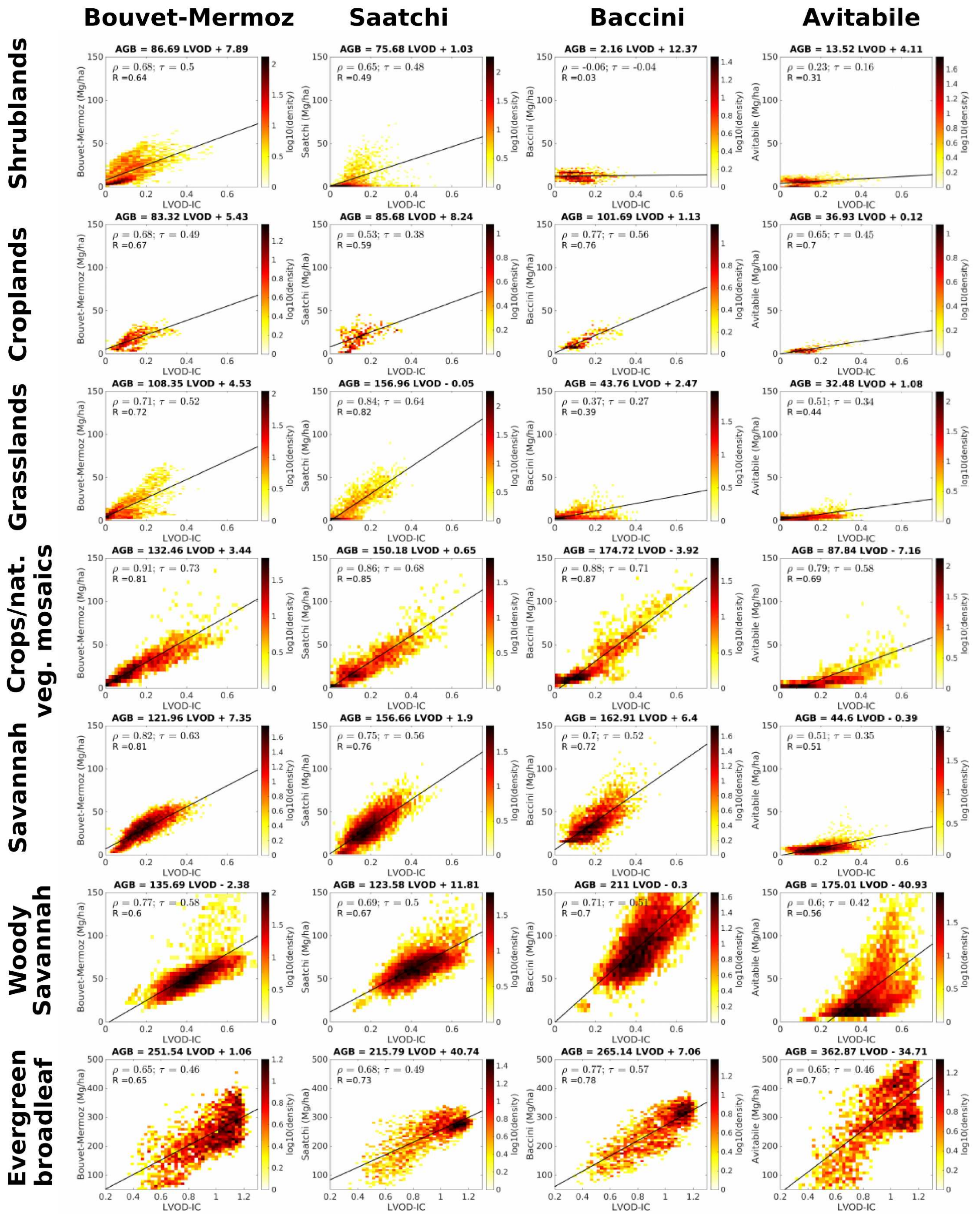

Figure 6. SMOS IC L-VOD relationships ~~to NDVI~~ versus the four AGB data sets (~~**a, b**)~~from left to right: Bouvet-Mermoz, ~~precipitations (**c, d**)~~Saatchi, ~~tree height (**e, f**) and Bouvet-Mermoz AGB (**g, h**~~Baccini; Avitabile) for ~~two biomes groups. Panels **a, c, e, g** represent the results including~~ different IGBP land cover classes (from top to bottom: open shrublands~~,~~; croplands~~,~~; grasslands; croplands and natural vegetation ~~and grasslands,~~ mosaics; savannah~~and~~ ; woody savannah~~. Panels **b, d, f, h** show the results for~~ ; evergreen broadleaf~~rainforest~~). Each panel shows the regression line and equation, and values of the Pearson R, Spearman ρ and Kendall τ coefficients.

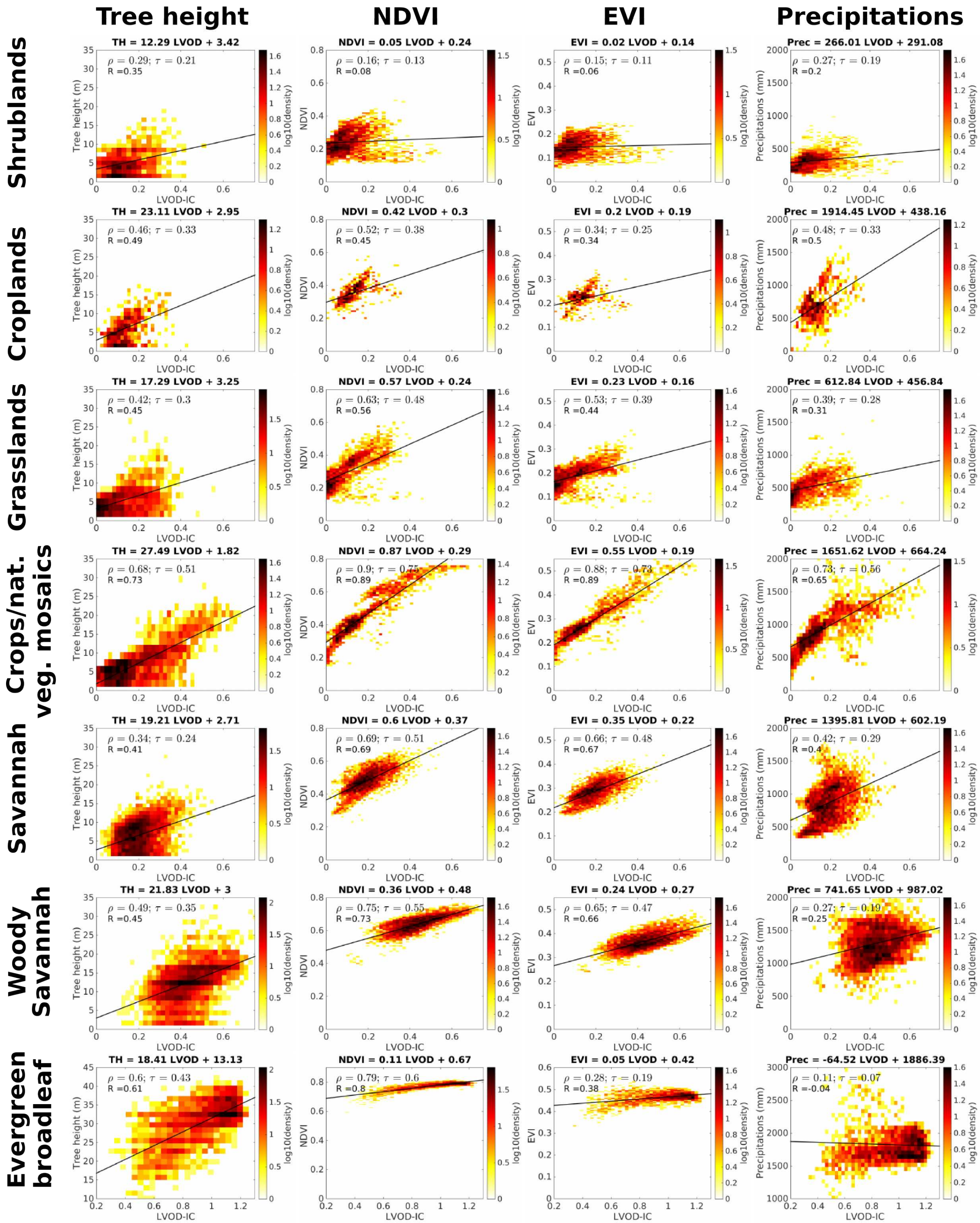

Figure 7. SMOS IC L-VOD relationships versus auxiliary data sets (from left to right: tree height, NDVI, EVI and average annual precipitations) for different IGBP land cover classes (from top to bottom: open shrublands; croplands; grasslands; croplands and natural vegetation mosaics; savannah; woody savannah; evergreen broadleaf). Each panel shows the regression line and equation, and values of the Pearson R, Spearman ρ and Kendall τ coefficients.

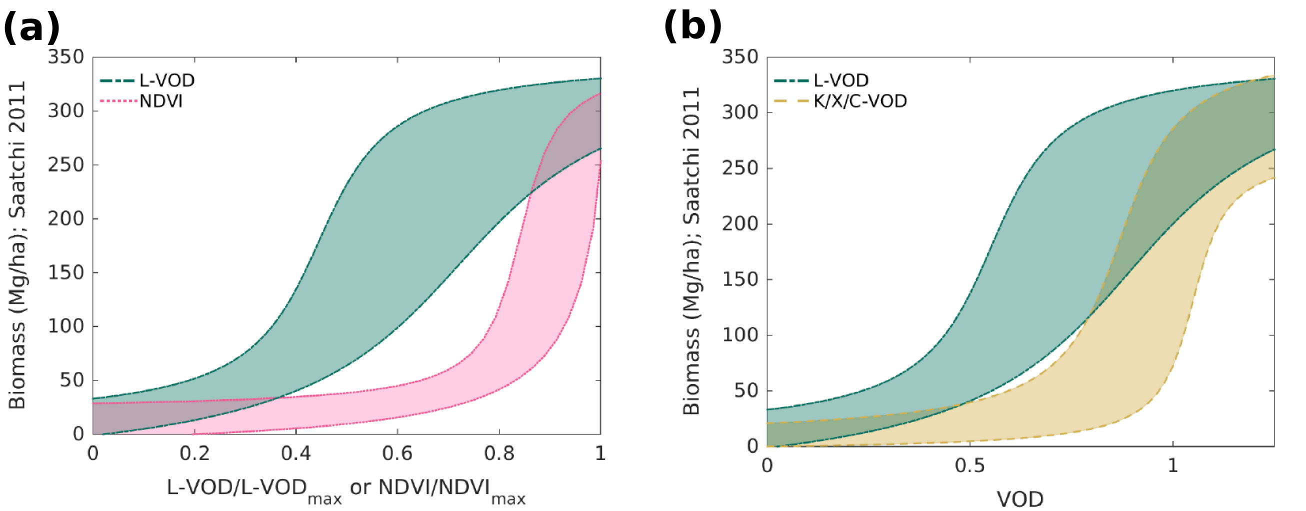

Figure 8. Left: Fits of the 5th and 95th percentile curves of the Saatchi et al. (2011) AGB with respect to SMOS-IC L-VOD (green) ~~, K/X/C-VOD from Liu et al. (2015) (brown),~~ and NDVI (pink). ~~The~~ To plot both distributions with the same scale, VOD and NDVI ~~distributions~~ were normalized from 0 to 1 using their respective maxima (0.83 for NDVI and 1.24 for L-VOD). Right: Fits of the 5th and 95th percentile curves of the Saatchi et al. (2011) AGB with respect to SMOS-IC L-VOD (green) overlaid in the K/X/C-VOD versus Saatchi et al. (2011) AGB curves of Fig. S4 from Liu et al. (2015) (brown). No normalization is needed in this case as both VODs span a similar range of values.

Table 1. Pearson's R, Spearman's ρ and Kendal's τ correlation coefficients of the three SMOS L-VOD data sets with respect to ~~cumulated~~ mean annual precipitations, tree height, MODIS NDVI and EVI and AGB from Saatchi et al. (2011), Avitabile et al. (2016), Baccini et al. (2012) and Bouvet-Mermoz.

	R			ρ			τ		
	IC	~~L2~~ iL2	L3	IC	~~L2~~ iL2	L3	IC	~~L2~~ iL2	L3
Precipitations	0.77	0.67	0.65	0.82	0.72	0.69	0.62	0.53	0.50
Tree Height	0.87	0.79	0.78	0.78	0.67	0.66	0.61	0.50	0.49
NDVI	0.81	0.75	0.73	0.88	0.81	0.78	0.72	0.63	0.60
EVI	0.80	0.74	0.73	0.86	0.79	0.76	0.69	0.60	0.57
Avitabile	0.85	0.78	0.78	0.84	0.73	0.72	0.65	0.54	0.53
Baccini	0.94	0.87	0.87	0.90	0.80	0.77	0.74	0.62	0.60
Saatchi	0.92	0.84	0.84	0.91	0.82	0.80	0.75	0.64	0.62
Bouvet-Mermoz	0.89	0.81	0.81	0.91	0.83	0.80	0.75	0.65	0.62

References

Al Bitar, A., Mialon, A., Kerr, Y., Cabot, F., Richaume, P., Jacquette, E., Quesney, A., Mahmoodi, A., Tarot, S., Parrens, M., Al-yaari, A., Pellarin, T., Rodriguez-Fernandez, N., and Wigneron, J.-P.: The Global SMOS Level 3 daily soil moisture and brightness temperature maps, Earth System Science Data, 9, 293–315, https://doi.org/10.5194/essd-2017-1, http://www.earth-syst-sci-data-discuss.net/essd-2017-1/, 2017.

Andela, N., Liu, Y., Van Dijk, A., De Jeu, R., and McVicar, T.: Global changes in dryland vegetation dynamics (1988-2008) assessed by satellite remote sensing: Comparing a new passive microwave vegetation density record with reflective greenness data, Biogeosciences, 10, 6657, 2013.

Asner, G. P., Knapp, D. E., Martin, R. E., Tupayachi, R., Anderson, C. B., Mascaro, J., Sinca, F., Chadwick, K. D., Higgins, M., Farfan, W., Llactayo, W., and Silman, M. R.: Targeted carbon conservation at national scales with high-resolution monitoring, Proceedings of the National Academy of Sciences, 111, E5016–E5022, https://doi.org/10.1073/pnas.1419550111, 2014.

Avitabile, V., Herold, M., Heuvelink, G., Lewis, S. L., Phillips, O. L., Asner, G. P., Armston, J., Ashton, P. S., Banin, L., Bayol, N., et al.: An integrated pan-tropical biomass map using multiple reference datasets, Global change biology, 2016.

Baccini, A., Goetz, S., Walker, W., Laporte, N., Sun, M., Sulla-Menashe, D., Hackler, J., Beck, P., Dubayah, R., Friedl, M., et al.: Estimated carbon dioxide emissions from tropical deforestation improved by carbon-density maps, Nature Climate Change, 2, 182–185, 2012.

Bouvet, A., Mermoz, S., Toan, T. L., Villard, L., Mathieu, R., Naidoo, L., and Asner, G. P.: An above-ground biomass map of African savannahs and woodlands at 25 m resolution derived from ALOS PALSAR, Remote Sensing of Environment, 206, 156 – 173, https://doi.org/https://doi.org/10.1016/j.rse.2017.12.030, https://www.sciencedirect.com/science/article/pii/S0034425717306053, 2018.

Brandt, M., Rasmussen, K., Peñuelas, J., Tian, F., Schurgers, G., Verger, A., Mertz, O., Palmer, J. R., and Fensholt, R.: Human population growth offsets climate-driven increase in woody vegetation in sub-Saharan Africa, Nature Ecology & Evolution, 1, 0081, 2017.

Brandt, M., Wigneron, J.-P., Chave, J., Tagesson, T., Penuelas, J., Ciais, P., Rasmussen, K., Tian, F., Mbow, C., Al-Yaari, A., et al.: Satellite passive microwaves reveal recent climate-induced carbon losses in African drylands, Nature ecology & evolution, 2, 827, 2018.

Brodzik, M. J., Billingsley, B., Haran, T., Raup, B., and Savoie, M. H.: EASE-Grid 2.0: Incremental but Significant Improvements for Earth-Gridded Data Sets., ISPRS International Journal of Geo-Information, 1(1), 32–45, https://doi.org/doi:10.3390/ijgi1010032, http://www.mdpi.com/2220-9964/1/1/32/, 2012.

Chave, J., Réjou-Méchain, M., Búrquez, A., Chidumayo, E., Colgan, M. S., Delitti, W. B., Duque, A., Eid, T., Fearnside, P. M., Goodman, R. C., et al.: Improved allometric models to estimate the aboveground biomass of tropical trees, Global change biology, 20, 3177–3190, 2014.

Entekhabi, D., Njoku, E. G., O'Neill, P. E., Kellogg, K. H., Crow, W. T., Edelstein, W. N., Entin, J. K., Goodman, S. D., Jackson, T. J., Johnson, J., et al.: The soil moisture active passive (SMAP) mission, Proceedings of the IEEE, 98, 704–716, 2010.

Esau, I., Miles, V. V., Davy, R., Miles, M. W., and Kurchatova, A.: Trends in normalized difference vegetation index (NDVI) associated with urban development in northern West Siberia, Atmospheric Chemistry and Physics, 16, 9563–9577, 2016.

Fernandez-Moran, R., Al-Yaari, A., Mialon, A., Mahmoodi, A., Al Bitar, A., De Lannoy, G., Rodriguez-Fernandez, N., Lopez-Baeza, E., Kerr, Y., and Wigneron, J.-P.: SMOS-IC: An alternative SMOS soil moisture and vegetation optical depth product, Remote Sensing, 9, 457, 2017.

Ferrazzoli, P. and Guerriero, L.: Passive microwave remote sensing of forests: A model investigation, IEEE Transactions on Geoscience and Remote Sensing, 34, 433–443, 1996.

Fick, S. E. and Hijmans, R. J.: WorldClim 2: new 1-km spatial resolution climate surfaces for global land areas, International Journal of Climatology, 2017.

Grant, J., Wigneron, J.-P., De Jeu, R., Lawrence, H., Mialon, A., Richaume, P., Al Bitar, A., Drusch, M., van Marle, M., and Kerr, Y.: Comparison of SMOS and AMSR-E vegetation optical depth to four MODIS-based vegetation indices, Remote Sensing of Environment, 172, 87–100, 2016.

Herrmann, S. M., Anyamba, A., and Tucker, C. J.: Recent trends in vegetation dynamics in the African Sahel and their relationship to climate, Global Environmental Change, 15, 394–404, 2005.

Hornbuckle, B. K., England, A. W., De Roo, R. D., Fischman, M. A., and Boprie, D. L.: Vegetation canopy anisotropy at 1.4 GHz, IEEE Transactions on Geoscience and Remote Sensing, 41, 2211–2223, 2003.

Huete, A., Didan, K., Miura, T., Rodriguez, E. P., Gao, X., and Ferreira, L. G.: Overview of the radiometric and biophysical performance of the MODIS vegetation indices, Remote sensing of environment, 83, 195–213, 2002.

Huete, A. R., Didan, K., Shimabukuro, Y. E., Ratana, P., Saleska, S. R., Hutyra, L. R., Yang, W., Nemani, R. R., and Myneni, R.: Amazon rainforests green-up with sunlight in dry season, Geophysical research letters, 33, 2006.

Jackson, T. and Schmugge, T.: Vegetation effects on the microwave emission of soils, Remote Sensing of Environment, 36, 203–212, 1991.

Jung, M., Reichstein, M., Margolis, H. A., Cescatti, A., Richardson, A. D., Arain, M. A., Arneth, A., Bernhofer, C., Bonal, D., Chen, J., et al.: Global patterns of land-atmosphere fluxes of carbon dioxide, latent heat, and sensible heat derived from eddy covariance, satellite, and meteorological observations, Journal of Geophysical Research: Biogeosciences, 116, 2011.

Kerr, Y., Waldteufel, P., Wigneron, J.-P., Delwart, S., Cabot, F., Boutin, J., Escorihuela, M.-J., Font, J., Reul, N., Gruhier, C., Juglea, S., Drinkwater, M., Hahne, A., Martin-Neira, M., and Mecklenburg, S.: The SMOS Mission: New Tool for Monitoring Key Elements ofthe Global Water Cycle, Proceedings of the IEEE, 98, 666–687, https://doi.org/10.1109/JPROC.2010.2043032, 2010.

Kerr, Y., Waldteufel, P., Richaume, P., Wigneron, J., Ferrazzoli, P., Mahmoodi, A., Al Bitar, A., Cabot, F., Gruhier, C., Juglea, S., Leroux, D., Mialon, A., and Delwart, S.: The SMOS Soil Moisture Retrieval Algorithm, IEEE Transactions on Geoscience and Remote Sensing, 50, 1384–1403, https://doi.org/10.1109/TGRS.2012.2184548, 2012.

Kerr, Y. H., Waldteufel, P., Wigneron, J. P., Martinuzzi, J., Font, J., and Berger, M.: Soil moisture retrieval from space: the Soil Moisture and Ocean Salinity (SMOS) mission, IEEE Transactions on Geoscience and Remote Sensing, 39, 1729–1735, https://doi.org/10.1109/36.942551, 2001.

Kirdiashev, K., Chukhlantsev, A., and Shutko, A.: Microwave radiation of the earth's surface in the presence of vegetation cover, Radiotekhnika I Elektronika, 24, 256–264, 1979.

Konings, A. G. and Gentine, P.: Global variations in ecosystem-scale isohydricity, Global change biology, 23, 891–905, 2017.

Konings, A. G., Piles, M., Rötzer, K., McColl, K. A., Chan, S. K., and Entekhabi, D.: Vegetation optical depth and scattering albedo retrieval using time series of dual-polarized L-band radiometer observations, Remote sensing of environment, 172, 178–189, 2016.

Konings, A. G., Piles, M., Das, N., and Entekhabi, D.: L-band vegetation optical depth and effective scattering albedo estimation from SMAP, Remote Sensing of Environment, 198, 460–470, 2017.

Kottek, M., Grieser, J., Beck, C., Rudolf, B., and Rubel, F.: World map of the Köppen-Geiger climate classification updated, Meteorologische Zeitschrift, 15, 259–263, 2006.

Lawrence, H., Wigneron, J.-P., Richaume, P., Novello, N., Grant, J., Mialon, A., Bitar, A. A., Merlin, O., Guyon, D., Leroux, D., Bircher, S., and Kerr, Y.: Comparison between SMOS Vegetation Optical Depth products and MODIS vegetation indices over crop zones of the USA, Remote Sensing of Environment, 140, 396 – 406, https://doi.org/http://dx.doi.org/10.1016/j.rse.2013.07.021, http://www.sciencedirect.com/science/article/pii/S0034425713002332, 2014.

Li, Y., Guan, K., Gentine, P., Konings, A. G., Meinzer, F. C., Kimball, J. S., Xu, X., Anderegg, W. R., McDowell, N. G., Martinez-Vilalta, J., et al.: Estimating Global Ecosystem Isohydry/Anisohydry Using Active and Passive Microwave Satellite Data, Journal of Geophysical Research: Biogeosciences, 2017.

Liu, Y., de Jeu, R. A., van Dijk, A. I., and Owe, M.: TRMM-TMI satellite observed soil moisture and vegetation density (1998–2005) show strong connection with El Niño in eastern Australia, Geophysical Research Letters, 34, 2007.

Liu, Y. Y., de Jeu, R. A., McCabe, M. F., Evans, J. P., and van Dijk, A. I.: Global long-term passive microwave satellite-based retrievals of vegetation optical depth, Geophysical Research Letters, 38, 2011.

Liu, Y. Y., van Dijk, A. I. J. M., de Jeu, R. a. M., Canadell, J. G., McCabe, M. F., Evans, J. P., and Wang, G.: Recent reversal in loss of global terrestrial biomass: supplementary information, Nature Climate Change, 5, 1–5, https://doi.org/10.1038/nclimate2581, http://www.nature.com/doifinder/10.1038/nclimate2581{%}5Cnpapers3://publication/doi/10.1038/nclimate2581, 2015.

Loveland, T. R., Reed, B. C., Brown, J. F., Ohlen, D. O., Zhu, Z., Yang, L., and Merchant, J. W.: Development of a global land cover characteristics database and IGBP DISCover from 1 km AVHRR data, International Journal of Remote Sensing, 21, 1303–1330, 2000.

Mermoz, S., Le Toan, T., Villard, L., Réjou-Méchain, M., and Seifert-Granzin, J.: Biomass assessment in the Cameroon savanna using ALOS PALSAR data, Remote sensing of environment, 155, 109–119, 2014.

Mermoz, S., Réjou-Méchain, M., Villard, L., Le Toan, T., Rossi, V., and Gourlet-Fleury, S.: Decrease of L-band SAR backscatter with biomass of dense forests, Remote Sensing of Environment, 159, 307–317, 2015.

Mo, T., Choudhury, B., Schmugge, T., Wang, J., and Jackson, T.: A model for microwave emission from vegetation-covered fields, Journal of Geophysical Research: Oceans, 87, 11 229–11 237, 1982.

Olson, D. M., Dinerstein, E., Wikramanayake, E. D., Burgess, N. D., Powell, G. V., Underwood, E. C., D'amico, J. A., Itoua, I., Strand, H. E., Morrison, J. C., et al.: Terrestrial Ecoregions of the World: A New Map of Life on Earth: A new global map of terrestrial ecoregions provides an innovative tool for conserving biodiversity, BioScience, 51, 933–938, 2001.

Parrens, M., Al Bitar, A., Mialon, A., Fernandez-Moran, R., Ferrazzoli, P., Kerr, Y., and Wigneron, J.-P.: Estimation of the L-band Effective Scattering Albedo of Tropical Forests using SMOS observations, IEEE Geoscience and Remote Sensing Letters, 14, 1223–1227, 2017a.

Parrens, M., Wigneron, J.-P., Richaume, P., Al Bitar, A., Mialon, A., Fernandez-Moran, R., Al-Yaari, A., O'Neill, P., and Kerr, Y.: Considering combined or separated roughness and vegetation effects in soil moisture retrievals, International Journal of Applied Earth Observation and Geoinformation, 55, 73–86, 2017b.

Pettorelli, N., Vik, J. O., Mysterud, A., Gaillard, J.-M., Tucker, C. J., and Stenseth, N. C.: Using the satellite-derived NDVI to assess ecological responses to environmental change, Trends in ecology & evolution, 20, 503–510, 2005.

Pettorelli, N., Ryan, S., Mueller, T., Bunnefeld, N., Jędrzejewska, B., Lima, M., and Kausrud, K.: The Normalized Difference Vegetation Index (NDVI): unforeseen successes in animal ecology, Climate Research, 46, 15–27, 2011.

Rahmoune, R., Ferrazzoli, P., Kerr, Y. H., and Richaume, P.: SMOS level 2 retrieval algorithm over forests: Description and generation of global maps, IEEE Journal of Selected Topics in Applied Earth Observations and Remote Sensing, 6, 1430–1439, https://doi.org/10.1109/JSTARS.2013.2256339, 2013.

Rahmoune, R., Ferrazzoli, P., Singh, Y., Kerr, Y., Richaume, P., and Al Bitar, A.: SMOS Retrieval Results Over Forests: Comparisons With Independent Measurements, Selected Topics in Applied Earth Observations and Remote Sensing, IEEE Journal of, 6-3, 1430 – 1439, https://doi.org/10.1109/JSTARS.2014.2321027, 2014.

Román-Cascón, C., Pellarin, T., Gibon, F., Brocca, L., Cosme, E., Crow, W., Fernández-Prieto, D., Kerr, Y. H., and Massari, C.: Correcting satellite-based precipitation products through SMOS soil moisture data assimilation in two land-surface models of different complexity: API and SURFEX, Remote Sensing of Environment, 200, 295–310, 2017.

Saatchi, S. S., Harris, N. L., Brown, S., Lefsky, M., Mitchard, E. T., Salas, W., Zutta, B. R., Buermann, W., Lewis, S. L., Hagen, S., et al.: Benchmark map of forest carbon stocks in tropical regions across three continents, Proceedings of the National Academy of Sciences, 108, 9899–9904, 2011.

Sahr, K., White, D., and Kimerling, A. J.: Geodesic discrete global grid systems cartography., Cartography and Geographic Information Science, 30(2), 30(2), 121–134, 2003.

Schwank, M., Matzler, C., Guglielmetti, M., and Fluhler, H.: L-band radiometer measurements of soil water under growing clover grass, IEEE Transactions on Geoscience and Remote Sensing, 43, 2225–2237, 2005.

Simard, M., Pinto, N., Fisher, J. B., and Baccini, A.: Mapping forest canopy height globally with spaceborne lidar, Journal of Geophysical Research: Biogeosciences, 116, 2011.

Todd, S., Hoffer, R., and Milchunas, D.: Biomass estimation on grazed and ungrazed rangelands using spectral indices, International journal of remote sensing, 19, 427–438, 1998.

Tucker, C. J.: Red and photographic infrared linear combinations for monitoring vegetation, Remote sensing of Environment, 8, 127–150, 1979.

Ulaby, F.: Passive microwave remote sensing of the Earth's surface, Antennas and Propagation, 1976.

Ulaby, F. T. and Wilson, E. A.: Microwave attenuation properties of vegetation canopies, IEEE Transactions on Geoscience and Remote Sensing, pp. 746–753, 1985.

Van de Griend, A. A. and Wigneron, J.-P.: The b-factor as a function of frequency and canopy type at H-polarization, IEEE Transactions on Geoscience and Remote Sensing, 42, 786–794, 2004.

Van der Werf, G. R., Randerson, J. T., Giglio, L., Collatz, G., Mu, M., Kasibhatla, P. S., Morton, D. C., DeFries, R., Jin, Y. v., and van Leeuwen, T. T.: Global fire emissions and the contribution of deforestation, savanna, forest, agricultural, and peat fires (1997–2009), Atmospheric Chemistry and Physics, 10, 11 707–11 735, 2010.

Van Marle, M., Van Der Werf, G., de Jeu, R., and Liu, Y.: Annual South American forest loss estimates based on passive microwave remote sensing (1990-2010), Biogeosciences, 13, 609, 2016.

Vicente-Serrano, S. M., Gouveia, C., Camarero, J. J., Beguería, S., Trigo, R., López-Moreno, J. I., Azorín-Molina, C., Pasho, E., Lorenzo-Lacruz, J., Revuelto, J., et al.: Response of vegetation to drought time-scales across global land biomes, Proceedings of the National Academy of Sciences, 110, 52–57, 2013.

Vittucci, C., Ferrazzoli, P., Kerr, Y., Richaume, P., Guerriero, L., Rahmoune, R., and Laurin, G. V.: SMOS retrieval over forests: Exploitation of optical depth and tests of soil moisture estimates, Remote Sensing of Environment, 180, 115–127, https://doi.org/10.1016/j.rse.2016.03.004, http://dx.doi.org/10.1016/j.rse.2016.03.004, 2016.

Wigneron, J.-P., Chanzy, A., Calvet, J.-C., and Bruguier, N.: A simple algorithm to retrieve soil moisture and vegetation biomass using passive microwave measurements over crop fields, Remote Sensing of Environment, 51, 331–341, 1995.

Wigneron, J.-P., Pardé, M., Waldteufel, P., Chanzy, A., Kerr, Y., Schmidl, S., and Skou, N.: Characterizing the dependence of vegetation model parameters on crop structure, incidence angle, and polarization at L-band, Geoscience and Remote Sensing, IEEE Transactions on, 42, 416–425, 2004.

Wigneron, J.-P., Kerr, Y., Waldteufel, P., Saleh, K., Escorihuela, M.-J., Richaume, P., Ferrazzoli, P., de Rosnay, P., Gurney, R., Calvet, J.-C., Grant, J., Guglielmetti, M., Hornbuckle, B., Mätzler, C., Pellarin, T., and Schwank, M.: L-band Microwave Emission of the Biosphere (L-MEB) Model: Description and calibration against experimental data sets over crop fields, Remote Sensing of Environment, 107, 639 – 655, https://doi.org/https://doi.org/10.1016/j.rse.2006.10.014, http://www.sciencedirect.com/science/article/pii/S0034425706004238, 2007.

Supplementary information

Correlation computation

To get a quantitative assessment of the correlation and the dispersion of L-VOD versus the evaluation datasets, three correlation coefficients were computed. First, the Pearson correlation coefficient R of two variables $x_1,...x_n$ and $y_1...y_n$ was computed as:

$$R = \frac{\sum_{i=1}^{n}(x_i - \overline{x})(y_i - \overline{y})}{\sqrt{\sum_{i=1}^{n}(x_i - \overline{x})^2}\sqrt{\sum_{i=1}^{n}(y_i - \overline{y})^2}} \tag{S1}$$

where, $\overline{x}$ and $\overline{y}$ are the means of each variable. R is a measure of the linear correlation between two variables. If the relationship linking these variables is linear with no dispersion, R equals 1 (both variables increase together) or -1 (one variable increases when the other decreases).

However, the relationships between L-VOD and the evaluation data are not expected to be linear in most of the cases. Therefore, two rank correlations were also computed to quantify monotonic relationships whether linear or not. The Spearman's correlation coefficient ρ is the Pearson correlation coefficient R computed on the rank of the two variables instead of the variables themselves. If there are no repeated data values, a perfect Spearman correlation of +1/-1 occurs when each of the variables is a perfect monotonic function of the other. In addition, Kendall's rank correlation was also computed. Kendall's correlation coefficient τ is given by:

$$\tau = \frac{n_{\text{concordant}} - n_{\text{discordant}}}{n(n-1)/2} \tag{S2}$$

where $n_{\text{concordant}}$ and $n_{\text{discordant}}$ are the number of concordant and discordant pairs, respectively. Given a pair of observations (x_i, y_i) and (x_j, y_j), they are said to be concordant if $y_j > y_i$ for $x_j > x_i$ or $y_j < y_i$ for $x_j < x_i$. Otherwise, the pair is said to be discordant. The denominator is the total number of pair combinations, so τ is in the range [-1,1].

~~Non-linear fits to the AGB versus L-VOD relationship~~

~~The relationships linking L-VOD to the evaluation data for different biomes were fitted using linear fits. In addition, fits to the global relationships linking AGB and L-VOD were computed following the approach used by Liu et al. (2015) . The~~

~~SMOS-IC L-VOD data was binned in 0.05-width bins. For each L-VOD bin, the 5th and 95th percentiles and the mean of the AGB distribution were computed, obtaining three AGB curves as a function of L-VOD. The three curves were fitted with Liu's function, with a logistic function or with a generalized logistic function, obtaining results of the same quality. Figure 5 shows the fitted curves and Table S3 presents the parameters of the fits obtained using a logistic function:~~

$$AGB = \frac{a}{1+e^{-b(VOD-c)}} + d$$

~~where a, b, c, d are four best-fit parameters. The fitted curves give AGB in Mg/h units as a function of L-VOD, which is dimensionless quantity. Therefore the units of a and d are Mg/h and b and c are dimensionless quantities. Table S3 also gives the values of the best-fit parameters and the correlation coefficients between the observed and fitted L-VOD data.~~

~~To compare the performance of L-VOD to estimate AGB with respect to other vegetation indices, scatter plots similar to those of Fig. 3 were computed using Saatchi's AGB with respect to MODIS NDVI and EVI (Fig. 4). There is a close-to-linear relationship for AGB lower than ~ 90 Mg/h and EVI or NDVI lower than 0.4 and 0.7, respectively. However, in contrast to L-VOD, the relationship saturates for higher AGB values and both EVI and NDVI show a very low sensitivity to AGB with increments of 90 to 300 Mg/h in the 0.5-0.6 and 0.7-0.8 ranges for EVI and NDVI, respectively. This is expected as the visible/infra-red indices are sensible to the greenness of the canopy, which is not closely related to the total AGB in densely vegetated regions.~~

~~L-VOD versus AGB and tree height for different biomes~~

~~Figure S1 shows the distribution of the two biomes groups used to compute Fig. **??**. In addition, Fig. **??** shows the L-VOD versus the AGB and tree height data sets using the more specific land cover classes shown in Fig. S1. Most of the relationships are close to linear with $R \sim 0.7$ or higher, and ρ values similar to R. For all land cover classes, the correlations with respect to Avitabile AGB are the lowest of all the AGB data sets, except for the Mermoz AGB for evergreen broadleaf rainforest. The highest correlations for shrublands, croplands, natural vegetation and grasslands and savannahs were found with Saatchi's and Bouvet's AGB ($R = 0.73-0.79$ and $\rho = 0.73-0.78$), while the highest correlations were found with Baccini's AGB for woody savannah. For dense evergreen broadleaf forest the highest correlations were found with Baccini's and Saatchi's AGB. For the latter vegetation type, the values of the correlation coefficient values are comparable to those obtained for the other land cover classes but the slope of the regression lines are significantly higher (by factors of 1.3-1.9) than those obtained for shrublands, croplands, grasslands, and savannahs, which are rather similar for Baccini, Saatchi and Bouvet-Mermoz data sets ($\sim 110-140$ Mg/h). Once again, the L-VOD relationships obtained between L-VOD with respect to and Avitabile AGB are very different to those found with the other AGB data sets, with slopes changing by a factor of 8 from that computed for savannahs to that obtained for evergreen broadleaf forest, leading to the highly non-linear global relationship discussed in Sect 4. Baccini's AGB data set shows a high dynamical range for low AGBs, as AGB is as high as ~ 150 Mg/h for IC L-VOD ~ 0.6, while for the other data sets, the maximum AGB for this L-VOD value is less than 100 Mg/h.~~

~~AGB versus L-VOD scatter plots of Fig. 3 but plotted as point scatter plots. In addition, on the right-hand panels, the 5th and 95th percentiles of the AGB distribution in bins of L-VOD are displayed as blue circles while the mean is displayed as black circles. Solid blue and black lines are the fits obtained using a logistic function (Eq. 2) with the parameters given in Table S3 for the 5th and 95th percentiles and the mean curves.~~

~~Scatter plots of MODIS NDVI and EVI with respect to Saatchi et al. (2011) AGB.~~

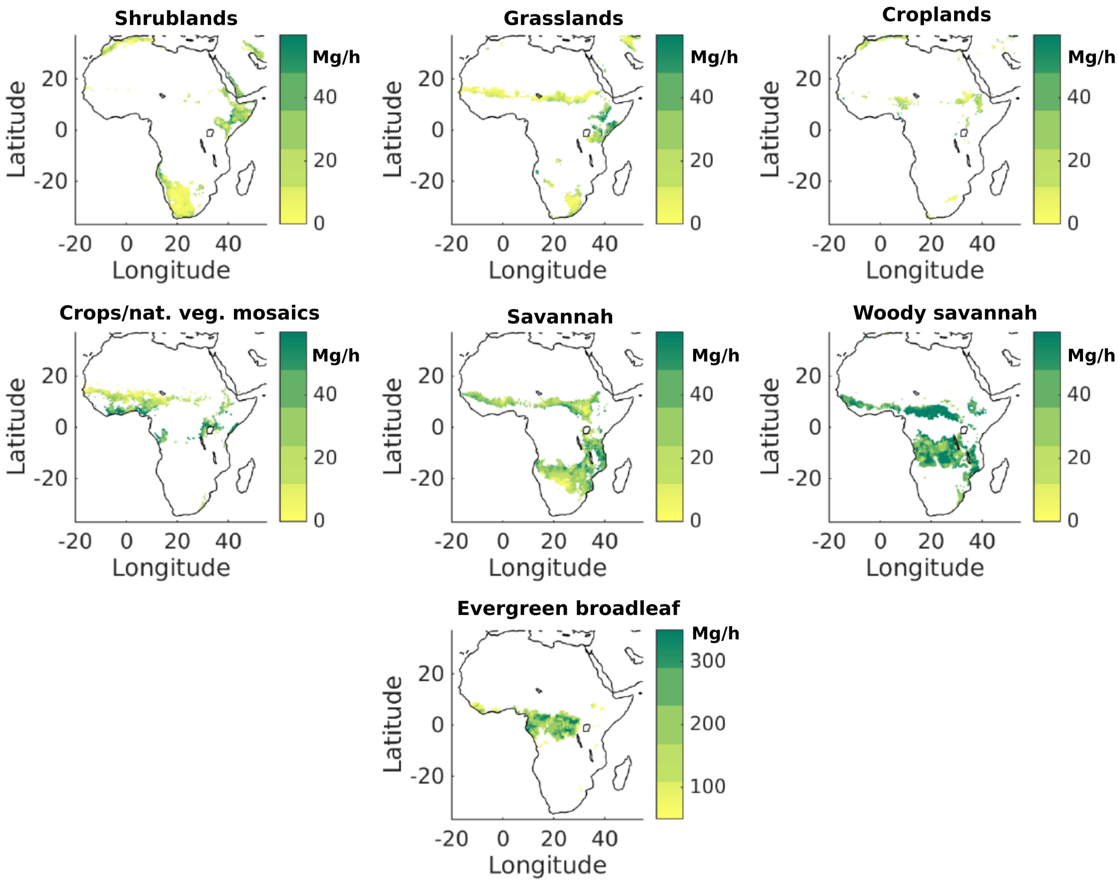

Figure S1. ~~Bouvet-Mermoz data set showing the spatial~~ Spatial distribution of the IGBP land cover classes used ~~to compute Fig. ??~~in this study (Table S2) shown in the Bouvet-Mermoz AGB map.

~~Density scatter plots of the 2011 annual mean of SMOS L2 L-VOD respect to (from top to bottom and from left to right): tree height, EVI, NDVI, cumulated precipitation, Baccini et al. (2012) , Avitabile et al. (2016) , Saatchi et al. (2011) and Bouvet-Mermoz AGB datasets.~~

~~Density scatter plots of the 2011 anual mean of SMOS L3 L-VOD respect to (from top to bottom and from left to right): tree height, EVI, NDVI, cumulated precipitation, Baccini et al. (2012) , Avitabile et al. (2016) , Saatchi et al. (2011) and Bouvet-Mermoz AGB datasets.~~

Table S1. Main characteristics of the three SMOS L-VOD products used in this study.

	ESA Level 2	CATDS Level 3	INRA-CESBIO
Reference	Kerr et al. (2012)	Al Bitar et al. (2017)	Fernandez-Moran et al. (2017)
Version used	620	300	100
Soil texture	Ecoclimap	Ecoclimap	Ecoclimap
Land cover	Ecoclimap	Ecoclimap	IGBP
Soil temperature	ECMWF	ECMWF	ECMWF
Forward model	L-MEB (Wigneron et al., 2007)	L-MEB (Wigneron et al., 2007)	L-MEB (Wigneron et al., 2007)
Single-scattering albedo	Low vegetation: 0 Tropical and subtropical forest: 0.06 Boreal forest: 0.08	Low vegetation:0 Tropical and subtropical forest: 0.06 Boreal forest: 0.08	Parrens et al. (2017b, a)
Roughness	Low vegetation: 0.1 Forest: 0.3	Low vegetation: 0.1 Forest: 0.3	Parrens et al. (2017b, a)
Multi-orbit	no	yes, three orbits, L-VOD assumed to be correlated	no
L-VOD first guess	Computed from Ecoclimap LAI	Computed from Ecoclimap LAI	First inversion using a constant value of ~~0.2 and a local average of previous IC retrievals in a~~ **0.5** a ~~second step~~ a local average of the first retrievals
SM first guess	ECMWF	ECMWF	0.2 m^3/m^{-3}
Footprints with inhomogeneous land cover	SM and L-VOD retrieval only for major fraction. Contribution from minor fraction using ECMWF SM and Ecoclimap LAI	SM and L-VOD retrieval only for major fraction. Contribution from minor fraction using ECMWF SM and Ecoclimap LAI	SM and L-VOD retrieval for the whole footprint assumed to be homogeneous
Grid Sampling	ISEA 15 km	EASEv2 25 km	EASEv2 25 km

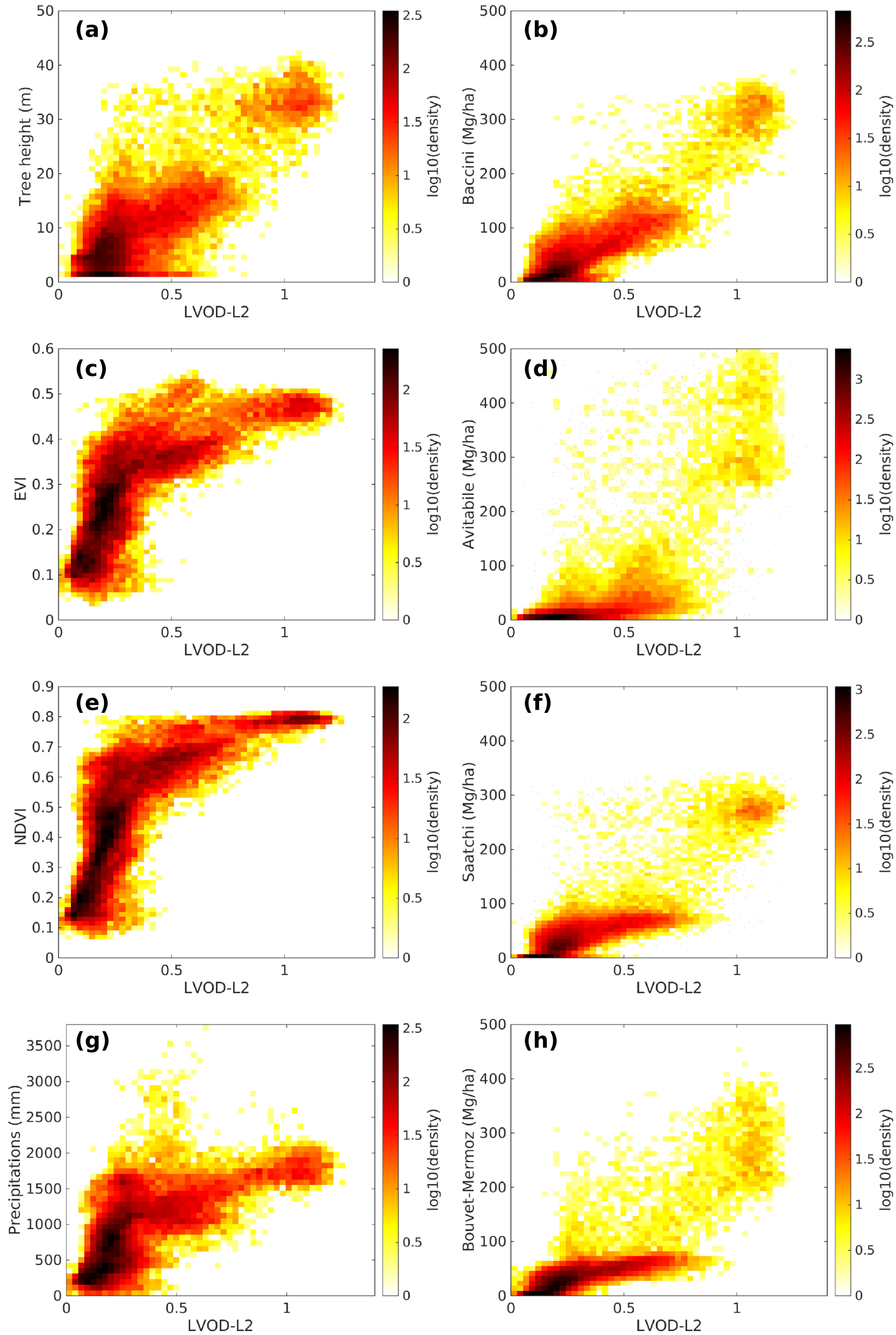

Figure S2. Density scatter plots of the 2011 annual mean of SMOS ~~IC~~ iL2 L-VOD ~~relationships~~ respect to ~~the AGB~~ (from top to bottom and ~~tree heigh evaluation datasets for different land cover classes: From~~ from left to right): ~~*(i)* Shrublands~~tree height, ~~croplands~~EVI, ~~natural vegetation and grasslands~~NDVI, ~~*(ii)* Savannah *(ii)* Woody savannah~~cumulated precipitation, ~~*(iv)* Evergreen broadleaf~~Baccini et al. (2012) , Avitabile et al. (2016) , Saatchi et al. (2011) and Bouvet-Mermoz AGB datasets.

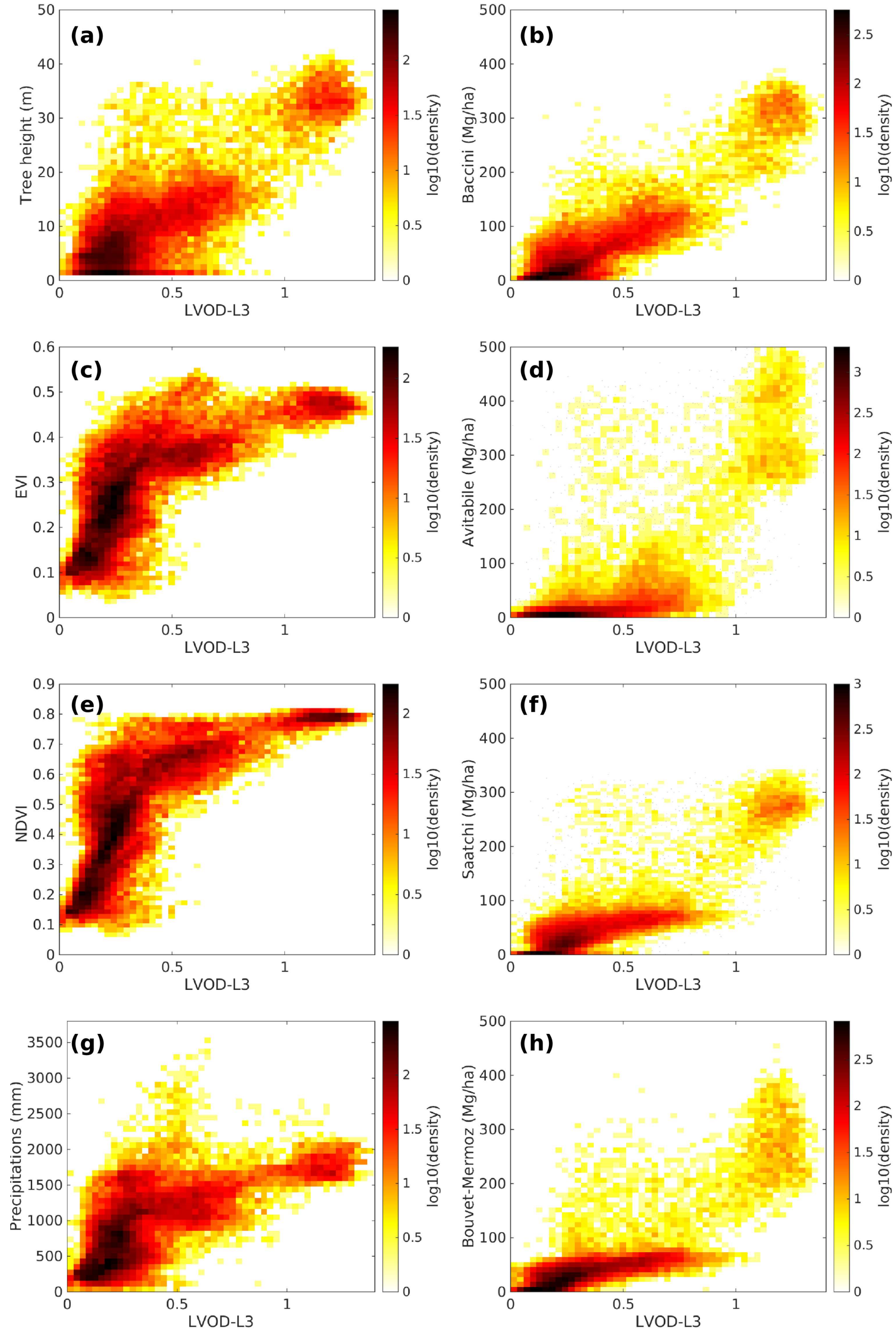

Figure S3. ~~Spatial distribution of the Bouvet-Mermoz AGB for the land cover classes used to compute the~~ Density scatter plots of ~~Fig. ??. (a)~~ ~~Shrublands~~the 2011 annual mean of SMOS L3 L-VOD respect to (from top to bottom and from left to right): tree height, ~~croplands~~EVI, ~~natural vegetation and grasslands~~NDVI, ~~(b)~~ ~~Savannah~~ ~~(c)~~ ~~Woody savannah~~cumulated precipitation, ~~(d)~~ ~~Evergreen broadleaf~~Baccini et al. (2012) , Avitabile et al. (2016) , Saatchi et al. (2011) and Bouvet-Mermoz AGB datasets.

Table S2. Land cover classes of the International Geosphere-Biosphere Program (IGBP) dataset (Loveland et al., 2000) used in this study.

Number	Name	Description
2	Evergreen broadleaf	Lands dominated by broadleaf woody vegetation with a percent cover >60% and height exceeding 2 m. Almost all trees and shrubs remain green year round. Canopy is never without green foliage.
7	Open shrublands	Lands with woody vegetation less than 2 m tall and with shrub canopy cover between 10% and 60%. The shrub foliage can be either evergreen or deciduous.
8	Woody savannah	Lands with herbaceous and other understory systems, and with forest canopy cover between 30% and 60%. The forest cover height exceeds 2 m.
9	Savannah	Lands with herbaceous and other understory systems, and with forest canopy cover between 10% and 30%. The forest cover height exceeds 2 m.
10	Grasslands	Lands with herbaceous types of cover. Tree and shrub cover is less than 10%.
12	Croplands	Lands covered with temporary crops followed by harvest and a bare soil period (e.g., single and multiple cropping systems). Note that perennial woody crops will be classified as the appropriate forest or shrub land cover type.
14	Croplands and natural vegetation mosaics	Lands with a mosaic of croplands, forests, shrubland, and grasslands in which no one component comprises more than 60% of the landscape.

Table S3. Parameters of the fits of the AGB vs IC L-VOD of relationship of Fig. 5 using a logistic function (Eq. 2).

AGB	line	a [Mg/h]	b[-]	c[-]	d [Mg/h]	R^2
Avitabile	05th	264.367	13.115	0.846	4.351	0.998
Avitabile	Mean	369.890	8.921	0.732	5.158	0.999
Avitabile	95th	463.091	9.466	0.583	2.135	0.990
Saatchi	05th	345.590	4.458	0.926	-4.387	0.993
Saatchi	Mean	280.159	6.680	0.689	14.794	0.993
Saatchi	95th	289.762	9.857	0.548	33.859	0.993
Baccini	05th	455.774	2.785	0.964	-40.357	0.990
Baccini	Mean	422.744	3.400	0.729	-29.252	0.999
Baccini	95th	393.863	4.685	0.558	-6.444	0.997
Bouvet-Mermoz	05th	296.709	4.511	0.966	2.129	0.987
Bouvet-Mermoz	Mean	325.043	5.116	0.774	7.651	0.996
Bouvet-Mermoz	95th	355.989	7.267	0.589	19.731	0.994

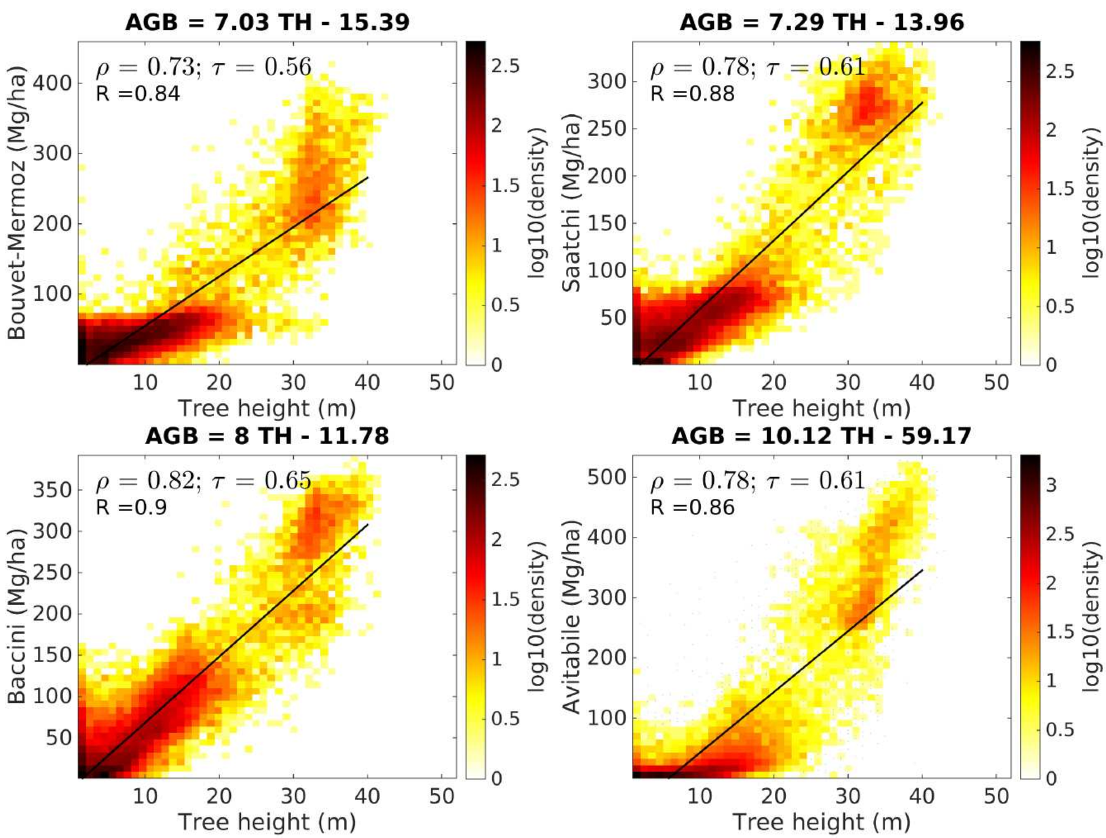

Figure S4. Scatter plots of the four AGB datasets as a function of Simard et al. (2011) tree height.